

FLOOD RISK MAPPING

A DISSERTATION

*Submitted in partial fulfillment of the
requirements for the award of the degree*

of
MASTER OF TECHNOLOGY
in
HYDROLOGY

By

DHRUV DHIRENDRA



**DEPARTMENT OF HYDROLOGY
INDIAN INSTITUTE OF TECHNOLOGY ROORKEE
ROORKEE - 247 667 (INDIA)
JUNE, 2006**

CANDIDATE'S DECLARATION

I hereby certify that the work which is being presented in this dissertation entitled "**FLOOD RISK MAPPING**" in partial fulfillment of the requirement for the award of the degree of **Master of Technology in Hydrology**, submitted in the Department of Hydrology of Indian Institute of Technology Roorkee is an authentic record of my work carried out during the period from July, 2005 to June, 2006 under the supervision of **Dr. D. S. Arya, Asstt. Professor**, Department of Hydrology, and **Dr. N.K. Goel, Professor**, Department of Hydrology Indian Institute of Technology, Roorkee.

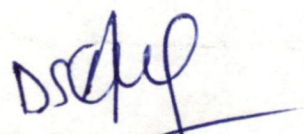
The matter embodied in this dissertation has not been submitted by me for the award of any other degree or diploma.



(Dhruv Dhirendra)

Candidate's Signature

Dated: June 15, 2006

This is to certify that the above statement made by the candidate is correct to the best of our knowledge.


(**D. S. Arya**)
Asstt. Professor,
Department of Hydrology
Indian Institute of Technology,
Roorkee


(**N. K. Goel**)
Professor,
Department of Hydrology
Indian Institute of Technology,
Roorkee

ACKNOWLEDGEMENTS

It is my great pleasure to express my profound sense of respect and gratitude to my guide Dr. D. S. Arya, Asst. Professor, Department of Hydrology, and Dr. N.K. Goel, Professor, Department of Hydrology, Indian Institute of Technology, Roorkee for their valuable and timely guidance, constant encouragement, moral support and pains taking supervision to complete this study. Indeed, I will remain ever indebted to them for their keen interest and whole-hearted cooperation all through the pursuance of this study.

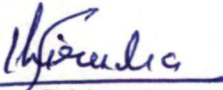
I am extremely grateful to Department of Hydrology for providing me all academic and technical assistance throughout the preparation of this work. My sense of gratitude goes to Dr. B. S. Mathur, Professor, Dr. D. K. Srivastava, Professor, Dr. Ranvir Singh, Professor, Dr. D.C.Signal, Professor, Dr. Himanshu Joshi, Associate professor and Dr. M. Perumal, Associate Professor, Department of Hydrology, Indian Institute of technology, Roorkee for their valuable teaching, guidance, assistance and encouragement during the entire course of study at Roorkee.

I would like to thank my fellow trainee officers and all my friends for their immense cooperation, constant interaction and advice during this work. I also wish to express my deep thanks to Mr. Harish G. Gundekar (Research Scholar) for his help in carrying out this study. I wish to thank all others who have directly or indirectly contributed in this work.

I bow with reverence to my parents and my brother for their blessings to complete this study.

IIT Roorkee, India

Dated: 15 June, 2006


(Dhruv Dhirendra)

SYNOPSIS

Flood is one of the natural disasters which occur in Myanmar every year. Floods generally occur during the southwest monsoon period i.e. from June to October, when the westerly depression system and the low latitude tropical cyclone system causes the rainstorm. These floods had caused appreciable damage to livestock, agricultural crops, roads, bridges and buildings in the past. It is evident from the past record that the problem of river flooding is getting more and more acute due to human intervention in the flood plain at an ever increasing scale. It has been gradually realized that it is more rational to try minimizing the risk and damage involved the floods rather than formulating structural measures for containing the river.

The computation of flood water level is needed because this level delineates the flood plain and determines the required height of structures such as bridges and levees. The computation of flood flow rate is also important; first, because the flow rate determines the water level, and second, because the design of any flood storage structure such as a detention pond or reservoir requires an estimate of its inflow hydrograph.

It is envisaged to predict the water level using kinematic wave model. Kinematic wave modelling is an important hydraulic engineering practice because it deals with the modeling of movement of flow along the channel over time. Results of channel flow routing provide information regarding to the temporal and spatial distributions of flood wave which is essential for flood warning and protection. In this study, the daily stage, annual peak flow and rainfall from six gauging stations from Chindwin basin have been analyzed.

The efficiency of stage-discharge relationship for Hkamti, Homalin, Mawalaik, Kalewa and Monywa is found to be 88%, 99.02%, 86%, 89%, and 89% respectively. Similarly efficiency of Kinematic wave model has been tested separately for daily stage prediction and for daily discharge prediction. Efficiency of the Kinematic wave model for daily stage prediction at station Kalewa and Monywa is found to be 82% and 87% respectively. The efficiency of same model for daily discharge prediction for Kalewa and Monywa is found to be 85.75% and 84% respectively. The stages computed from stage discharge relationship are found to be satisfactory. Similarly the model efficiency of the Kinematic wave model for stage and discharge prediction is also found to be acceptable.

CONTENTS

	Page No.
CANDIDATE'S DECLARATION	i
ACKNOWLEDGEMENTS	ii
SYNOPSIS	iv
CONTENTS	vi
LIST OF TABLES	x
LIST OF FIGURES	xii
Chapter 1 INTRODUCTION	
1.1 General	1
1.2 Work Done So Far	2
1.3 Scope Of The Study	3
1.4 Layout Of The Thesis	3
Chapter 2 STUDY AREA	
2.1 Study Area	5
2.2 Hydrological, Meteorological and Topographic Data Used	10
Chapter 3 DATA ANALYSIS AND DEVELOPMENT OF RATING CURVES	
3.1 PRELIMINARY ANALYSIS OF HYDROMETEOROLOGICAL DATA	15
3.1.1 Statistical Parameters	15
3.1.2 Randomness Analysis	16
3.1.3 Trends Identification	16
3.1.4 Long Term Persistence	18
3.1.5 Test for Outliers	18
3.2 DEVELOPMENT OF RATING CURVES	19
3.2.1 Introduction	19
3.2.2 Methods Of Development Of Rating Curves	20
3.2.3 Arithmetic Plot Of Stage Data Versus Discharge Data For All Stations	26
3.3 STAGE-DISCHARGE RELATIONSHIP	28

3.3.1	Performance Of Stage-Discharge Relationship At Different Stations For Different Seasons	29
3.3.2	Summary Of Stage-Discharge Relationship At Different Stations For Different Seasons	32
Chapter 4	KINEMATIC WAVE THEORY	
4.1	INTRODUCTION	42
4.2	SAINT-VENANT EQUATIONS	42
4.2.1	Continuity Equation	43
4.2.2	Momentum Equation	46
4.3	FORCES	47
4.3.1	Gravity	47
4.3.2	Friction	47
4.3.3	Contraction/Expansion	48
4.3.4	Wind Shear	48
4.3.5	Pressure	49
4.4	MOMENTUM	51
4.4.1	Net Momentum Outflow	51
4.4.2	Momentum Storage	53
4.5	WAVE MOTION	57
4.5.1	Kinematic Wave Celerity	58
4.5.2	Solution Of the Kinematic Wave	62
4.6	FINITE-DIFFERENCE APPROXIMATION	62
4.6.1	Finite Differences	64
4.6.2	Numerical Solution Of The Kinematic Wave Equations	68
4.7	DEVLOPMENT OF KINEMATIC WAVE MODEL FOR CHINDWIN RIVER	72
4.7.1	Variables List	72
4.7.2	Data Used	72
4.8	PERFORMANCE OF KINEMATIC WAVE MODEL AT DIFFERENT STATION FOR DIFFERENT SEASONS	73
4.9	SUMMARY OF KINEMATIC WAVE MODEL AT DIFFERENT STATION FOR DIFFERENT SEASONS	79

4.9.1	Summary Of Kinematic Wave Model At Different Stations For Daily Discharge Prediction	79
4.9.2	Summary Of Kinematic Wave Model At Different Stations For Daily Stage Prediction	83
Chapter 5	CONCLUSIONS	
5.1	General	87
5.2	Conclusions	87
5.3	Suggestions For Further Work	89
	REFERENCES	90
	APPENDIX	97

LIST OF TABLES

Table No.		Page No.
2.1	The length of Myanmar Rivers	5
2.2	Distribution of Monthly Mean Rainfall of Chindwin basin	8
2.3	Annual Maximum Water Level for Chindwin River at Different Stations in Myanmar in 1966 to 2002	10
2.4	Summary of data availability in this study Daily stages, annual peak flow and rainfall data	11
3.1	Statistical Characteristics of original series of annual peak flow data	15
3.2	Statistical Characteristics of log transform series annual peak flow data	15
3.3	Turning Point test results	16
3.4	Anderson's Correlogram test results	16
3.5	Kendal's rank correlation test results	16
3.6	Mann Kendal test results	17
3.7	Spearman's Rho test results	17
3.8	Long-term dependence Test results	17
3.9	Outlier test results	18
3.10a	Summary of Hkamti station for rest and pre-monsoon	32
3.10b	Summary of Hkamti station for monsoon and post-monsoon	33
3.11a	Summary of Homalin station for rest and pre-monsoon	34
3.11b	Summary of Homalin station for monsoon and post-monsoon	35
3.12a	Summary of Mawalaik station for rest and pre-monsoon	36
3.12b	Summary of Mawalaik station for monsoon and post-monsoon	37
3.13a	Summary of Kalewa station for rest and pre-monsoon	38
3.13b	Summary of Kalewa station for monsoon and post-monsoon	39
3.14a	Summary of Monywa station for rest and pre-monsoon	40
3.14b	Summary of Monywa station for monsoon and post-monsoon	41
4.1a	Summary of Kalewa station for rest and pre-monsoon	79
4.1b	Summary of Kalewa station for monsoon and post-monsoon	80

4.2a	Summary of Monywa station for rest and pre-monsoon	81
4.2b	Summary of Monywa station for monsoon and post-monsoon	82
4.3a	Summary of Kalewa station for rest and pre-monsoon	83
4.3b	Summary of Kalewa station for monsoon and post-monsoon	84
4.4a	Summary of Monywa station for rest and pre-monsoon	85
4.4b	Summary of Monywa station for monsoon and post-monsoon	86

LIST OF FIGURES

Fig. No.		Page No.
2.1	Map showing Chindwin Basin	7
2.2	Monthly Average Rainfall of Chindwin Basin at different Site	8
2.3	Mean Monthly Discharge of Chindwin River at Different Site (1972-2002)	9
2.4	Flood frequency in Chindwin Basin (1966-2000)	10
2.5a	Annual Peak Flow Series for Hkamti station	12
2.5b	Annual Peak Flow Series for Homalin station	12
2.5c	Annual Peak Flow Series for Mawalaik station	13
2.5d	Annual Peak Flow Series for Kalewa station	13
2.5e	Annual Peak Flow Series for Mingin station	14
2.5f	Annual Peak Flow Series for Monywa station	14
3.1	Running's Method for estimation of the constant H_0	25
3.2	Plot of stage data versus discharge data at Hkamti station	26
3.3	Plot of stage data versus discharge data at Homalin station	26
3.4	Plot of stage data versus discharge data at Mawalaik station	27
3.5	Plot of stage data versus discharge data at Kalewa station	27
3.6	Plot of stage data versus discharge data at Monywa station	27
3.7	Percentage efficiency of computed stage at Hkamti station over a year	29
3.8	Percentage efficiency of computed stage at Homalin station over a year	29
3.9	Percentage efficiency of computed stage at Mawalaik station over a year	30
3.10	Percentage efficiency of computed stage at Kalewa station over a year	30
3.11	Percentage efficiency of computed stage at Monywa station over a year	31
3.12	Percentage efficiency of different stations	31

4.1	An element reach of channel for derivation of the Saint-Venant equations	
4.1a	Elevation view	44
4.1b	Plan view	44
4.1c	Cross section	44
4.2	Kinematic and dynamic waves in a short reach of channel as seen by a stationary observer	58
4.3	The grid The grid on the x-t plane used for numerical solution of the Saint-Venant equations by finite differences.	63
4.4	Finite difference box for solution of the linear kinematic wave equation showing the finite difference equations.	69
4.5	Flow chart for linear Kinematic wave computation.	73
4.6	Percentage efficiency of Kalewa station over a year for daily discharge prediction	74
4.7	Percentage efficiency of Monywa station over a year for daily discharge prediction.	75
4.8	Average Percentage efficiency of Monywa and Kalewa for daily discharge prediction	75
4.9	Percentage variation in computed discharge with observed discharges at Kalewa station over a year.	76
4.10	Percentage variation in computed discharge with observed discharges at Monywa station over a year.	76
4.11	Percentage efficiency of Kalewa station in different seasons for daily stage prediction	77
4.12	Percentage efficiency of Monywa station over a year for daily stage prediction	77
4.13	Average Percentage efficiency of Monywa and Kalewa for daily stage prediction.	78
4.14	Percentage variation in computed stage with observed stage at Kalewa station over a year.	78
4.15	Percentage variation in computed stage with observed stage at	79

CHAPTER- 1

INTRODUCTION

1.1 GENERAL

Flood is one of the natural disasters which occur in Myanmar every year. Floods in Myanmar generally occur during the southwest monsoon season (June to October), when the westerly depression system and the low latitude tropical cyclone system causes the rainstorm. Floods are generated by the random coincidence of several meteorological factors, but human activities in the river catchment also has an impact upon the severity and consequences of the events. A flood can be treated as a hazard if it poses threat to human life and their welfare. The risk of floods is treated as the probability of occurrence of the specific hazard.

With the economic growth, urbanization and successive concentration of population, more people who have never experienced a flood move to flood prone areas in many countries. The residents are conversely less aware of the threat of floods in those areas, where flood control facilities have been improved and the frequency and magnitude of inundation are decreased. In such cases, they are hardly prepared for floods and by no means assured of proper actions to take, and accordingly serious damage may be suffered once a flood occurs.

It is time and money consuming to thoroughly construct structural flood control facilities to lower the risk of flood damage. It is advisable to enhance local residents' awareness of the importance of protection efforts, whereas the flood control facilities shall steadily be developed so that overall flood damage shall be mitigated. Flood warning assumes a critical role in minimizing flood losses.

Prediction of flood inundation is not straightforward since the flood inundation extent is highly dependent on topography and it changes with time (dynamic). When bankful flow depth is reached in a flood event, water ceases to be contained solely in the main river channel and water spills onto adjacent floodplains.

Propagation of flood waves in an open channel can be mathematically approximated by the Saint-Venant equations (dynamic wave) or by their simplifications including the kinematic wave, noninertia wave, gravity wave, and quasi-steady dynamic wave models. All of these wave approximations differ not only in the physical propagation mechanism, but also in the degree of complexity involved in computation.

The flow of water through the stream channels of a watershed is a distributed process because the flow rate, velocity, and depth vary in space & throughout the watershed. Estimates of the flow rate or water level at important locations in the channel system can be obtained using a distributed flow routing model. This type of model is based on partial differential equations (the Saint Venant equations for one-dimensional flow) that allow the flow rate and water level to be computed as functions of space and time, rather than of time alone as in the lumped models.

1.2 WORK DONE SO FAR

Chindwin River has already being done. Work has been completed in period July, 2004 to June, 2005. In this work of Htay Htay Than the following aspects were covered:

- (i) Preliminary statistical analysis of Hydrometeorological Data
- (ii) Estimation of flood quantiles for different return period using L-moments
- (iii) Prediction of the daily water level using ANN for 1 day in advance
- (iv) Development of Digital Elevation Model (DEM)

She had used HEC-RAS for hydraulic modeling and HEC-GeoRAS for flood plain mapping on DEM prepared from 1: 63360 (1 inch = 1 mile) Topographical maps

1.3 OBJECTIVES OF THE STUDY

The present work extends the study of Chindwin river basin by the :

- development of stage discharge relationship for different stations of Chindwin river.
- development of Kinematic wave model for lower part of Chindwin basin.
- Testing and validation of the model developed.

CHAPTER- 2

STUDY AREA

2.1 STUDY AREA

Location: In the present study, flood plain mapping of lower part of Chindwin basin (Myanmar) has been attempted. Chindwin is the great tributary of Ayeyarwady river system. The other river systems of Myanmar are Thanlwin, Sittoung and Bago Rivers. The lengths of the main river are shown in Table (2.1). The Chindwin basin occupies almost the entire Northwestern part of Myanmar. It is situated between $22^{\circ} 06'$ and $26^{\circ} 45'$ N Latitude and between $94^{\circ} 30'$ and $96^{\circ} 45'$ E Longitude as shown in Fig (2.1).

Table (2.1) The length of Myanmar Rivers

River	Length(km)
Ayeyarwady	1786
Chindwin	901
Thanlwin	1223
Sittoung	407

The length of Chindwin River is 901 km and this river rises from the Kachin plateau. Saramali which is the second highest mountain in Myanmar is also located on the upper Chindwin catchment area. Since it passes through the mountainous region numerous streams, flow into the Chindwin River. The important tributaries of Chindwin River are U Yu and Myitha, where U Yu flows into Chindwin near Homalin and Myittha near Kalewa respectively. Hkamti, Homalin, Mawlaik, Kalewa and Monywa are main hydrometeorological stations of Chindwin Basin.

Topography: The Chindwin River in its upper reaches is known as the Tanai Hka, and originates near the Ayeyarwady watershed in the Kachin hills in Lat 25⁰ 40' N and Long 97⁰ E to enters the southeast corner of the Hukawng valley. In Hukawng valley, two important tributaries, the Taran and Tawan Hka from the north, join it.

The Chindwin River near Homalin receives an important tributary on the left bank which is the U Yu River. On the right bank it is joined by the Yu and Myittha from which it receives the drainage of Chin Hills. Generally, the Basin of Chindwin River is a mountainous forested terrain with the only exception of its lowest southern part which is a vast plain. The highest mountains which are 10,000 feet and more are to be found to the west and north of the basin. In the East, the watershed passes a mountain chain of 3000 – 5000 feet high.

Climate: Myanmar has a longer period of rainy season than most other places in South and Southwest Asia. The Southwest monsoon season begins about last week of May and extends up to the middle of October. The lowest southern part of Chindwin basin lies in Subhumid region and receives less rainfall than other parts because of the subsidence of lower layer of air and rain shadowing effects. The Northern part of Chindwin basin experiences heavy rainfall due to the western disturbance, and tropical cyclone in the Bay of Bengal. Nearly 90 percent rainfall for Northern part of Chindwin basin and 75 percent rainfall for Southern part occur between June to October as shown in Table (2.2), which presents the monthly average rainfall at different stations based on data from 1972 to 2002.

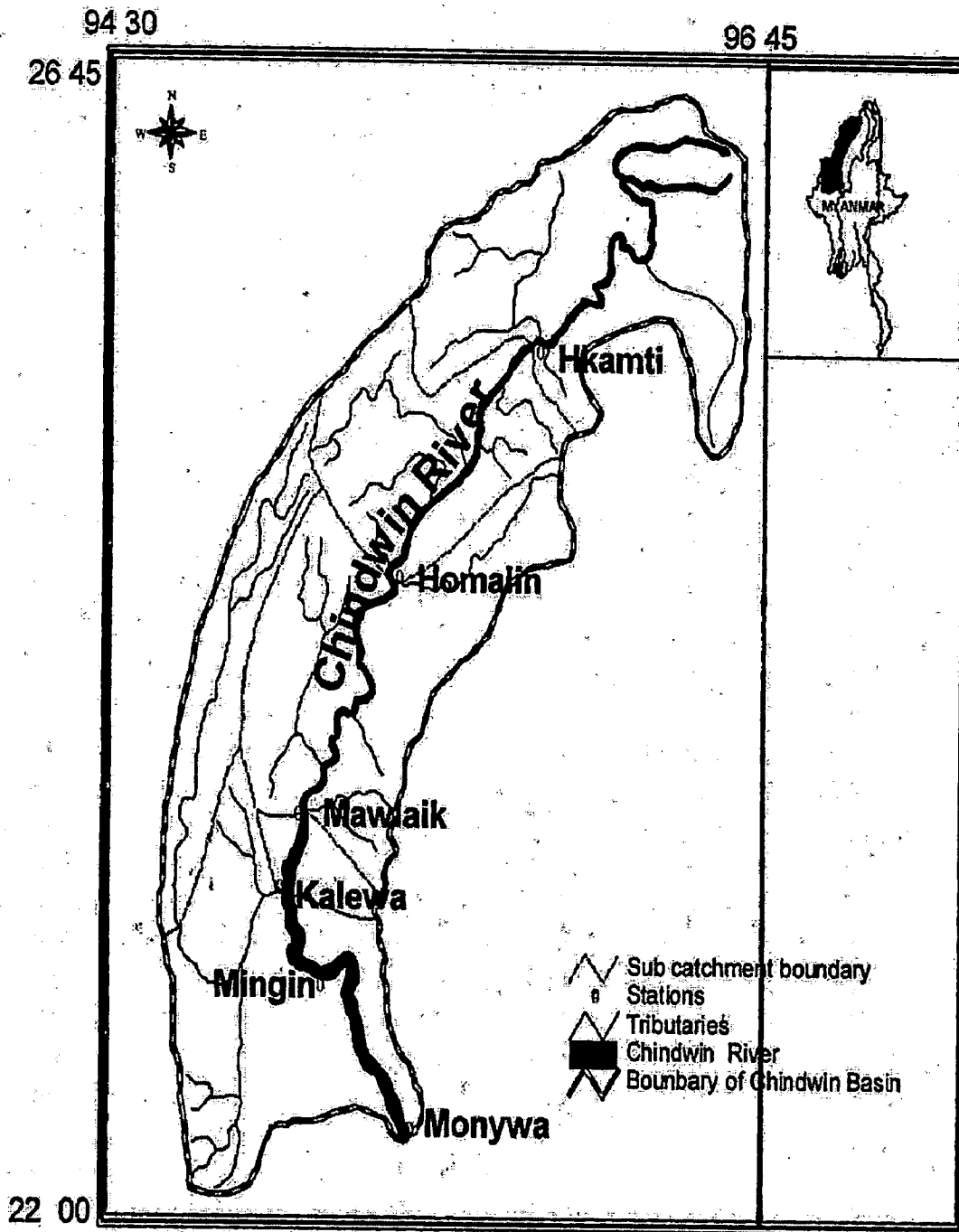


Fig (2.1) Map showing Chindwin basin

Table (2.2) Distribution of Monthly Mean Rainfall of Chindwin basin

Station	Record length(Yrs)	June - Sep (%)	June - Oct (%)
Hkamti	31	85	91
Homalin	31	79	87
Mawlaik	31	73	84
Kalewa	31	72	83
Mingin	17	68	81
Monywa	31	61	77

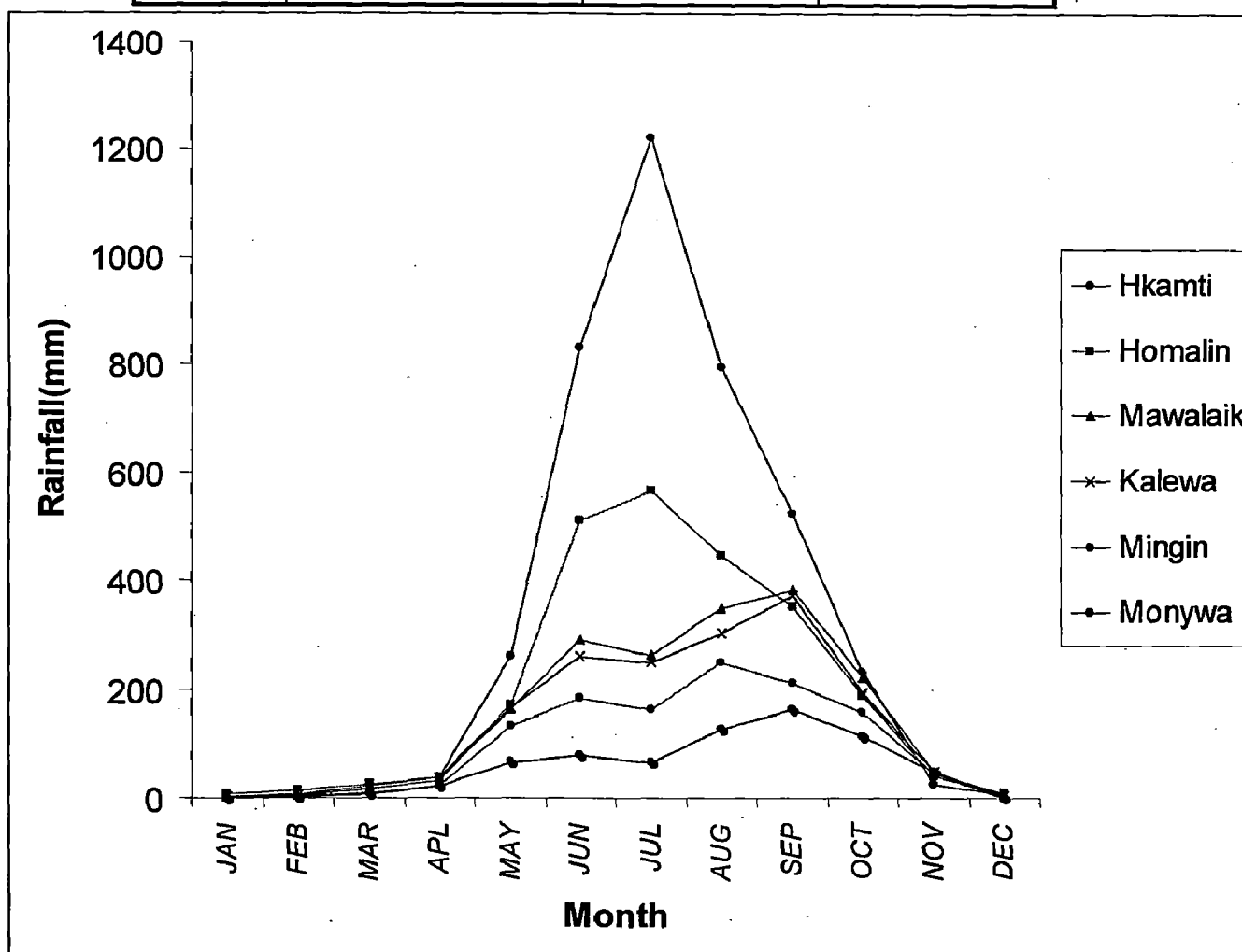


Fig (2.2) Monthly Average Rainfall of Chindwin Basin at different Sites

Floods in Chindwin Basin: Monthly average discharges (1972- 2002) at different sites of Chindwin river basin are shown in Fig (2.3). Information about history of floods (years of first highest, second highest and third highest year when water level have been above danger level etc) are tabulated in Table 2.3. Fig (2.4) shows the frequency of floods experienced in Chindwin basin during (1966-2000). It is quite evident that Chindwin basin is a highly flood prone basin.

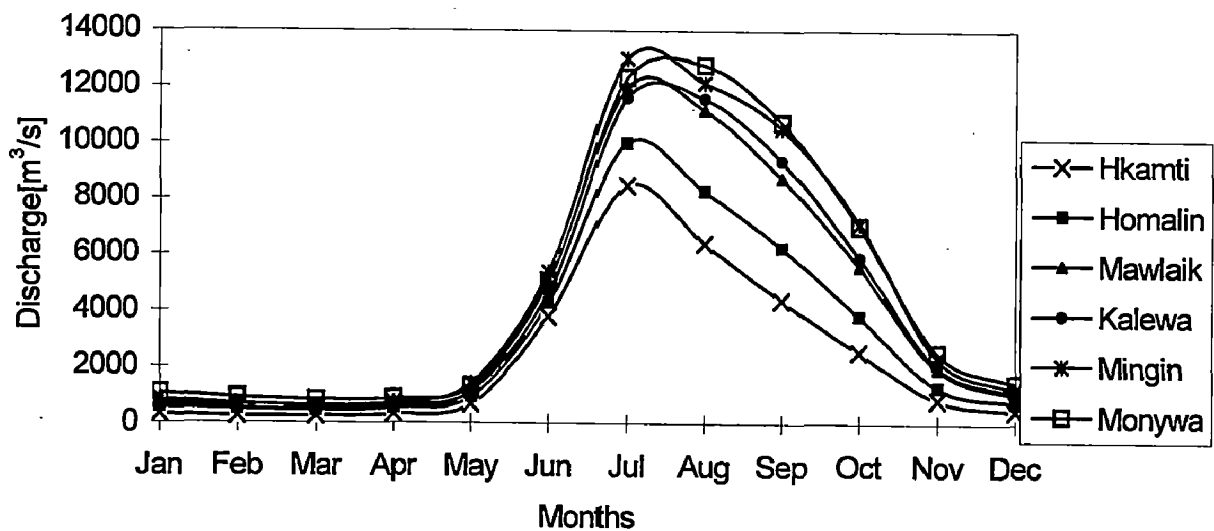


Fig (2.3) Mean Monthly Discharge of Chindwin River at Different Sites (1972-2002)

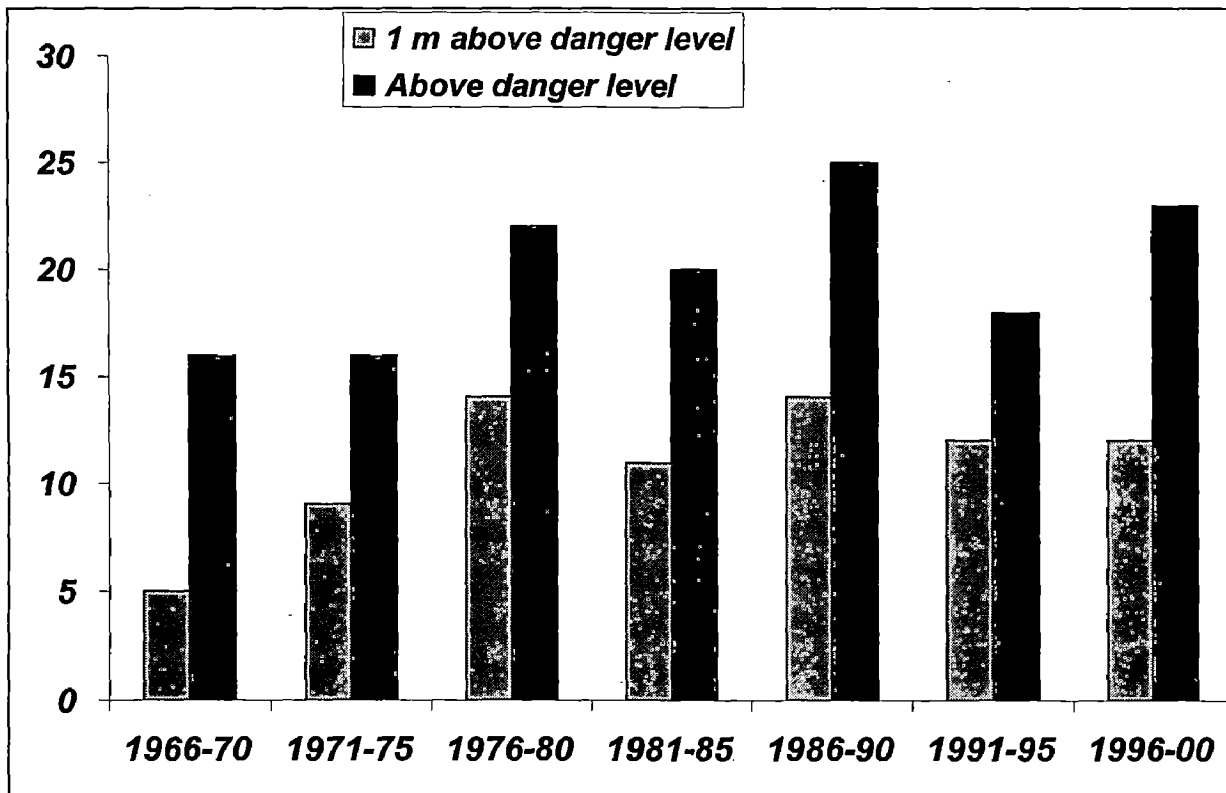


Fig (2.4) Flood frequency in Chindwin Basin (1966-2000)

2.2 HYDROLOGICAL, METEOROLOGICAL AND TOPOGRAPHIC

DATA USED

In the present study, Hydrological Division, Department of Meteorology and Hydrology (DMH), Myanmar has provided the required data. DMH has established 6 Hydrological and Meteorological stations such as Hkamti, Homalin, Mawlaik, Kalewa, Mingin and Monywa. Daily stages, annual peak flow, rainfall and topographic data from these stations were used for this study. The length of data varies from 17 to 31 years. Table 2.4 shows the summary of data availability. Annual peak flows of this study area are plotted in Fig (2.5).

Hydrometeorological data for entire reach of Chindwin river is obtained, but the Kinematic wave modelling is confined to lower reach only, due to paucity of time and unavailability of data.

Table (2.4) Summary of data availability in this study Daily stages, annual peak flow and Rainfall data:

No.	Stations	Lat. ⁰ N	Long ⁰ E	Catchment area (km ²)	Period of Record	Record Length (Years)
1.	Hkamti	26 ⁰ 00'	95 ⁰ 42'	27420	1972-2002	31
2.	Homalin	24 ⁰ 52'	94 ⁰ 55'	43124	1972-2002	31
3.	Mawlaik	23 ⁰ 38'	94 ⁰ 25'	69339	1972-2002	31
4.	Kalewa	23 ⁰ 12'	94 ⁰ 18'	72848	1972-2002	31
5.	Mingin	22 ⁰ 53'	94 ⁰ 30'	85283	1985-2001	17
6.	Monywa	22 ⁰ 06'	95 ⁰ 08'	110350	1972-2002	31

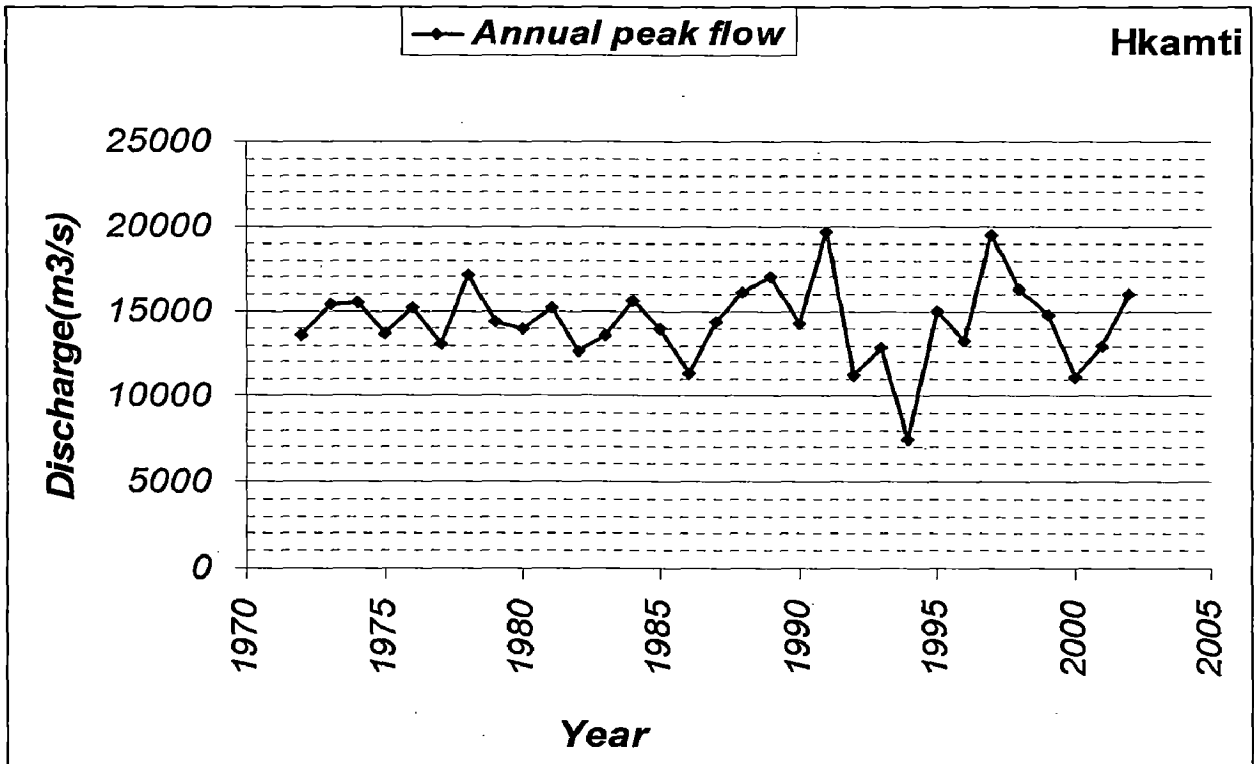


Fig (2.5a) Annual Peak Flow plot for Hkamti station.

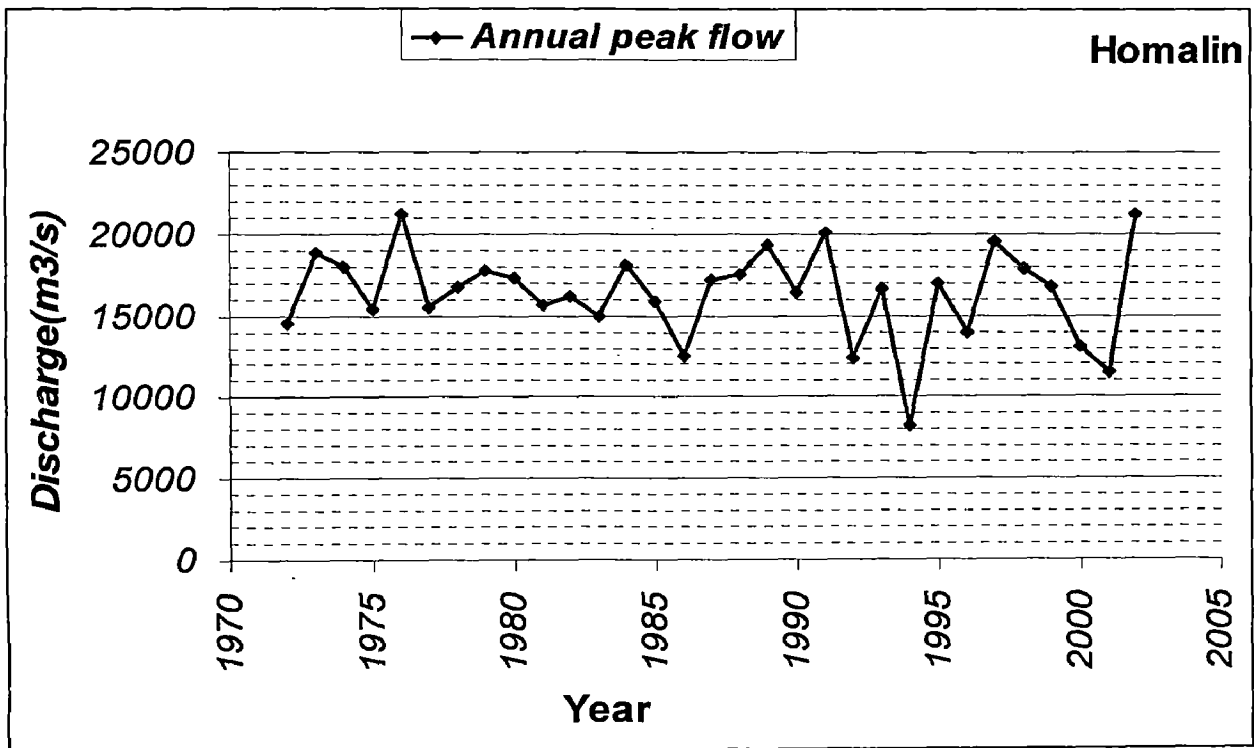


Fig (2.5b) Annual Peak Flow plot for Homalin station

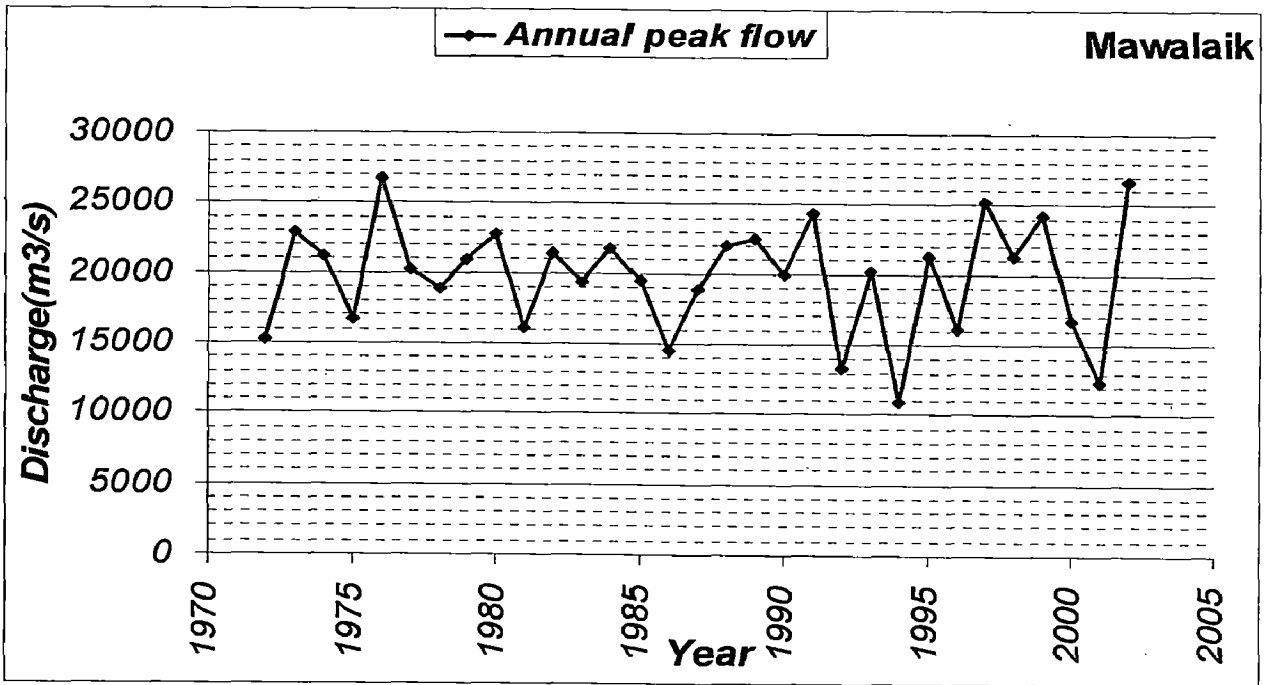


Fig (2.5c) Annual Peak Flow plot for Mawalaik station

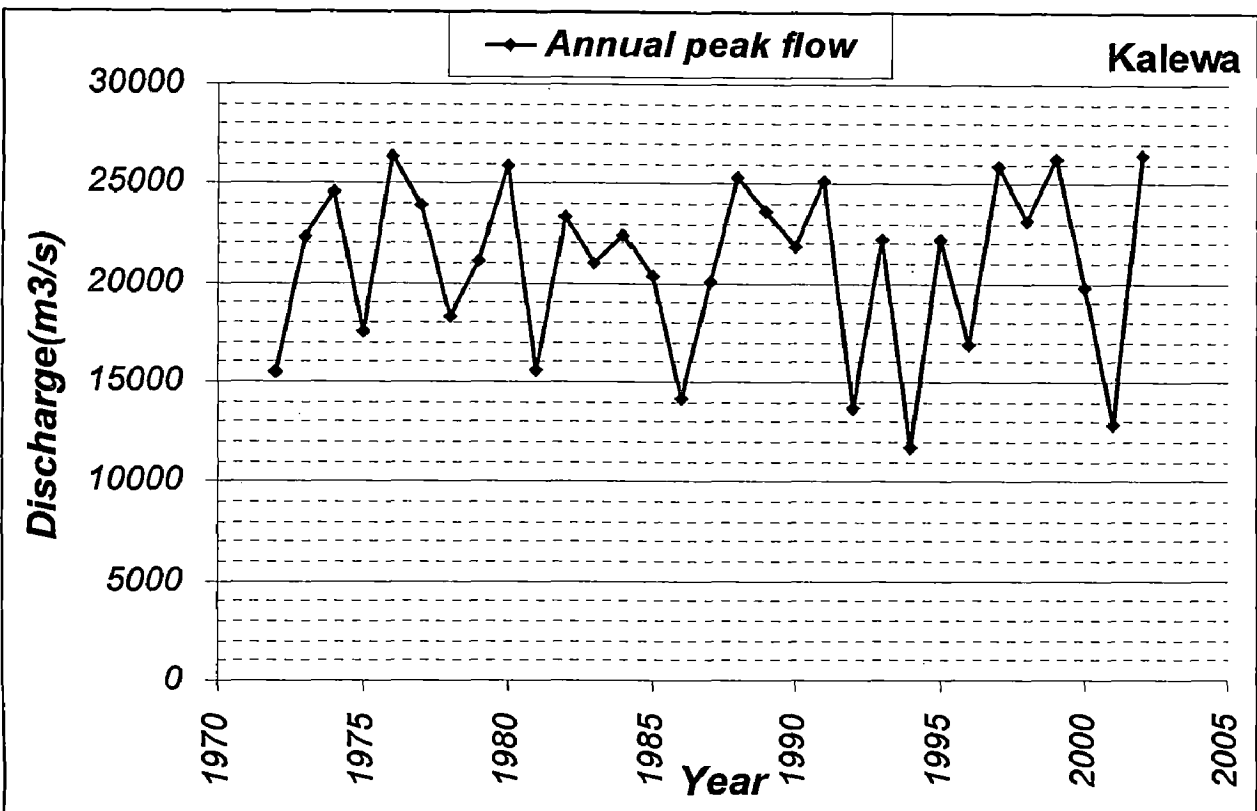


Fig (2.5d) Annual Peak Flow plot for Kalewa station

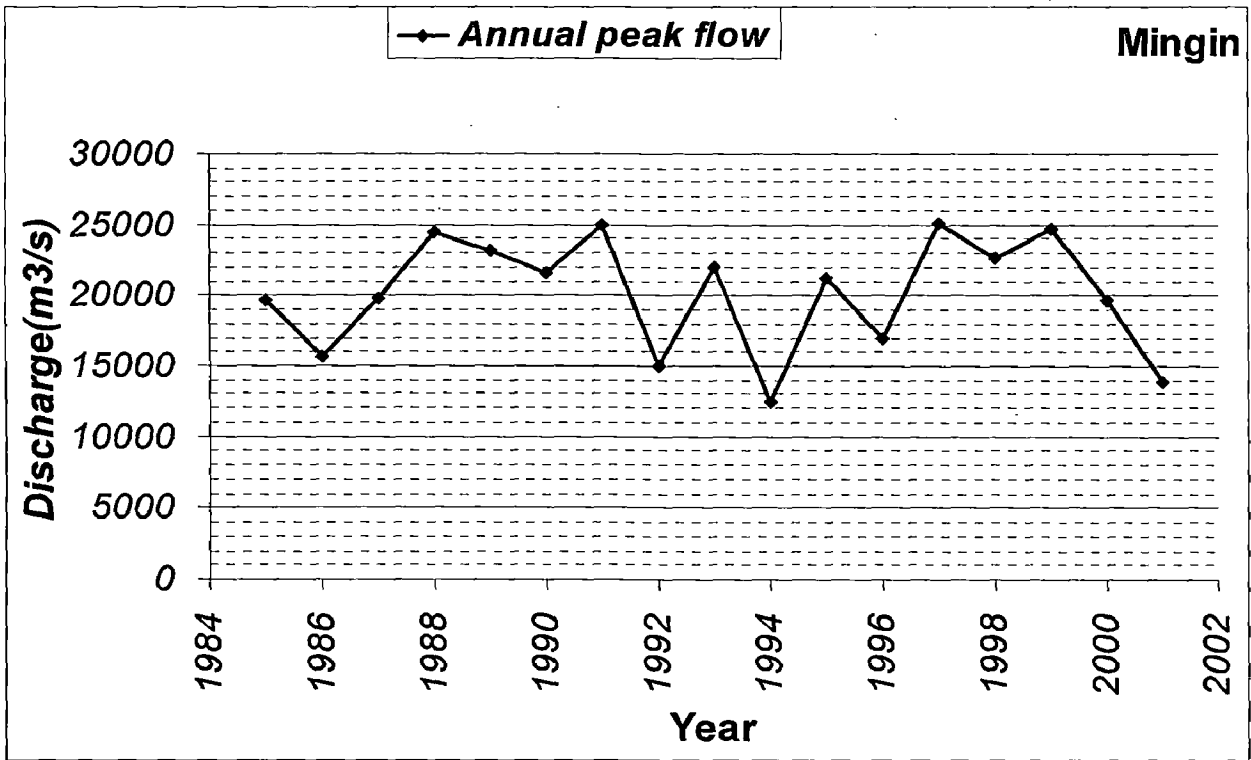


Fig (2.5e) Annual Peak Flow plot for Mingin station

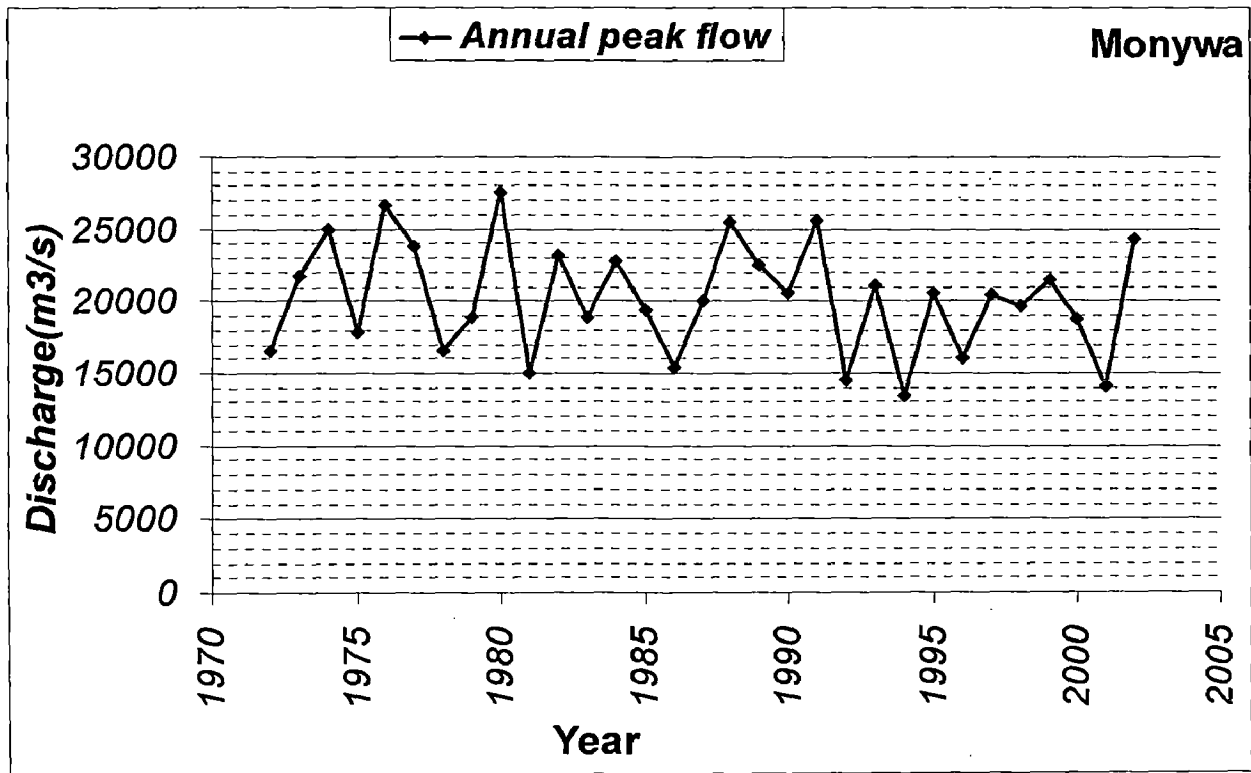


Fig (2.5f) Annual Peak Flow plot for Monywa station

DATA ANALYSES AND DEVELOPMENT OF RATING CURVES

3.1 PRELIMINARY ANALYSIS OF HYDROMETEOROLOGICAL DATA

The results of preliminary analysis of hydrometeorological data which has been already completed by Htay Htay Than and which has been recalculated are presented in section 3.1.1, Section 3.1.4, Section 3.1.5 deals with Long Term Persistence and Test of Outliers.

3.1.1 Statistical Parameters

Statistical parameters of original series as well as log transform series of annual peak flow data of six gauging stations are given in Table (3.1) and (3.2).

Table (3.1) Statistical Characteristics of original series of annual peak flow data

Stations	Hkamti	Homalin	Mawlaik	Kalewa	Mingin	Monywa
Max	19720	21250	26790	26460	25140	27550
Min	7448	8266	10910	11750	12360	13410
Mean	14401.87	16366.97	19803.23	20945.81	20154.12	20241.94
Std.dev	2412.65	2842.73	4011.46	4338.39	4094.36	3888.4
Skew	-0.27	-0.70	-0.39	-0.63	-0.55	0.01
Kurtosis	4.97	4.25	2.95	2.58	2.64	2.41
Cor.coeff(r_1)	-0.2	-0.201	-.308	-0.273	-0.106	-.298
(r_2)	0.101	0.169	0.088	0.043	0.24	0.063
(r_3)	-0.561	-0.35	-0.219	-0.139	-0.567	0.046

Table(3.2) Statistical Characteristics of log transformed series annual peak flow data

Stations	Hkamti	Homalin	Mawlaik	Kalewa	Mingin	Monywa
Max	9.89	9.96	10.2	10.18	10.13	10.22
Min	8.92	9.02	9.3	9.37	9.42	9.5
Mean	9.56	9.69	9.87	9.93	9.89	9.9
Std	0.18	0.19	0.22	0.23	0.22	0.2
Skew	-1.3	-1.46	-0.88	-0.96	-0.83	-0.32
Kurtosis	7.43	6.57	3.63	3.17	3.10	2.49
Cor. oeff(r_1)	-0.006	-0.167	-0.278	-0.267	-0.131	-0.307
(r_2)	0.131	0.206	0.135	0.082	0.265	0.092
(r_3)	-0.548	-0.352	-0.259	-0.173	-0.545	0.009

3.1.2 Randomness Analysis

The randomness of the data sets has been computed using Turning Point test and Anderson's Correlogram test (for r_1 only). The results are given in Table (3.3) and (3.4).

Table (3.3) Turning Point test results

Stations	Record length	Scores	$Z_{\text{calculated}}$	Z_{critical}	Remarks
Hkamti	31	20	0.2927	1.96	Random
Homalin	31	20	0.2927	1.96	Random
Mawlaik	31	22	1.1707	1.96	Random
Kalewa	31	22	1.1707	1.96	Random
Mingin	17	12	1.2172	1.96	Random
Monywa	31	22	1.1707	1.96	Random

Table (3.4) Anderson's Correlogram test results

Stations	r_1	95 % confidence limits		Remarks
		Lower	Upper	
Hkamti	-0.02	-0.385	0.318	Random
Homalin	-0.20	-0.385	0.318	Random
Mawlaik	-0.31	-0.385	0.318	Random
Kalewa	-0.27	-0.385	0.318	Random
Mingin	-0.11	-0.537	0.412	Random
Monywa	-0.30	-0.385	0.318	Random

3.1.3 Trends Identification

Trend identification of the data sets has been computed using Kendall's rank correlation test, Mann Kendal test and Spearman Rho test. The results are given in Table (3.5) to (3.7).

Table (3.5) Kendal's rank correlation test results

Stations	Record Length	P	$Z_{\text{calculated}}$	Z_{critical}	Remarks
Hkamti	31	223	-0.32293	1.96	No Trend
Homalin	31	221	-0.39092	1.96	No Trend
Mawlaik	31	234	-0.05099	1.96	No Trend
Kalewa	31	235	0.08498	1.96	No Trend
Mingin	17	68	0	1.96	No Trend
Monywa	31	207	-0.89524	1.96	No Trend

Table (3.6) Mann Kendal test results

Stations	Record length	C_{ite}	S	$Var(s)$	$Z_{calculated}$	$Z_{critical}$	Remarks
Hkamti	31	36	-17	3459	-0.27205	1.96	<i>No Trend</i>
Homalin	31	0	-23	3461	-0.37396	1.96	<i>No Trend</i>
Mawlaik	31	36	5	3459	0.06801	1.96	<i>No Trend</i>
Kalewa	31	0	5	3461	0.06799	1.96	<i>No Trend</i>
Mingin	17	18	1	588	0.0	1.96	<i>No Trend</i>
Monywa	31	18	-54	3460	-0.90103	1.96	<i>No Trend</i>

Table (3.7) Spearman's Rho test of annual peak flow series for all stations

Stations	Record length	$[R(x_i)-I]^2$	D	$Z_{calculated}$	$Z_{critical}$	Remarks
Hkamti	31	5222	-0.05282	-0.28932	1.96	<i>No Trend</i>
Homalin	31	5374	-0.08347	-0.45717	1.96	<i>No Trend</i>
Mawlaik	31	4916	0.00887	0.04859	1.96	<i>No Trend</i>
Kalewa	31	4898	0.0125	0.06847	1.96	<i>No Trend</i>
Mingin	17	804	0.01471	0.05882	1.96	<i>No Trend</i>
Monywa	31	5832	-0.17581	-0.96293	1.96	<i>No Trend</i>

3.1.4 Long Term Persistence

Long-term dependence is measured by the magnitude of Hurst's coefficient. In this study the Hurst's coefficient is estimated by Hurst's K. The results are shown in Table (3.8).

Table (3.8) Long-term dependence Test results

Stations	Sample Size	R_n	R_n^*	K	r_1	Remark
Hkamti	31	12151.4	5.04	0.59	-0.02	<i>Independence</i>
Homalin	31	16593.7	5.84	0.64	-0.20	<i>Independence</i>
Mawlaik	31	17226.0	4.29	0.53	-0.31	<i>Independence</i>
Kalewa	31	18009.0	4.15	0.52	-0.27	<i>Independence</i>
Mingin	17	13453.5	3.29	0.56	-0.11	<i>Independence</i>
Monywa	31	22429.4	5.77	0.64	-0.30	<i>Independence</i>

From this analysis, the results showed that the time series are randomness and have no trend.

3.1.5 Test for Outliers

Testing the presence of low and high outliers has been computed by using Grubs and Beck (1972) test. The results are given in Table (3.9).

Table (3.9) Outlier test results

Stations	Sample Size	k_n	Computed $Q_H(m^3/s)$	Computed $Q_L(m^3/s)$	Observed $Q_H(m^3/s)$	Observed $Q_L(m^3/s)$	Remark
Hkamti	31	2.577	22558	8921	19720	7448	R
Homalin	31	2.577	26361	9901	21250	8266	R
Mawlaik	31	2.577	34095	10972	26790	10910	R
Kalewa	31	2.577	37150	11354	26370	11750	A
Mingin	17	2.309	32843	11843	25140	12360	A
Monywa	31	2.577	33370	11904	27550	13410	A

Where “A” is Accept “R” is Reject

Outlier test has been used to check for any errors or inconsistencies in the data.

One low outlier value each in Hkamti, Homalin and Mawlaik stations for annual peak flow was found and these were in years 1998. This year was an El Nino year in Myanmar (Tun Lwin, Myanmar 1999). So we can comment that the outlier values were due to the natural causes.

3.2 DEVELOPMENT OF RATING CURVES

3.2.1 Introduction

The primary objective of a gauging station is to provide a record of the stage and discharge of a river. The water level and the volume of water passing a site of a river provides useful information about the flow, which can be used for many purpose in water resources planning and management. The water levels are easily measured in comparison to discharge even at very short intervals. The measurement of the discharge of a river by direct measurements is laborious and also costly. But the data of the discharge at shorter intervals are needed for unit hydrograph studies. This is achieved by computing the discharge using the data of water level observations. To enable such computation a

relationship between stage and discharge is established. Such relationships are known as the rating curves.

The relationship between stage and discharge is expressed in the following form:

$$Q = a (H - H_o)^b \quad (3.1)$$

Where

Q = stream discharge (m³/sce)

H = Gauge height (stage) (metre)

H_o = A constant which represent the gauge reading corresponding to zero discharge

a, b = Rating curve constants

The relationship given by Eq. (3.37) can be graphically expressed by plotting the observed stage against the corresponding values of discharge in arithmetic or logarithmic plot

3.2.2 Methods Of Development Of Rating Curves:

- (a) Data analysis
- (b) Physical analysis
- (c) Double log plot
- (d) Least Square method

3.2.2.1 Data Analysis:

The steps involved in developing the rating curve by this method are:

(i) Grouping the measured discharge and corresponding stage values for different years pertaining to the site under investigation.

(ii) Plotting the data with stages on the Y-axis and discharges on the X-axis.

(iii) Marking off the data points which are obviously away from general trend.

(iv) Being not misled however to remove peak discharge measurements since the deviation could be a possible physical mechanism.

3.2.2.2 Physical Analysis:

In physical analysis the cross section of the river reveals certain important information regarding the uniformity of rating curve. The following steps may be followed in physical analysis.

(i) Noting the elevation up to which the cross section is uniform.

(ii) Choosing the exponent b in the Eq. (3.1) as follows:

For rectangular shape : 1.6

For triangular shape : 2.5

For parabolic shape : 2.0

For irregular shape : 1.6 to 1.9

(iii) Taking the average bed level as the value for H_0 in Eq. (3.1).

(iv) Computing the value of the co-efficient a appeared in Eq (3.1) using the following relationship

$$a = \frac{1}{n} WS^{\frac{1}{2}} \quad (3.2a)$$

where

W is the top width of the channel,

S is the bed slope

n is manning coefficient

In Eq. (3.2) W and S would be known from the available cross section of the river at the gauging site and longitudinal section of the river. The value of n can be evaluated as follows:

For gravel bed river the empirical equation given by Strickler may be used. The equation is :

$$n = 0.034 d^{1/n} \quad (3.2b)$$

where d is median size of the bed material in mm.

Typical values of 'n' for natural rivers are: (Henderson (1966))

clean and straight river channel (0.025-- 0.03)

winding with pools and shoals (0.033 - 0.04)

very weedy, winding and overgrown (0.075—0.15)

3.2.2.3 Double Log Plot

The grouped data, obtained from step (i) of the data analysis are plotted on a double logarithmic paper. The advantage of using double logarithmic plot is two fold - Firstly, the plot would produce straight line, since general form of rating curve is parabolic. Secondly, different straight lines allow further grouping of data. A part of the entire range of stage may form a straight line. It gives an indication about the stage at which the slope line changes, if more than one straight lines are used for representing the rating curve. Use of different symbols for different periods (years) of data would enable one to identify the

uniform deviations, if any, present from the mean. In case of such deviations different rating curves should be developed for each year.

While plotting the data on double log plot a prior knowledge about the value of H_0 in Eq. (3.1) is necessary. As a first approximation the value of H_0 is assumed to be the level of the bottom of the channel as determined from the cross section of the gauging site. Marginal adjustment in the value of H_0 may be required in order, to produce a straight line giving better fit to the plotted points. In case if a single straight line could not be fitted inspite of trials with various values of H_0 , it should be concluded that the data need grouping for different relations and dealt accordingly as explained in the previous paragraph.

3.2.2.4 Least Square Method

The best values of a and b in Eq. (3.1) for a given stage are obtained by the least square error method. Thus by taking logarithms of Eq (3.1).

$$\text{Log}_e Q = \log_e a + b \log_e (H - H_0) \quad (3.3)$$

Or

$$Y = \alpha + \beta X \quad (3.3a)$$

$$Y = \log_e Q \quad (3.3b)$$

$$X = \log_e (H - H_0) \quad (3.3c)$$

$$\alpha = \log_e a \quad (3.3d)$$

$$\beta = b \quad (3.3e)$$

For the best fit straight line on N observations of X and Y

$$\beta = \frac{N(\sum XY) - (\sum X)(\sum Y)}{N(\sum X^2) - (\sum X)^2} \quad (3.4)$$

$$\alpha = \frac{\sum Y - \beta(\sum X)}{N} \quad (3.5)$$

In the above it should be noted that H_0 is an unknown and its determination poses some difficulties. The following alternate methods are available for its determination:

Plotting Q versus H on an arithmetic graph paper and drawing a best fit curve. By extrapolating the curve by eye judgment finding H_0 as the value of H corresponding to $Q = 0$. Using this value of H_0 plotting Q versus $\log(H - H_0)$ and verifying whether data plots as a straight line. If not set another acceptable value of H_0 is selected which - gives a straight line plot of $\log Q$ versus $\log(H - H_0)$. In order to avoid the plotting for each trial value of H_0 , the least square method discussed and the value of a fitting parameter 'r' which may be computed using Eq. 3.6a are compared for each trial run. That value of H_0 is finally accepted which gives the fitting parameter closest to one

$$r = \sqrt{1 - \frac{F_1}{F_0}} \quad (3.6a)$$

Where

$$F_0 = \frac{\sum_{i=1}^N (Y_i - \bar{Y})^2}{(N-1)} \quad (3.6b)$$

$$F_1 = \frac{\sum_{i=1}^N \left(\hat{Y}_i - \bar{Y} \right)^2}{(N-2)} \quad (3.6c)$$

Y_i = logarithms of observed discharge values

\bar{Y} = Mean of the logarithms of observed discharge values

\hat{Y}_i = logarithms of computed discharge values obtained from Eq.

(3.3a)

(ii) A graphical method due to Running is as follows (Wisler and Brater (1959)).

The Q versus H data are plotted to arithmetic scale and smooth curve through plotted points are drawn. Three points A, B and C on the curve are selected such that their discharges are in geometric progression (Fig. 3.4) .i.e.

$$\frac{Q_A}{Q_B} = \frac{Q_B}{Q_C} \quad (3.7)$$

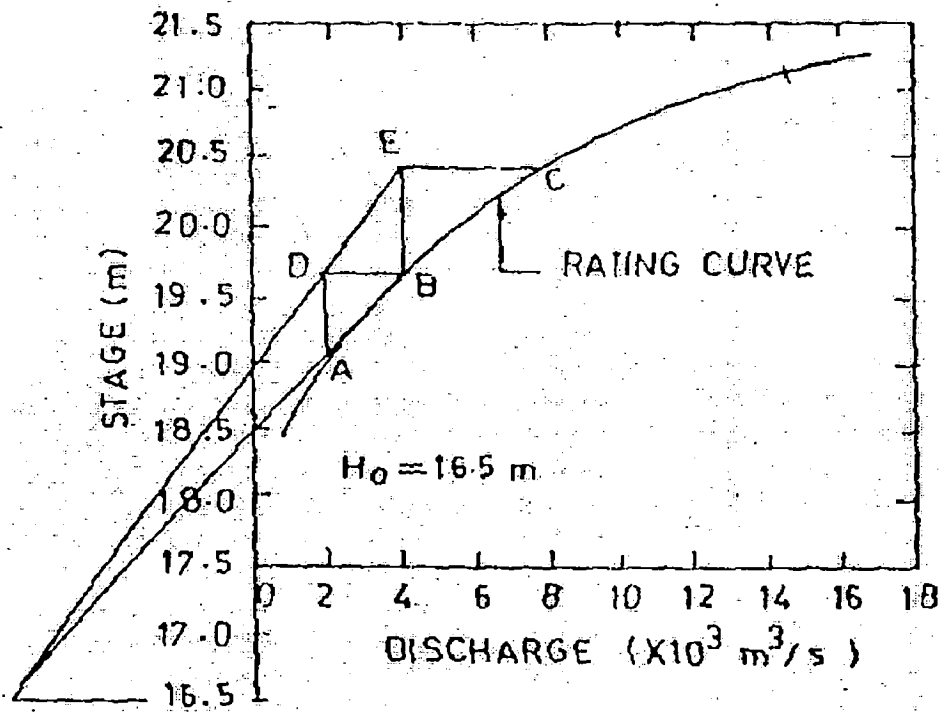


Fig 3.1: Running's Method for estimation of the constant H_0

At A and B vertical lines are drawn and then horizontal lines are drawn at B and C to get D and E as intersection point with the verticals. Two straight lines ED and BA are drawn intersect at F. The ordinate at F is the required value of H_0 , the gauge height corresponding to zero discharge. This method assumes the lower part of stage discharge curve to be a parabola.

- (i) Plotting Q versus H to an arithmetic scale and drawing a smooth good fitting curve by eye judgment. Selection of three discharges $Q_1, Q_2,$ and Q_3 such that $Q_1/Q_2 = Q_2/Q_3$ and noting from the curve the corresponding values of gauge reading H_1, H_2, H_3 from Eq. (3.39)

$$\frac{(H_1 - H_0)}{(H_2 - H_0)} = \frac{(H_2 - H_0)}{H_3 - H_0}$$

$$H_o = \frac{H_1 H_3 - H_2^2}{(H_1 + H_3) - 2H_2} \quad (3.8)$$

- (ii) A number optimization procedure that are based on the use of computers are available to estimate the best value of H_o . A trial and error search for H_o which gives the best value of the correlation co-efficient (fitting parameter 'r' as expressed by Eq (3.6) is one of them.

3.2.3 Arithmetic plot of stage data versus discharge data for all stations:

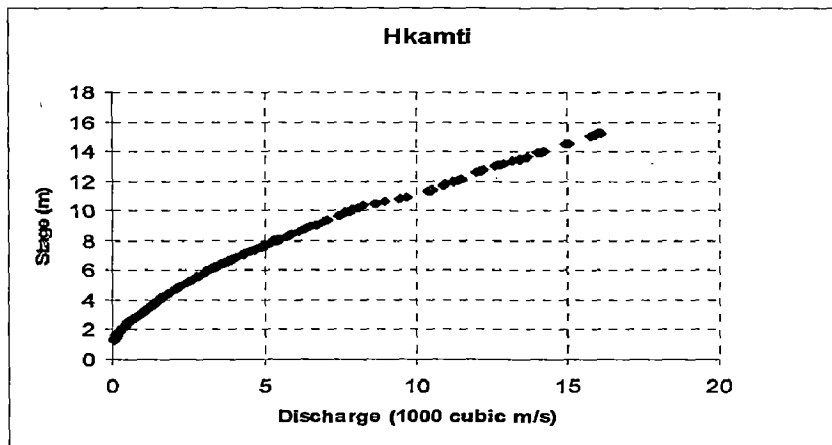


Fig 3.2: Plot of stage data versus discharge data at Hkamti station.

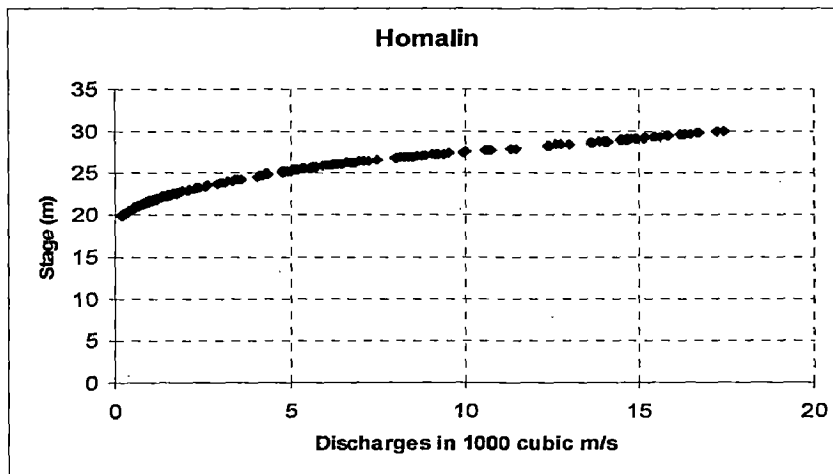


Fig 3.3: Plot of stage data versus discharge data at Homalin station.

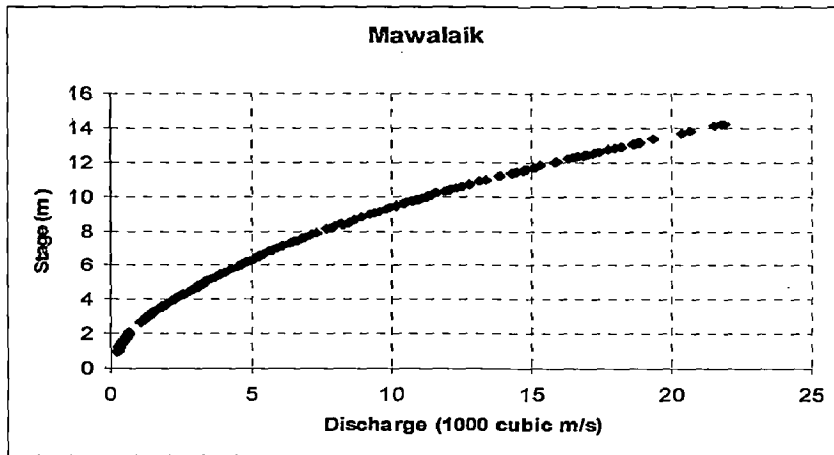


Fig 3.4: Plot of stage data versus discharge data at Mawalaik station.

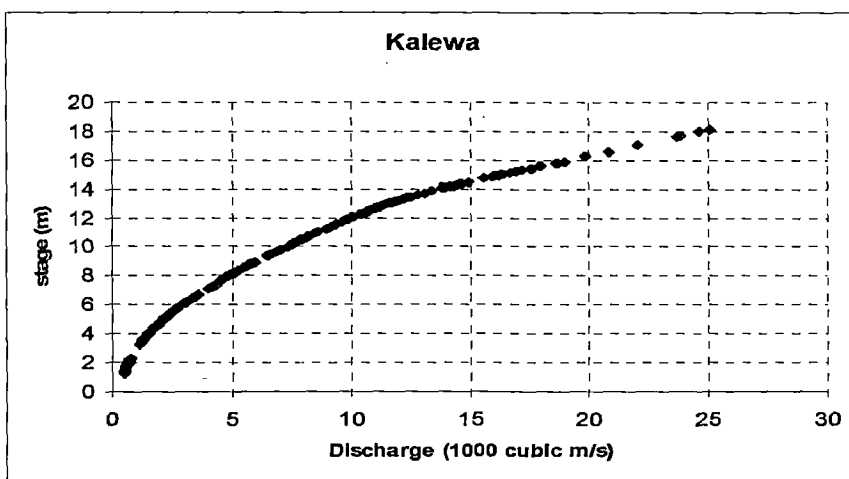


Fig 3.5: Plot of stage data versus discharge data at Kalewa station.

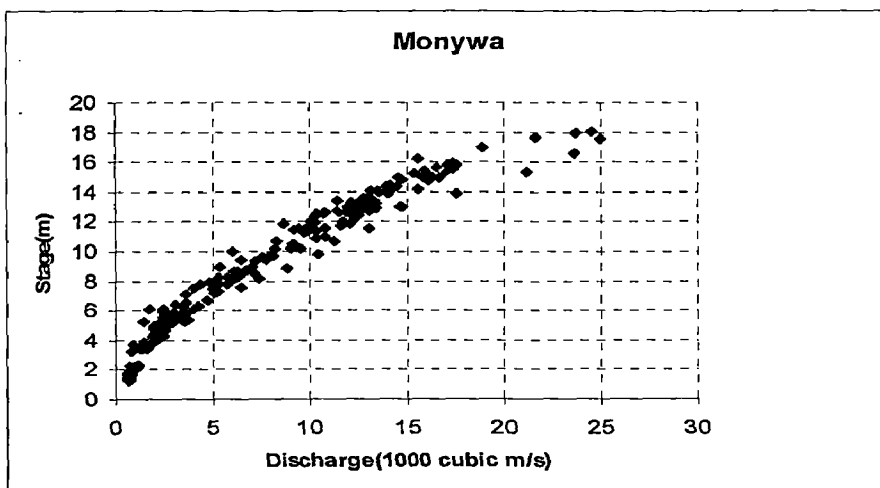


Fig 3.6: Plot of stage data versus discharge data at Monywa station.

3.3 STAGE-DISCHARGE RELATIONSHIP

The flood quantiles of different return periods can be converted into peak stage by developing the stage-discharge relationship. The relationships between discharge and stage have been developed for different stations as follow:

$$Q = 267.67(H - 1.50)^{1.51} \quad (\text{For Hkamti Station})$$

$$Q = 112.23(H - 19.0)^{2.11} \quad (\text{For Homalin Station})$$

$$Q = 242.60(H - 0.80)^{1.732} \quad (\text{For Mawlaik Station})$$

$$Q = 64.20(H - 0.70)^{2.08} \quad (\text{For Kalewa Station})$$

$$Q = 993.57(H - 0.90)^{1.307} \quad (\text{For Monywa Station})$$

Where H is the stage (m) and Q is the discharge (m³/s) of corresponding station. The zero discharge gauge values of Hkamti, Homalin, Mawlaik, Kalewa, and Monywa stations are 0.25 m, 19.0 m, 0.80 m, 0.70 m, and 0.90 m respectively.

3.3.1: Performance Of Stage-Discharge Relationship At Different Station For Different Seasons

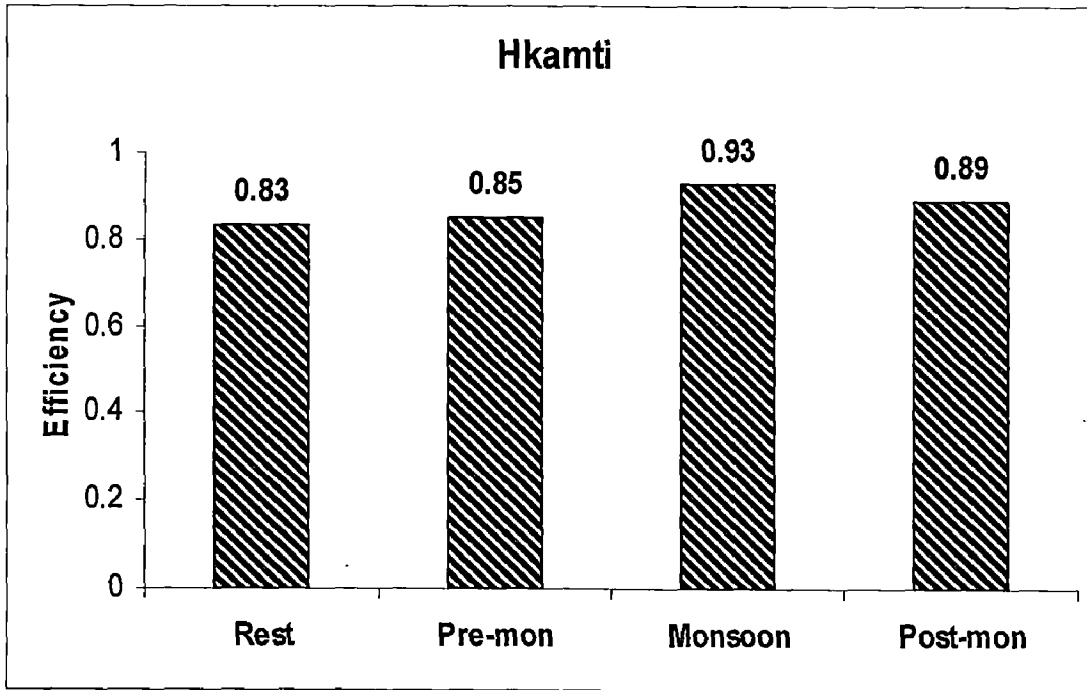


Fig (3.7): Efficiency of computed stage at Hkamti station over a year

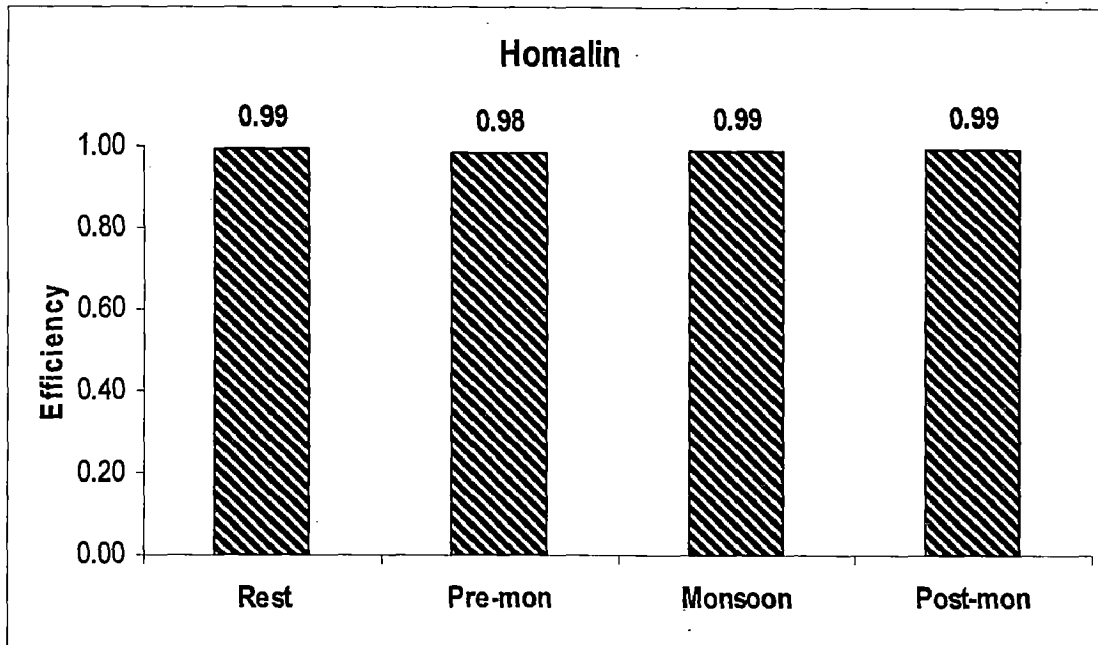


Fig (3.8): Efficiency of computed stage at Homalin station over a year

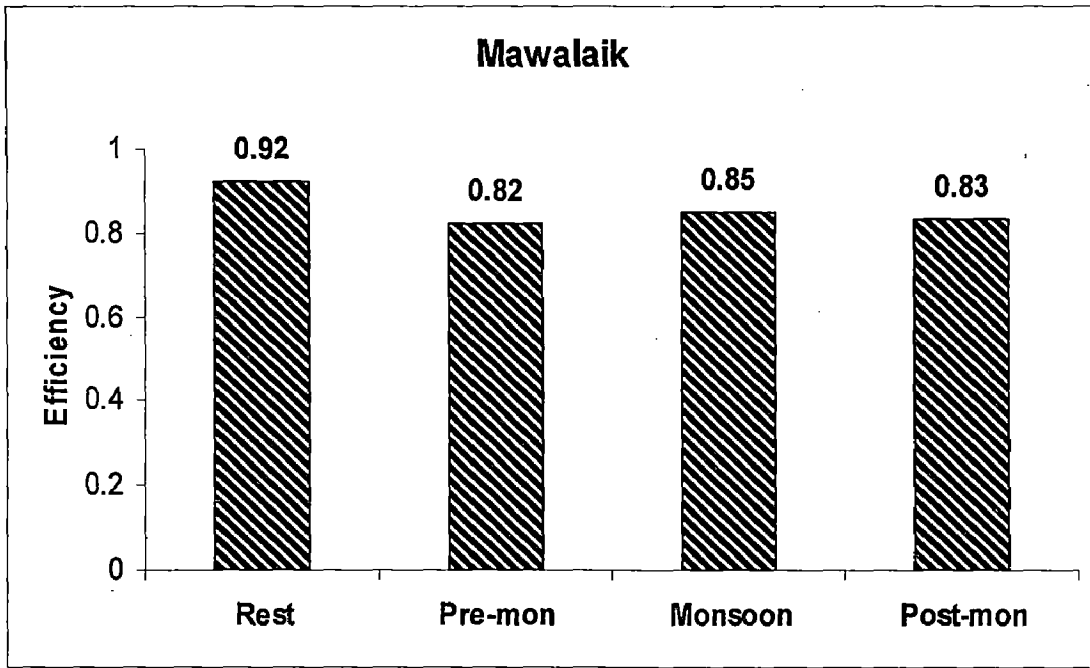


Fig (3.9): Percentage Efficiency of computed stage at Mawalaik station over a year

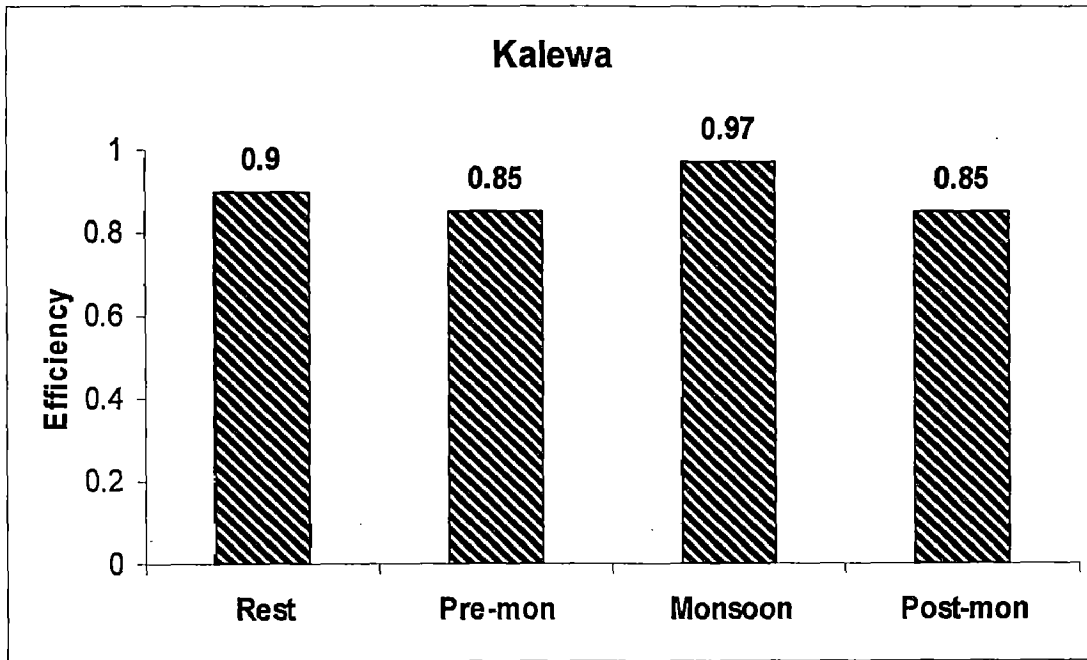


Fig (3.10): Percentage Efficiency of computed stage at Kalewa station over a year

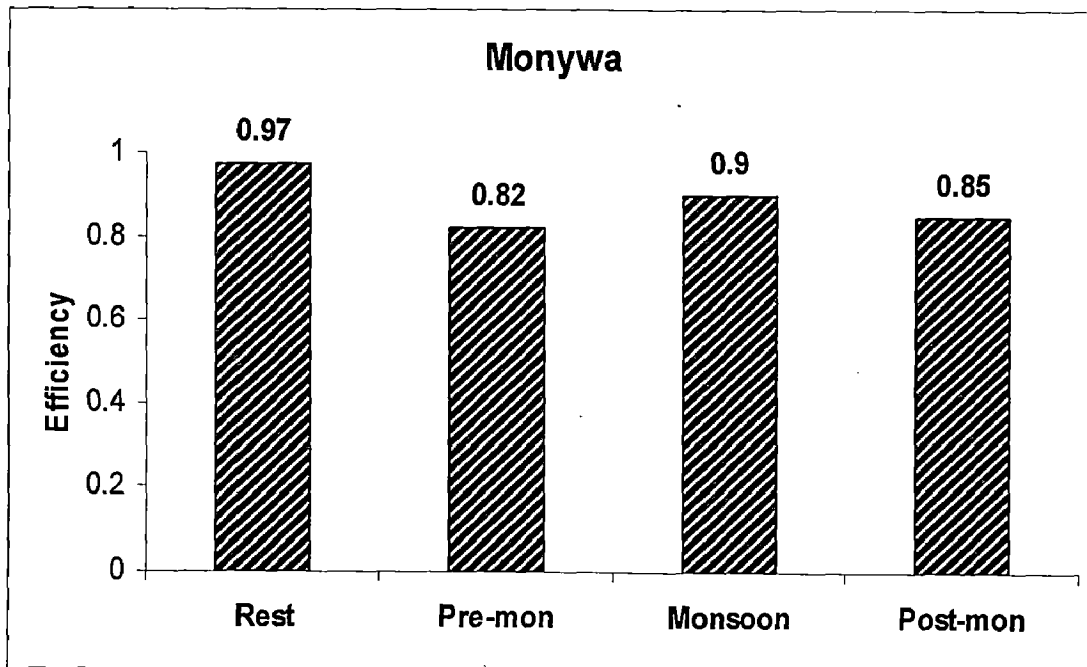


Fig (3.11): Efficiency of computed stage at Monywa station over a year

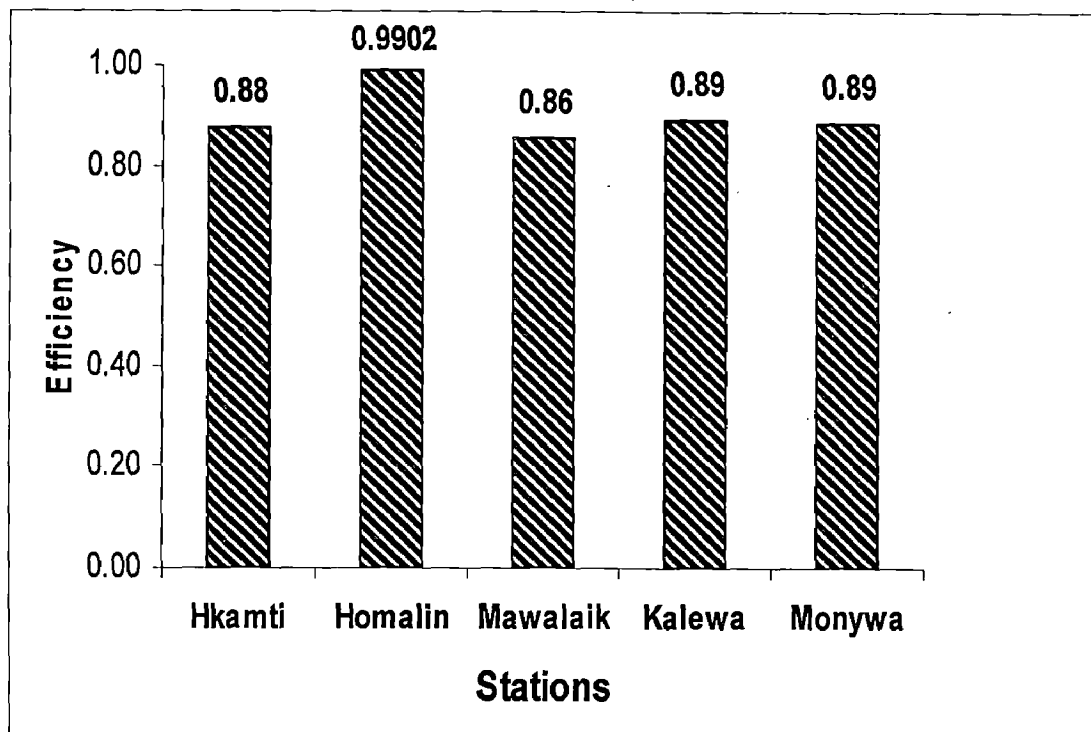


Fig (3.12): Efficiency of different stations

3.3.2 Summary Of Stage-Discharge Relationship At Different Station For Different Seasons

Table (3.10a) Summary of Hkamti station for rest and pre-monsoon

Rest			Pre-monsoon		
Observed	Computed	Efficiency	Observed	Computed	Efficiency
2.11	1.8841911	0.8929816	1.32	1.0370537	0.7856467
2.1	1.8687812	0.8898958	1.31	1.0230909	0.7809854
2.09	1.8532961	0.8867445	1.32	1.0370537	0.7856467
2.08	1.8377343	0.8835261	1.31	1.0230909	0.7809854
2.07	1.8220944	0.8802388	1.31	1.0300882	0.7863269
2.06	1.8095251	0.8784102	1.4	1.1117211	0.7940865
2.05	1.7937404	0.8749953	1.43	1.1575551	0.8094791
2.04	1.777873	0.8715064	1.58	1.3944465	0.8825611
2.03	1.7619211	0.8679414	1.98	2.1817865	0.8980876
2.02	1.7523086	0.8674795	2.02	2.2730188	0.8747432
2.01	1.7362177	0.8637899	1.94	2.1107757	0.9119713
1.99	1.7102856	0.85944	1.8	1.8551485	0.969362
1.97	1.6775361	0.8515412	1.69	1.6398436	0.9703217
1.95	1.6510582	0.8466965	1.67	1.592631	0.9536713
1.92	1.6175973	0.8424986	1.59	1.4116063	0.8878027
1.9	1.5837134	0.8335334	1.5	1.2022374	0.8014916
1.87	1.5493847	0.8285479	1.46	1.1640061	0.7972645
1.85	1.514587	0.8186957	1.41	1.124941	0.7978305
1.83	1.4863935	0.8122369	1.41	1.1183439	0.7931517
1.81	1.4578682	0.805452	1.68	1.6137172	0.960546
1.78	1.4217204	0.7987193	1.67	1.592631	0.9536713
1.76	1.3849947	0.7869288	1.56	1.3421569	0.860357
1.74	1.3551722	0.7788346	1.5	1.2148076	0.8098717
1.72	1.3249335	0.7703102	1.49	1.1959205	0.8026312
1.7	1.2981144	0.7635967	1.57	1.3713604	0.8734779
1.71	1.3173061	0.7703544	1.95	2.1286563	0.9083814
1.71	1.3096507	0.7658776	2.35	2.9148522	0.7596374
1.7	1.2942546	0.7613262	2.22	2.6702487	0.7971853
1.68	1.2670286	0.7541837	2.1	2.4205976	0.8473345
Average efficiency		0.829887	Average efficiency		0.849067

Table (3.10b) Summary of Hkamti station for monsoon and post monsoon

Monsoon			Post-monsoon		
Observed	Computed	Efficiency	Observed	Computed	Efficiency
8.21	7.782076	0.947878	4.57	3.971398	0.869015
7.33	6.834877	0.932453	5.39	4.802825	0.891062
6.57	6.006322	0.914204	8.04	7.598939	0.945142
5.91	5.306243	0.897842	8.86	8.464485	0.95536
5.32	4.693656	0.882266	8.52	8.108042	0.951648
4.96	4.350316	0.87708	7.96	7.512795	0.943819
5.26	4.636811	0.881523	7.32	6.81973	0.931657
5	4.385178	0.877036	6.87	6.332995	0.921833
4.82	4.208099	0.87305	6.44	5.870732	0.911604
6.38	5.809016	0.910504	6.06	5.460938	0.901145
7.1	6.573922	0.925904	6.62	6.059902	0.915393
7.24	6.736098	0.9304	6.64	6.088106	0.916883
7.34	6.837715	0.931569	6.54	5.972833	0.913277
7.44	6.95355	0.934617	6.04	5.444934	0.901479
7.49	7.004082	0.935124	5.69	5.070662	0.891153
7.83	7.372597	0.941583	5.23	4.611166	0.881676
7.3	6.794128	0.930702	5	4.379178	0.875836
6.74	6.192264	0.918734	4.9	4.289852	0.87548
6.54	5.976897	0.913899	5.37	4.742087	0.88307
7.62	7.151766	0.938552	5.14	4.518436	0.879073
8.09	7.656083	0.946364	4.89	4.277704	0.874786
8.24	7.814729	0.948389	4.79	4.185988	0.873902
7.56	7.081378	0.93669	4.56	3.954924	0.867308
6.8	6.2559	0.919985	4.16	3.555533	0.854695
7.33	6.837715	0.93284	3.93	3.325502	0.846184
8.35	7.932389	0.949987	3.82	3.232712	0.84626
8.55	8.142587	0.952349	3.67	3.103749	0.845708
8.9	8.501634	0.95524	3.53	2.977678	0.843535
9.49	9.084115	0.95723	3.44	2.898485	0.842583
10.51	10.19055	0.969606	3.35	2.807348	0.838014
12.84	12.89827	0.995461	3.3	2.762701	0.837182
Average efficiency		0.928004	Average efficiency		0.8889

Table (3.11a) Summary of Homalin station for rest and pre-monsoon

Rest			Pre-monsoon		
Observed	Computed	Efficiency	Observed	Computed	Efficiency
21.4	21.536626	0.9936156	20.57	20.890052	0.9844408
21.38	21.524572	0.993238	20.6	20.914869	0.9847151
21.37	21.513972	0.9932629	20.59	20.904572	0.9847221
21.35	21.501798	0.99289	20.55	20.873304	0.9842674
21.34	21.497215	0.9926329	20.53	20.854262	0.9842054
21.33	21.489556	0.9925196	20.53	20.854262	0.9842054
21.31	21.474161	0.9922965	20.59	20.906636	0.9846218
21.3	21.46332	0.9923324	20.64	20.947413	0.985106
21.29	21.452426	0.9923708	20.59	20.906636	0.9846218
21.27	21.436769	0.9921594	20.54	20.866981	0.9840808
21.24	21.419417	0.9915529	20.5	20.83069	0.9838688
21.23	21.405116	0.9917515	20.48	20.813332	0.983724
21.21	21.392325	0.9914038	20.46	20.800192	0.9833728
21.2	21.38107	0.991459	20.45	20.791373	0.983307
21.19	21.376228	0.9912115	20.45	20.793582	0.9831989
21.18	21.364888	0.9912707	20.46	20.802389	0.9832654
21.26	21.43205	0.9919073	20.48	20.81115	0.9838306
21.25	21.424163	0.9918041	20.56	20.881699	0.9843532
21.24	21.413073	0.9918516	20.71	21.00491	0.98576
21.24	21.413073	0.9918516	20.78	21.054945	0.9867688
21.24	21.413073	0.9918516	20.71	21.00491	0.98576
21.23	21.405116	0.9917515	20.67	20.969441	0.9855132
21.21	21.389115	0.9915552	20.6	20.912814	0.9848148
21.09	21.290495	0.9904934	20.54	20.864868	0.9841837
21.08	21.285439	0.9902543	20.51	20.837152	0.9840492
21.08	21.285439	0.9902543	20.49	20.824202	0.9836895
21.11	21.307257	0.9906558	20.48	20.817689	0.9835113
21.13	21.330499	0.9905112	20.48	20.815512	0.9836176
21.14	21.335446	0.9907547	20.48	20.815512	0.9836176
21.13	21.327194	0.9906676	20.48	20.817689	0.9835113
21.4	21.536626	0.9936156	20.57	20.890052	0.9844408
Average efficiency		0.9917	Average efficiency		0.98429

Table (3.11b) Summary of Homalin station for monsoon and post monsoon

Monsoon			Post-monsoon		
Observed	Computed	Efficiency	Observed	Computed	Efficiency
26.34	26.07222	0.9898337	24.06	23.93934	0.994985
26.78	26.55557	0.9916195	24	23.88957	0.995399
26.31	26.02146	0.9890331	24.24	24.11516	0.99485
25.75	25.452317	0.9884395	26.47	26.28347	0.992953
24.99	24.784491	0.9917763	27.33	27.18091	0.994545
24.43	24.289169	0.9942353	27.25	27.08235	0.993848
24.24	24.111708	0.9947074	27.02	26.83356	0.9931
24.32	24.189073	0.9946165	26.63	26.37786	0.990532
24.21	24.08123	0.9946811	26.02	25.71506	0.988281
24.25	24.122742	0.9947522	25.76	25.46882	0.988696
25.07	24.851468	0.9912831	25.46	25.18216	0.989087
25.39	25.122578	0.9894674	25.51	25.22393	0.988786
25.48	25.198344	0.988946	25.74	25.45285	0.988844
25.95	25.647878	0.9883575	25.24	24.99394	0.990251
26.07	25.762309	0.9881975	24.82	24.63179	0.992417
26.19	25.891007	0.9885837	24.54	24.3833	0.993614
26.44	26.161634	0.9894718	24.28	24.15295	0.994767
26.3	26.011745	0.9890397	24.21	24.07914	0.994595
25.92	25.61789	0.9883445	24.19	24.06243	0.994726
25.65	25.364219	0.9888584	24.32	24.18568	0.994477
25.72	25.426671	0.9885953	24.33	24.19518	0.994459
26.34	26.054862	0.9891747	24.18	24.05195	0.994704
26.34	26.047616	0.9888996	23.95	23.84511	0.99562
25.94	25.640653	0.98846	23.67	23.60322	0.997179
25.44	25.165359	0.9892043	23.57	23.5273	0.998188
25.7	25.408436	0.9886551	23.41	23.39806	0.99949
26.29	25.997632	0.9888791	23.25	23.24755	0.999895
26.44	26.161634	0.9894718	23.11	23.11554	0.99976
26.74	26.509327	0.9913735	23	23.01945	0.999155
27.03	26.837858	0.9928915	22.94	22.95761	0.999232
27.28	27.123751	0.9942724	23.01	23.02125	0.999511
Average efficiency		0.990456	Average efficiency		0.994385

Table(3.12a) Summary of Mawalaik station for rest and pre-monsoon

Rest			Pre-monsoon		
Observed	Computed	Efficiency	Observed	Computed	Efficiency
2.2	2.2973606	0.9557452	1.28	1.4461554	0.8701911
2.2	2.2838977	0.9618647	1.28	1.4687408	0.8525463
2.17	2.2703475	0.9537569	1.27	1.4873479	0.8288599
2.14	2.2544259	0.9465299	1.32	1.5422388	0.8316373
2.14	2.244125	0.9513434	1.34	1.5638285	0.8329638
2.14	2.244125	0.9513434	1.32	1.5606178	0.8177138
2.14	2.2303088	0.9577996	1.3	1.5552452	0.8036575
2.13	2.2163971	0.959438	1.28	1.5433289	0.7942743
2.12	2.2023877	0.9611379	1.31	1.5400554	0.8243852
2.1	2.1882782	0.9579628	1.34	1.5134864	0.8705325
2.08	2.1752545	0.9542046	1.34	1.4804126	0.8952145
2.08	2.1609462	0.9610836	1.29	1.4722574	0.8587152
2.06	2.1609462	0.950997	1.24	1.4509564	0.8298739
2.04	2.1465303	0.9477793	1.22	1.448559	0.8126565
2.02	2.1465303	0.9373613	1.2	1.448559	0.7928675
2	2.135646	0.932177	1.2	1.4401184	0.7999014
2	2.1246984	0.9376508	1.18	1.4401184	0.7795607
1.98	2.1198122	0.9293878	1.18	1.4376922	0.7816168
1.96	2.1026081	0.9272408	1.16	1.4328201	0.7648103
1.94	2.1026081	0.9161814	1.16	1.4328201	0.7648103
1.92	2.1026081	0.9048916	1.16	1.4328201	0.7648103
1.9	2.0914627	0.8992302	1.31	1.4328201	0.9062442
1.88	2.0839943	0.8914924	1.34	1.4242291	0.9371424
1.86	2.0689642	0.8876537	1.34	1.4242291	0.9371424
1.84	2.0563418	0.8824229	1.33	1.4757611	0.8904052
1.82	2.0512676	0.8729299	1.32	1.5498454	0.8258747
1.8	2.0449043	0.8639421	1.3	1.6067887	0.7640087
1.78	2.0449043	0.8511774	1.28	1.6098682	0.7422904
1.76	2.0877323	0.8137885	1.26	1.5807929	0.7454024
1.76	2.1210349	0.7948665	1.23	1.5444178	0.7443758
2.2	2.2973606	0.9557452	1.28	1.4461554	0.8701911
Average efficiency		0.915904	Average efficiency		0.826177

Table(3.12b) Summary of Mawalaik station for monsoon and post monsoon

Monsoon			Post-monsoon		
Observed	Computed	Efficiency	Observed	Computed	Efficiency
7.69	6.3691985	0.8282443	6.28	9.406794	0.502103
9.43	6.6675261	0.7070547	6.34	10.14579	0.399718
9.79	7.2891726	0.7445529	6.31	10.42902	0.347224
9.55	6.3834925	0.6684285	7.36	10.61236	0.558104
8.91	7.4761512	0.8390742	8.85	9.843568	1.112268
8.15	6.4205046	0.787792	9.36	9.445681	1.009154
7.68	6.7974131	0.8850798	9.53	8.658147	0.908515
7.65	7.2260365	0.9445799	9.4	8.266265	0.87939
7.11	7.2591215	0.9790265	9.27	7.410826	0.799442
6.89	7.5408492	0.9055371	8.97	6.981659	0.778334
7.41	7.7950177	0.9480408	8.88	6.757532	0.760983
7.93	7.9318697	0.9997642	8.44	6.577144	0.779282
8.33	8.0842241	0.9704951	8.25	6.343608	0.768922
8.36	8.1313723	0.9726522	8.19	6.099756	0.744781
8.51	8.2094781	0.964686	8.15	5.930901	0.727718
8.97	8.2351249	0.9180741	7.57	5.853027	0.773187
9.4	8.3700961	0.8904358	7.54	5.760177	0.763949
9.65	8.183378	0.8480184	6.83	5.672684	0.830554
9.55	7.9864883	0.8362815	7.13	5.809993	0.814866
9.25	7.6476007	0.8267676	6.78	5.752566	0.848461
8.97	7.5624612	0.8430837	6.69	5.708909	0.85335
8.83	7.8532086	0.8893781	6.61	5.874447	0.888721
9.31	8.4136903	0.9037261	6.36	6.056079	0.952214
9.29	8.8963386	0.9576252	6.07	5.990075	0.986833
8.97	9.3572559	0.9568277	5.79	5.760177	0.994849
8.5	9.8225085	0.8444108	5.55	5.72422	1.031391
8.31	9.8909303	0.8097557	5.38	5.368743	0.997908
8.62	10.986346	0.725482	5.18	5.240732	1.011724
8.8	11.286447	0.7174492	5.02	5.153123	1.026518
9	11.627007	0.7081104	5.09	4.970341	0.976491
9.27	11.685446	0.7394341	5.25	4.901095	0.933542
Average efficiency		0.85667	Average efficiency		0.8309804

Table(3.13a) Summary of Kalewa station for rest and pre-monsoon

Rest			Pre-monsoon		
Observed	Computed	Efficiency	Observed	Computed	Efficiency
2.2637	2.64	0.857	2.3116	1.47	0.427
2.2637	2.64	0.857	1.687	1.46	0.845
2.2605	2.63	0.859	1.6852	1.45	0.838
2.2564	2.62	0.861	1.6887	1.47	0.851
2.2457	2.59	0.867	1.6887	1.47	0.851
2.2308	2.55	0.875	1.6895	1.48	0.858
2.2157	2.51	0.883	1.6895	1.48	0.858
2.2022	2.47	0.892	1.6895	1.48	0.858
2.2013	2.47	0.891	1.6887	1.47	0.851
2.197	2.46	0.893	1.687	1.46	0.845
2.2637	2.64	0.857	1.6887	1.47	0.851
2.1936	2.45	0.895	1.6938	1.51	0.878
2.1936	2.45	0.895	1.6947	1.51	0.878
2.1825	2.42	0.902	1.693	1.5	0.871
2.1712	2.39	0.908	1.6947	1.51	0.878
2.1668	2.38	0.91	1.6956	1.52	0.885
2.1633	2.37	0.913	1.6947	1.51	0.878
2.159	2.36	0.915	1.693	1.5	0.871
2.1554	2.35	0.917	1.6913	1.49	0.865
2.151	2.34	0.919	1.6895	1.48	0.858
2.1475	2.33	0.922	1.6878	1.46	0.844
2.1341	2.3	0.928	1.6852	1.45	0.838
2.1243	2.27	0.936	1.6835	1.44	0.831
2.1143	2.24	0.944	1.6818	1.43	0.824
2.1043	2.21	0.952	1.7754	1.41	0.741
2.1052	2.21	0.953	1.6765	1.4	0.802
2.1052	2.21	0.953	1.6826	1.43	0.823
2.1052	2.21	0.953	1.715	1.65	0.961
2.0988	2.19	0.958	1.7184	1.67	0.971
2.0988	2.19	0.958	1.7184	1.67	0.971
2.1016	2.2	0.955	2.3116	1.47	0.427
Average efficiency		0.909	Average efficiency		0.847

Table(3.13b) Summary of Kalewa station for monsoon and post monsoon

Monsoon			Post-monsoon		
Observed	Computed	Efficiency	Observed	Computed	Efficiency
8.5717	7.87	0.911	7.0115	7.97	0.88
8.5499	7.85	0.911	6.997	7.95	0.88
9.2859	8.67	0.929	7.1357	8.14	0.877
9.7601	9.22	0.941	7.4099	8.53	0.869
9.8833	9.37	0.945	8.8476	10.68	0.828
9.8064	9.29	0.944	9.5309	11.77	0.81
10.111	9.63	0.95	9.6369	11.94	0.807
10.615	10.23	0.962	9.5882	11.86	0.808
10.809	10.47	0.968	9.4444	11.63	0.812
11.198	10.96	0.978	9.2072	11.25	0.818
11.486	11.31	0.984	9.3112	11.41	0.816
11.727	11.61	0.99	9.0283	10.97	0.823
12.018	11.99	0.998	8.7686	10.57	0.83
12.017	11.99	0.998	8.6947	10.45	0.832
12.084	12.07	0.999	8.8858	10.75	0.827
12.216	12.22	1	8.5101	10.16	0.838
12.427	12.47	0.997	8.2851	9.82	0.844
12.312	12.33	0.999	7.8479	9.19	0.854
11.975	11.93	0.996	8.1287	9.59	0.848
11.711	11.59	0.99	7.9334	9.31	0.852
11.475	11.3	0.985	7.5552	8.76	0.862
11.63	11.49	0.988	7.6434	8.9	0.859
12.168	12.16	0.999	7.3986	8.51	0.869
12.721	12.83	0.992	7.009	7.97	0.879
13.391	13.51	0.991	6.7297	7.48	0.9
14.086	14.15	0.995	6.5292	7.13	0.916
14.764	14.76	1	6.2367	6.8	0.917
15.711	15.58	0.992	6.1295	6.66	0.92
16.513	16.29	0.986	5.962	6.42	0.929
17.009	16.77	0.986	6.069	6.57	0.924
17.142	16.9	0.986	6.0487	6.54	0.925
Average efficiency		0.977	Average efficiency		0.859

Table(3.14a) Summary of Monywa station for rest and pre-monsoon

Rest			Pre-monsoon		
Observed	Computed	Efficiency	Observed	Computed	Efficiency
2.151	2.29	0.9395	1.701	1.43	0.8102
2.144	2.28	0.9401	1.697	1.42	0.8047
2.132	2.26	0.9433	1.688	1.41	0.8027
2.12	2.24	0.9466	1.682	1.4	0.7989
2.109	2.22	0.9499	1.686	1.41	0.8044
2.097	2.2	0.9532	1.724	1.46	0.8194
2.088	2.18	0.9576	1.76	1.53	0.8496
2.08	2.17	0.9583	1.711	1.55	0.896
2.07	2.15	0.9628	1.71	1.55	0.8969
2.07	2.15	0.9628	1.708	1.55	0.8979
2.064	2.14	0.9646	1.696	1.52	0.884
2.056	2.13	0.9653	1.681	1.49	0.8716
2.05	2.12	0.9671	1.663	1.46	0.8609
2.043	2.1	0.9728	1.649	1.44	0.8551
2.038	2.1	0.9707	1.639	1.42	0.846
2.029	2.08	0.9754	1.684	1.4	0.7971
2.023	2.07	0.9772	1.682	1.4	0.7989
2.023	2.07	0.9772	1.675	1.39	0.795
2.017	2.06	0.9791	1.668	1.38	0.7911
2.011	2.05	0.9809	1.662	1.37	0.7872
2.005	2.04	0.9828	1.662	1.37	0.7872
1.997	2.03	0.9836	1.668	1.38	0.7911
1.987	2.01	0.9885	1.666	1.38	0.7929
1.981	2	0.9905	1.662	1.37	0.7872
1.975	1.99	0.9924	1.655	1.36	0.7832
1.967	1.97	0.9987	1.641	1.34	0.7751
1.963	1.96	0.9985	1.641	1.34	0.7751
1.963	1.96	0.9985	1.668	1.38	0.7911
1.963	1.96	0.9985	1.721	1.46	0.8211
1.963	1.96	0.9985	1.767	1.54	0.8529
1.961	1.96	0.9993	1.701	1.43	0.8102
Average efficiency		0.9734	Average efficiency		0.8208

Table(3.14b) Summary of Monywa station for monsoon and post monsoon

Monsoon			Post-monsoon		
Observed	Computed	Efficiency	Observed	Computed	Efficiency
5.002	6.08	0.8228	4.938	6.03	0.819
4.647	5.71	0.8138	4.803	5.88	0.8168
4.607	5.67	0.8124	4.957	6.03	0.822
5.017	6.1	0.8225	5.341	6.4	0.8345
5.472	6.52	0.8393	5.476	6.52	0.8398
5.582	6.61	0.8445	6.382	7.32	0.8719
5.509	6.55	0.841	7.15	7.91	0.9039
5.666	6.69	0.8469	7.317	8.03	0.9113
6.084	7.06	0.8617	7.313	8.03	0.9107
6.302	7.25	0.8692	7.267	7.99	0.9095
6.571	7.49	0.8774	7.011	7.81	0.8976
6.907	7.73	0.8936	6.973	7.78	0.8962
7.165	7.92	0.9046	6.658	7.56	0.8807
7.456	8.14	0.916	6.375	7.32	0.8709
7.43	8.12	0.9151	6.437	7.38	0.8722
7.508	8.19	0.9167	6.559	7.49	0.8757
7.639	8.3	0.9203	6.287	7.24	0.8684
7.7	8.37	0.92	6.024	7	0.8606
7.662	8.33	0.9198	5.746	6.76	0.85
7.423	8.12	0.9142	5.685	6.7	0.8485
7.203	7.94	0.9071	5.658	6.68	0.8471
6.944	7.76	0.8949	5.449	6.5	0.8383
7.039	7.83	0.899	5.337	6.39	0.8352
7.472	8.16	0.9157	5.161	6.23	0.8284
7.954	8.55	0.9303	4.8	5.88	0.8163
8.501	8.91	0.9541	4.532	5.59	0.8108
9.059	9.29	0.9752	4.383	5.42	0.8088
9.306	9.46	0.9838	4.243	5.26	0.8066
9.813	9.78	0.9966	4.106	5.1	0.8051
10.22	10.05	0.9833	3.95	4.92	0.8028
10.39	10.19	0.9802	3.976	4.95	0.8032
Average efficiency		0.8977	Average efficiency		0.8504

CHAPTER-4

KINEMATIC WAVE THEORY

4.1 INTRODUCTION

Lighthill and Whitham developed the Kinematic Wave theory in 1955. Over a decade later, the theory started to receive wide acceptance. By the 1980s, the theory became an accepted tool for modeling not only surface runoff but also for subsurface flow, soil moisture movement, macropore flow, snowmelt runoff, and soil erosion. Many watershed models began incorporating the kinematic wave method for modeling overland flow. The decade of the 1990s witnessed applications of the theory to a variety of other hydrologic processes.

The true flow process varies in all three space dimensions; for example, the velocity in a river varies along the river, across it, and also from the water surface to the river bed. However, for many practical purposes, the spatial variation in velocity across the channel and with respect to the depth can be ignored, so that the flow process can be approximated as varying in only one space dimension—along the flow channel, or in the direction of flow. The Saint- Venant equations, first developed by Bane de Saint-Venant in 1871, describe one-dimensional unsteady open channel flow, which is applicable in this case.

4.2 SAINT-VENANT EQUATIONS

The following assumptions are necessary for derivation of the Saint-Venant equations:

1. The flow is one-dimensional; depth and velocity vary only in the longitudinal direction of the channel. This implies that the velocity is constant and the water surface is horizontal across any section perpendicular to the longitudinal axis

2. Flow is assumed to vary gradually along the channel so that hydrostatic pressure prevails and vertical accelerations can be neglected (Chow, 1959).

3. The longitudinal axis of the channel is approximated as a straight line.

4. The bottom slope of the channel is small and the channel bed is-fixed; that is, the effects of scour and deposition are negligible.

5. Resistance coefficients for steady uniform turbulent flow are applicable so that relationships such as Manning's equation can be used to describe resistance effects.

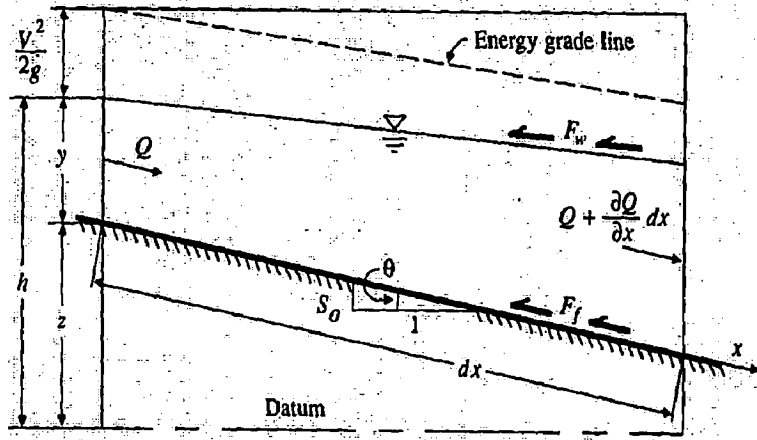
6. The fluid is incompressible and of constant density throughout the flow.

4.2.1 Continuity Equation

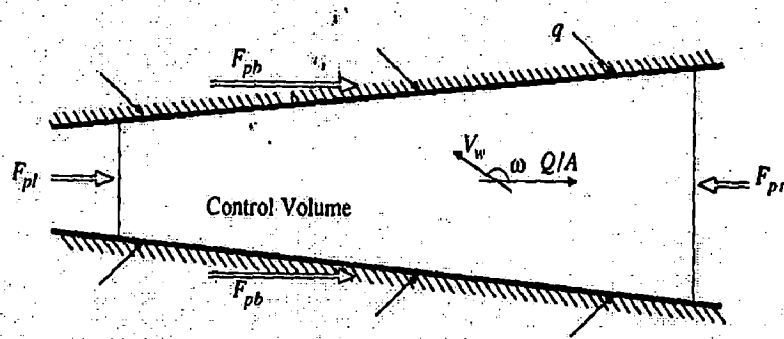
The continuity equation for an unsteady variable-density flow through a control volume can be written as:

$$0 = \frac{d}{dt} \iiint_{\text{c.v.}} \rho dv + \iint_{\text{c.s.}} \rho V \cdot dA \quad (4.1.1)$$

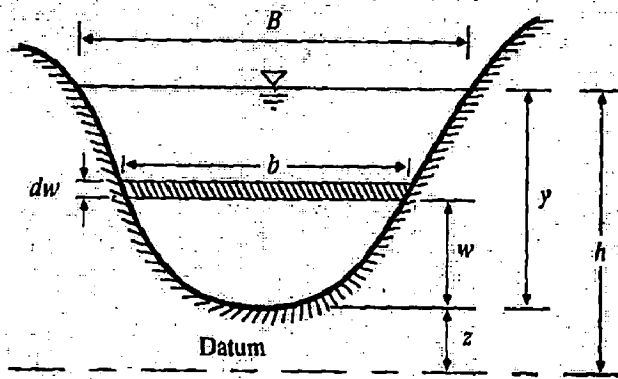
Consider an elemental control volume of length dx in a channel. Fig. 4.1.1 shows three views of the control volume: (a) an elevation view from the side, (b) a plan view from above, and (c) a channel cross section. The inflow to the control volume is the sum of the flow Q entering the control volume at the upstream end of the channel and the lateral inflow q entering the control volume as a distributed flow along the side of the channel. The dimensions of q are those of flow per unit length of channel so the rate of lateral inflow is qdx and the mass inflow rate is



(a) Elevation view.



(b) Plan view.



(c) Cross section.

Figure 4.1 An elemental reach of channel for derivation of the Saint-venant equations

$$\iint_{\text{inlet}} \rho V \cdot dA = -\rho(Q + qdx) \quad (4.1.2)$$

This is negative because inflows are considered to be negative in the Reynolds transport theorem. The mass outflow from the control volume is

$$\iint_{\text{outlet}} \rho V \cdot dA = \rho \left(Q + \frac{\partial Q}{\partial x} dx \right) \quad (4.1.3)$$

Where $\frac{\partial Q}{\partial x}$ is the rate of change of channel flow with distance. The volume of the channel element is $A dx$, where A is the average cross-sectional area, so the rate of change of mass stored within the control volume is

$$\frac{d}{dt} \iiint_{\text{c.v.}} \rho dv = \frac{\partial(\rho A dx)}{\partial t} \quad (4.1.4)$$

Where the partial derivative is used because the control volume is defined to be fixed in size (though the water level may vary within it). The net outflow of mass from the control volume is found by substituting Eqs. (4.1.2) to (4.1.4) into (4.1.1):

$$\frac{\partial(\rho A dx)}{\partial t} - \rho(Q + qdx) + \rho \left(Q + \frac{\partial Q}{\partial x} dx \right) = 0 \quad (4.1.5)$$

Assuming the fluid density ρ as constant, (4.1.5) is simplified by dividing through by ρdx and rearranging to produce the conservation form of the continuity equation,

$$\frac{\partial Q}{\partial x} + \frac{\partial A}{\partial t} - q = 0 \quad (4.1.6)$$

which is applicable at a channel cross section. This equation is valid for a prismatic or a nonprismatic channel; a prismatic channel one in which the cross-sectional shape does not vary along the channel and the bed slope is constant. For some methods of solving the Saint-Venant equations, the nonconservation form of the continuity equation is used, in which the average flow velocity V is a dependent variable, instead of Q . This form, of the continuity equation can be derived for a unit width of flow within the channel, neglecting lateral inflow, as follows, for a unit width of flow $A = y$, $x = 1 = y$ and $Q = VA = Vy$. Substituting into (4.1.6)

$$\frac{\partial(Vy)}{\partial x} + \frac{\partial y}{\partial t} = 0 \quad (4.1.7)$$

or

$$V \frac{\partial y}{\partial x} + y \frac{\partial V}{\partial x} + \frac{\partial y}{\partial t} = 0 \quad (4.1.8)$$

4.2.2 Momentum Equation

Newton's second law is written in the form of Reynold's transport theorem as:

$$\sum F = \frac{d}{dt} \underbrace{\iiint \rho dv}_{\text{c.v.}} + \underbrace{\iint \rho V \cdot dA}_{\text{c.s.}} \quad (4.1.9)$$

This states that the sum of the forces applied is equal to the rate of change of momentum stored within the control volume plus the net outflow of momentum across the control surface. This equation, in the form $\sum F = 0$, was applied to steady uniform flow in an open channel. Here, unsteady nonuniform flow is considered.

4.2 FORCES.

There are five forces acting on the control volume:

$$\sum F = F_g + F_f + F_e + F_w + F_p \quad (4.1.10)$$

where F_g is the gravity force along the channel due to the weight of the water in the control volume, F_f is the friction force along the bottom and sides of the control volume, F_e is the contraction/expansion force produced by abrupt changes in the channel cross section, F_w is the wind shear force on the water surface, and F_p is the unbalanced pressure force [Fir. 4.1.1(b)]. Each of these five forces is evaluated in the following paragraphs.

4.3.1 Gravity.

The volume of fluid in the control volume is $A dx$ and its weight is $\rho g A dx$. For a small angle of channel inclination θ , $S_0 \approx \sin \theta$ and the gravity force is given by

$$F_g = \rho g A dx \sin \theta \approx \rho g A dx S_0 \quad (4.1.11)$$

Where the channel bottom slope S_0 equals $-\frac{\partial z}{\partial x}$

4.3.2 Friction.

Frictional forces created by the shear stress along the bottom and sides of the control volume are given by $-\tau_0 P dx$ where τ_0 is the bed shear stress and P is the

wetted perimeter. From Eq. $\tau_0 = \gamma R S_f = \rho g (A/p) S_f$ hence the friction force is written as

$$F_f = \rho g A S_f dx \quad (4.1.12)$$

where the friction slope S_f is derived from resistance equations such as Manning's equation.

4.3.3 Contraction/Expansion.

Abrupt contraction or expansion of the channel causes energy loss through eddy motion. Such losses are similar to minor losses in pipe system. The magnitude of eddy losses is related to the change in velocity head $V^2/2g = (Q/A)^2/2g$ through the length of channel causing the losses. The drag forces creating these eddy losses are given by

$$F_e = -\rho g A S_e dx \quad (4.1.13)$$

where S_e is the eddy loss slope

$$S_e = \frac{K_e}{2g} \frac{\partial(Q/A)^2}{\partial x} \quad (4.1.14)$$

in which K_e is the nondimensional expansion or contraction coefficient, negative for channel expansion [$\frac{\partial(Q/A)^2}{\partial x}$ is negative] and positive for channel contraction.

4.3.4 Wind Shear.

The wind shear force is caused by frictional resistance of wind against the free surface of the water and is given by

$$F_w = \tau_w B dx \quad (4.1.15)$$

where τ_w is the wind shear stress. The shear of a boundary on a fluid may be written in general as

$$\tau_w = \frac{-\partial C_f |V_r| V_r}{2} \quad (4.1.16)$$

where V_r is the velocity of the fluid relative to the boundary, the notation $V_r|V_r$ is used so that τ_w will act opposite to the direction of V_r and C_f is a shear stress coefficient. As shown in Fig. 4.1.1(b), the average water velocity is Q/A , and the wind velocity is V_w in a direction at angle ω to the water velocity, so the velocity of the water relative to the air is

$$V_r = \frac{Q}{A} - V_w \cos \omega \quad (4.1.17)$$

The wind force is, from above,

$$\begin{aligned} F_w &= \frac{-\partial C_f |V_r| V_r B dx}{2} \\ &= -W_f B \rho dx \end{aligned} \quad (4.1.18)$$

where the wind shear factor W_f equals $C_f |V_r| V_r / 2$. Note that from this equation - the direction of the wind force will be opposite to the direction of the water flow.

4.3.5 Pressure.

Referring to Fig. 4.1.1(b) the unbalanced pressure force is the resultant of the hydrostatic force on the left side of the control volume, F_{pl} the hydrostatic force on the right side of the control volume, F_{pr} and the pressure force exerted by the banks on the control volume, F_{pb} .

$$F_p = F_{pl} - F_{pr} + F_{pb} \quad (4.1.19)$$

As shown in Fig. 4.1.1(c), an element of fluid of thickness d_w at elevation

w from the bottom of the channel is immersed at depth $y - w$, so the hydrostatic pressure on the element is $\rho g(y - w)$ and the hydrostatic force is $\rho g(y - w)b dw$. where b is the width of the element across the channel. Hence, the total hydrostatic

force on the left end of the control volume is

$$F_{pl} = \int' \rho g(y - w)b dw \quad (4.1.20)$$

The hydrostatic force on the right end of the control volume is

$$F_{pr} = (F_{pl} + \frac{\partial F_{pl}}{\partial x} dx) \quad (4.1.21)$$

where $\frac{\partial F_{pl}}{\partial x}$ is determined using the Leibnitz rule for differentiation of an integral

(Abramowitz and Stegun, 1972):

$$\begin{aligned} \frac{\partial F_{pl}}{\partial x} &= \int' \rho g \frac{\partial y}{\partial x} b dw + \int' \rho g(y - w) \frac{\partial b}{\partial x} dw \\ &= \rho g A \frac{\partial y}{\partial x} + \int' \rho g(y - w) \frac{\partial b}{\partial x} dw \end{aligned} \quad (4.1.22)$$

because $A = \int' b dw$. The force due to the banks is related to the rate of change in width of the channel, $\frac{\partial b}{\partial x}$, through the element dx as

$$F_{pb} = [\int' \rho g(y - w) \frac{\partial b}{\partial x} dw] dx \quad (4.1.23)$$

Substituting Eq. (4.1.21) into (4.1.19) gives



$$F_p = F_{pl} - \left(F_{pl} + \frac{\partial F_{pl}}{\partial x} dx \right) + F_{pb}$$

$$F_p = \frac{\partial F_{pl}}{\partial x} dx + F_{pb} \quad (4.1.24)$$

Now substituting Eqs. (4.1.22) and (4.1.23) into (4.1.24) and simplifying gives

$$F_p = -\rho g A \frac{\partial y}{\partial x} dx \quad (4.1.25)$$

The sum of the five forces in Eq. (4.1.10) can be expressed, after substituting (4.1.11) (4.1.12), (4.1.13), (4.1.18), and (4.1.25), as

$$\sum F = \rho g A dx S_o - \rho g A S_f dx - \rho g A S_e dx - W_f B \rho dx - \rho g A \frac{\partial y}{\partial x} dx \quad (4.1.26)$$

4.4 MOMENTUM.

The two momentum terms on the right-hand side of Eq. (4.1.9) represent the rate of change of storage of momentum in the control volume, and (the net outflow of momentum across the control surface, respectively.

4.4.1 Net Momentum Outflow.

The mass inflow rate to the control volume [Eq(4.1.2)] is $-\rho(Q + qdx)$, representing both stream inflow and lateral inflow. The corresponding momentum is computed by multiplying the two mass inflow rates by their respective velocities and a momentum correction factor β :

$$\iint_{\text{inlet}} \rho V \cdot dA = -\rho (\beta V Q + \beta v_x q dx) \quad (4.1.27)$$

inlet

where $\rho \beta VQ$ is the momentum entering from the upstream end of the channel, and $\rho \beta v_x q dx$ is the momentum entering the main channel with the lateral inflow, which has a velocity v_x in the x direction. The term β is known as the momentum coefficient or Boussinesq coefficient; it accounts for the nonuniform distribution of velocity at a channel cross section in computing the momentum. The value of β is given by

$$\beta = \frac{1}{V^2 A} \iint v^2 dA \quad (4.1.28)$$

where v is the velocity through a small element of area dA in the channel cross section. The value of β ranges from 1.01 for straight prismatic channels to 1.33 for river valleys with floodplains (Chow, 1959; Henderson, 1966).

The momentum leaving the control volume is

$$\iint_{\text{outlet}} \rho V \cdot dA = \rho \left(\beta VQ + \frac{\partial(\beta VQ)}{\partial x} dx \right) \quad (4.1.30)$$

outlet

The net outflow of momentum across the control surface is the sum of (4. 1.27) and (4.1.29):

$$\begin{aligned} \iint_{\text{c.s.}} \rho V \cdot dA &= -\rho (\beta VQ + \beta v_x q dx) + \rho \left(\beta VQ + \frac{\partial(\beta VQ)}{\partial x} dx \right) \\ &= -\rho \left[\beta v_x q - \frac{\partial(\beta VQ)}{\partial x} \right] dx \end{aligned} \quad (4.1.30)$$

4.4.2 Momentum Storage

The time rate of change of momentum stored in the control volume is found by using the fact that the volume of the elemental channel is $A dx$, so its momentum is $\rho A dx V$ or $\rho Q dx$, and then

$$\frac{d}{dt} \iiint V \rho dv = \rho \frac{\partial Q}{\partial t} dx \quad (4.1.31)$$

After substituting the force terms from (4.1.26) and the momentum terms from (4.1.30) and (4.1.31) into the momentum equation (4.1.9), it reads

$$\begin{aligned} \rho g A dx S_o - \rho g A S_f dx - \rho g A S_e dx - W_f B \rho dx - \rho g A \frac{\partial y}{\partial x} dx \\ = -\rho [\beta v_x q - \frac{\partial(\beta V Q)}{\partial x}] dx + \rho \frac{\partial Q}{\partial t} dx \end{aligned} \quad (4.1.32)$$

dividing through by ρdx , replacing V with Q/A , and rearranging produces the conservation form of the momentum equation:

$$\frac{\partial Q}{\partial t} + \frac{\partial(\beta Q^2 / A)}{\partial x} + g A \left(\frac{\partial y}{\partial x} - S_o + S_f + S_e \right) - \beta v_x q + W_f B = 0 \quad (4.1.33)$$

The depth y in Eq. (4.1.33) can be replaced by the water surface elevation h using [see Fig. 4.1.1(a)]:

$$h = y + z \quad (4.1.34)$$

Where z is the elevation of the channel bottom above a datum such as mean sea level. the derivative of Eq. (4.1.34) With respect to the longitudinal distance x along the channel is

$$\frac{\partial h}{\partial x} = \frac{\partial y}{\partial x} + \frac{\partial z}{\partial x} \quad (4.1.35)$$

$$\text{But } \frac{\partial z}{\partial x} = -S_o,$$

$$\frac{\partial h}{\partial x} = \frac{\partial y}{\partial x} - S_o, \quad (4.1.36)$$

The momentum equation can now be expressed in terms of h by using (4.1.36) in (4.1.33):

$$\frac{\partial Q}{\partial t} + \frac{\partial(\beta Q^2 / A)}{\partial x} + gA \left(\frac{\partial h}{\partial x} + S_f + S_e \right) - \beta v_x q + W_f B = 0 \quad (4.1.37)$$

The Saint-Venant equations, (4.1.6) for continuity and (4.1.37) for momentum, are the governing equations for One-dimensional unsteady flow in an open channel. The use of the terms S_f and S_e in (4.1.37), which represent the rate of energy loss as the flow passes through the channel, illustrates the close relationship between energy and momentum considerations in describing the flow. Strelkoff (1969) showed that the momentum equation for the Saint-Venant equations can also be derived from energy principles, rather than by using Newton's second law as Presented here.

The nonconservation form of the momentum equation can be derived in a similar manner to the nonconservation form of the continuity equation. Neglecting eddy losses, Wind shear effect, and lateral inflow, the nonconservation form of the momentum equation for a unit width in the flow is

$$\frac{\partial V}{\partial t} + V \frac{\partial V}{\partial x} + \left(\frac{\partial y}{\partial x} - S_o + S_f \right) = 0 \quad (4.1.38)$$

The Saint-Venant equations have various simplified forms, each defining a one-dimensional distributed routing model. Variations of Eqs. (4.1.6) and (4.1.37) in conservation and nonconservation forms, neglecting lateral inflow, wind shear, and eddy losses, are used to define various one-dimensional distributed routing models as shown in Table 4.2.1

The momentum equation consists of terms for the physical processes that govern the flow momentum. These terms are: the local acceleration term, which describes the change in momentum due to the change in velocity over time the convective acceleration term, which describes the change in momentum due to change in velocity along the channel, pressure force term, proportional to the change in the water depth along the channel, the gravity force term, proportional to the bed slope S_o and the friction force term, proportional to the friction slope S_f . The local and convective acceleration terms represent the effect of inertial forces on the flow.

Summary of the Saint-Venant equations

Continuity equation

Conservation form
$$\frac{\partial Q}{\partial x} + \frac{\partial A}{\partial t} = 0$$

Nonconservation form
$$V \frac{\partial y}{\partial x} + y \frac{\partial V}{\partial x} + \frac{\partial y}{\partial t} = 0$$

Momentum equation

Conservation form

$$\frac{1}{A} \frac{\partial Q}{\partial t} + \frac{1}{A} \frac{\partial}{\partial x} \left(\frac{Q^2}{A} \right) + g \frac{\partial y}{\partial x} - g(S_o - S_f) = 0$$

Local acceleration
term

Convective
acceleration term

Pressure force
term

Gravity
force term

Friction
force term

Nonconservation form(unit width element)

$$\frac{\partial V}{\partial t} + V \frac{\partial V}{\partial x} + g \frac{\partial y}{\partial x} - g(S_o - S_f) = 0$$

* Neglecting lateral inflow, wind shear, and eddy losses and assuming $\beta = 1$

When the water level or flow rate is changed at a particular point in a channel carrying a subcritical flow, the effects of these changes propagate back upstream. These backwater effects can be incorporated into distributed routing methods through the local acceleration, convective acceleration, and pressure terms. Lumped routing methods may not perform well in simulating the flow conditions when backwater effects are significant and the river slope is mild, because these methods have no hydraulic mechanisms to describe upstream propagation of changes in flow momentum.

As shown, alternative distributed flow routing models are produced by using the full continuity equation while eliminating some terms of the momentum equation. The simplest distributed model is the kinematic wave model, which neglects the local acceleration, convective acceleration, and pressure terms in the momentum equation; that is, it assumes $S_o = S_f$ and the friction and gravity forces balance each other. The diffusion wave model neglects the local and convective acceleration terms but incorporates the pressure term. The dynamic wave model considers all the acceleration and pressure terms in the momentum equation.

The momentum equation can also be written in forms that take into account whether the flow is steady or unsteady, and uniform or nonuniform, as shown in

Eqs(4.2.1). In the continuity equation, $\frac{\partial A}{\partial t} = 0$ for a steady flow, and the lateral inflow q is zero for a uniform flow.

Conservation form:

$$-\frac{1}{gA} \frac{\partial Q}{\partial t} - \frac{1}{gA} \frac{\partial(Q^2/A)}{\partial x} - \frac{\partial y}{\partial x} + S_o = S_f \quad (4.2.1a)$$

Non conservation form:

$$-\frac{1}{g} \frac{\partial V}{\partial t} - \frac{V}{g} \frac{\partial V}{\partial x} - \frac{\partial y}{\partial x} + S_o = S_f \quad (4.2.1b)$$

4.5 WAVE MOTION

Kinematic waves govern flow when inertial and pressure forces are not important. Dynamic waves govern flow when these forces are important, such as in the movement of a large flood wave in a wide river. In a kinematic wave, the gravity and friction forces are balanced, so the flow does not accelerate appreciably. Fig. 4.3.1 illustrates the difference between kinematic and dynamic wave motion within a differential element from the viewpoint of a stationary observer on the river bank

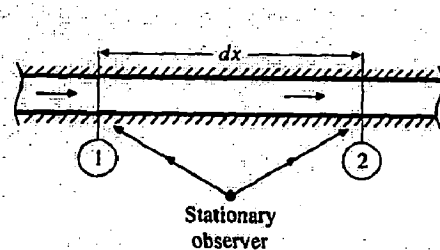




Figure 4.2 Kinematic and dynamic waves in a short reach of channel as seen by a stationary observer

For a kinematic wave, the energy grade line is parallel to the channel bottom and the flow is steady and uniform ($S_o = S_f$) within the differential length, while for a dynamic wave the energy grade line and water surface elevation are not parallel to the bed, even within a differential element.

4.5.1 Kinematic Wave Celerity

A wave is a variation in a flow, such as a change in flow rate or water surface elevation, and the wave celerity is the velocity with which this variation travels along the channel. The celerity depends on the type of wave being considered and may be quite different from the water velocity. For a kinematic wave the acceleration and pressure terms in the momentum equation are negligible, so the wave motion is described principally by the equation of continuity. The name kinematic is thus applicable, as kinematics refers to the study of motion exclusive of the influence of mass and force; in dynamics these quantities are included.

The kinematic wave model is defined by the following equations.

Continuity:

$$\frac{\partial Q}{\partial x} + \frac{\partial A}{\partial t} = q \quad (4.3.1)$$

Momentum:

$$S_o = S_f \quad (4.3.2)$$

The momentum equation can also be expressed in the form

$$A = \alpha Q^\beta \quad (4.3.3)$$

For example, Manning's equation written with $S_o = S_f$ and $R=A/P$ is

$$Q = \frac{1.49 S_o^{1/2}}{nP^{2/3}} A^{5/3} \quad (4.3.4)$$

This can be solved for A as

$$A = \left(\frac{nP^{2/3}}{1.49\sqrt{S_o}} \right)^{3/5} Q^{3/5} \quad (4.3.5)$$

$$\text{So } \alpha = \left(\frac{nP^{2/3}}{1.49\sqrt{S_o}} \right)^{3/5} \text{ and } \beta = 0.6 \text{ in this case}$$

Equation (4.3.1) contains two dependent variables, A and Q, but A can be eliminated by differentiating (4.3.3):

$$\frac{\partial A}{\partial t} = \alpha\beta Q^{\beta-1} \left(\frac{\partial Q}{\partial t} \right) \quad (4.3.6)$$

and substituting for and substituting for $\frac{\partial A}{\partial t}$ in (4.3.1) to give

$$\frac{\partial Q}{\partial x} + \alpha\beta Q^{\beta-1} \left(\frac{\partial Q}{\partial t} \right) = q \quad (4.3.7)$$

Kinematic waves result from changes in Q . An increment in flow, dQ , can be written as

$$dQ = \frac{\partial Q}{\partial x} dx + \frac{\partial Q}{\partial t} dt \quad (4.3.8)$$

Dividing through by dx and rearranging produces:

$$\frac{\partial Q}{\partial x} + \frac{dt}{dx} \frac{\partial Q}{\partial t} = \frac{dQ}{dx} \quad (4.3.9)$$

Equations (4.3.7) and (4.3.9) are identical if

$$\frac{dQ}{dx} = q \quad (4.3.10)$$

and

$$\frac{dx}{dt} = \frac{1}{\alpha\beta Q^{\beta-1}} \quad (4.3.11)$$

Differentiating Eq. (4.3.3) and rearranging gives

$$\frac{dQ}{dA} = \frac{1}{\alpha\beta Q^{\beta-1}} \quad (4.3.12)$$

and by comparing (4.3.11) and (4.3.12) it can be seen that

$$\frac{dx}{dt} = \frac{dQ}{dA} \quad (4.3.13)$$

$$C_k = \frac{dx}{dt} = \frac{dQ}{dA} \quad (4.3.14)$$

where C_k is the kinematic wave celerity. This implies that an observer moving at a velocity $dx/dt = C_k$ with the flow would see the flow rate increasing at a rate of dQ/dx

= q. If q = 0, the observer would see a constant discharge. Eqs. (4.3.10) and (4.3.14) are the characteristic equations for a kinematic wave, two ordinary differential equations that are mathematically equivalent to the governing continuity and momentum equations.

The kinematic wave celerity can also be expressed in terms of the depth y as

$$C_k = \frac{1}{B} \frac{dQ}{dy} \quad (4.3.15)$$

Where $dA = B dy$.

Both kinematic and dynamic wave motion are present in natural flood waves. In many cases the channel slope dominates in the momentum equation (4.2.1); Therefore, most of a flood wave moves as a kinematic wave. Lighthill and Whitham (1955) proved that the velocity of the main part of a natural flood wave approximates that of a kinematic wave. If the other momentum terms $[\partial V / \partial t, V(\partial V / \partial x), (1/g) \partial y / \partial x]$ are not negligible, then a dynamic wave front exists which can propagate both upstream and downstream from the main body of the flood wave. Lighthill and Whitham (1955) summarizes several criteria for determining when the kinematic wave approximation is applicable, but there is no single, universal criterion for making this decision.

As previously shown, if a wave is kinematic ($S_0 = S_f$) the kinematic wave celerity varies with dQ/dA . For Manning's equation, wave celerity increases as Q increases. As a result, the kinematic wave theoretically should advance downstream with its rising limb getting steeper. However, the wave does not get longer, or attenuate, so it does not subside, and the flood peak stays at the same maximum depth. As the wave becomes steeper the other momentum equation terms become more important and introduce dispersion and attenuation. The celerity of a flood wave departs from the kinematic wave

celerity because the discharge is not a function of depth alone, and, at the wave crest, Q and y do not remain constant.

Lighthill and Whitham (1955) illustrated the of a wave front can be determined by combining the Chezy equation

$$Q = CA \sqrt{RS_f} \quad (4.316)$$

with the momentum equation (4.2.1 b) to produce

$$Q = CA \sqrt{R \left(S_o - \frac{\partial y}{\partial x} - \frac{V}{g} - \frac{1}{g} \frac{\partial V}{\partial t} \right)} \quad (4.3.17)$$

in which C is the Chezy coefficient and R is the hydraulic radius.

4.5.2 Solution Of The Kinematic Wave

The solution of the kinematic wave equations specifies the distribution of the flow as a function of distance x along the channel and time t . The solution may be obtained numerically by using finite difference approximations to Eq. (4.3.7), or analytically by solving simultaneously the characteristic equations (4.3.10) and (4.3.14).

4.6 FINITE-DIFFERENCE APPROXIMATIONS

The Saint-Venant equations for distributed routing are not amenable to analytical solution except in a few special simple cases. They are partial differential equations that, in general, must be solved using numerical methods. Methods for solving partial differential equations may be classified as direct numerical methods and characteristic methods. In direct methods, finite-difference equations are formulated from the original partial differential equations for continuity and momentum. Solutions for the flow rate and water

surface elevation are then obtained for incremental times and distances along the stream or river. In characteristic methods, the partial differential equations are first transformed to a characteristic form, and the characteristic equations are solved analytically or by using a finite-difference representation.

In numerical methods for solving partial differential equations, the calculations are performed on a grid plotted over the $x-t$ plane. The $x-t$ grids a network of points defined by taking distance increments of length Δx and time increments of duration Δt . As shown in Fig. 4. 5.1, the distance points are denoted by index i and the time points by index j . A time line is a line parallel to the x axis through all the distance points at a given value of time.

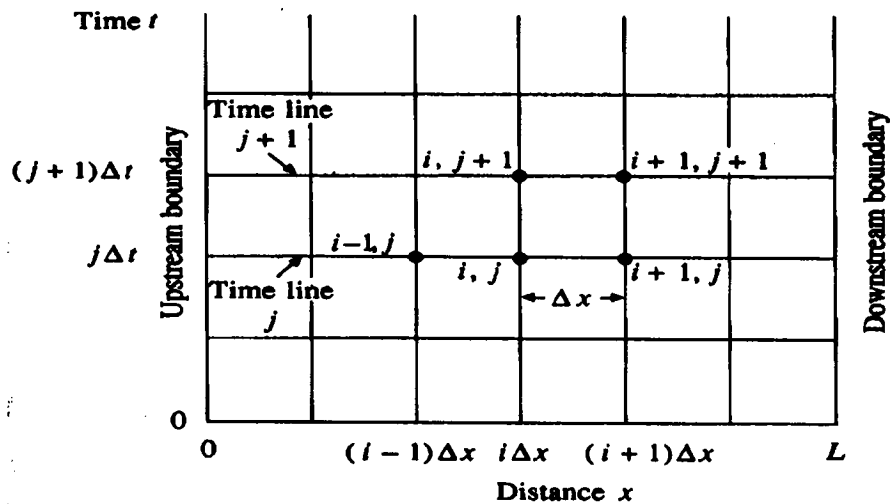


Figure 4.3 The grid on the $x-t$ plane used for numerical solution of the Saint-Venant equations by finite differences.

Numerical schemes transform the governing partial differential equations into a set of algebraic finite-difference equations, which may be linear or nonlinear. The finite-

difference equations represent the spatial and temporal derivatives in terms of the unknown variables on both the current time line, $j+1$, and the preceding time line, j , where all the values are known from previous computation (see Fig, 4.3). The solution of the Saint-Venant equations advances from one time line to the next.

4.6.1 Finite Difference Schemes

Finite-difference approximations can be derived for a function $u(x)$ as shown in Fig.

9.5.2. A Taylor series expansion of $u(x)$ at $x + \Delta x$ produces

$$u(x + \Delta x) = u(x) + \Delta x u'(x) + \frac{1}{2} \Delta x^2 u''(x) + \frac{1}{6} \Delta x^3 u'''(x) + \dots \quad (4.5.1)$$

where $u'(x) = \partial u / \partial x, u''(x) = \partial^2 u / \partial x^2, \dots$ and so on. The Taylor series expansion at $(x - \Delta x)$ is

$$u(x - \Delta x) = u(x) - \Delta x u'(x) + \frac{1}{2} \Delta x^2 u''(x) - \frac{1}{6} \Delta x^3 u'''(x) + \dots \quad (4.5.2)$$

A central-difference approximation uses the difference defined by subtracting (4.5.2) from (4.5.1)

$$u(x + \Delta x) - u(x - \Delta x) = 2 \Delta x u'(x) + 0(\Delta x^3) \quad (4.5.3)$$

where $0(\Delta x^3)$ represent a residual containing the third and higher order terms. Solving for $u'(x)$ assuming $0(\Delta x^3) \approx 0$ results in

$$u'(x) \approx \frac{u(x + \Delta x) - u(x - \Delta x)}{2 \Delta x} \quad (4.5.4)$$

which has an error of approximation of order Δx^2 . This approximation error, due to dropping the higher order terms, is also referred to as a truncation error.

A *forward difference* approximation is defined by subtracting $u(x)$ from (4.5.1):

$$u(x+\Delta x)-u(x) = \Delta x u'(x) + O(\Delta x^2) \quad (4.5.5)$$

Assuming second and higher order terms are negligible, solving for $u(x)$ gives

$$u'(x) \approx \frac{u(x+\Delta x) - u(x)}{\Delta x} \quad (4.5.6)$$

which has an error of approximation of order Δx .

The *backward-difference* approximation uses the difference defined by subtracting (4.5.2) from $u(x)$,

$$u(x)-u(x-\Delta x) = \Delta x u'(x) + O(\Delta x^2) \quad (4.5.7)$$

so that solving for $u'(x)$ gives

$$u'(x) \approx \frac{u(x) - u(x - \Delta x)}{\Delta x} \quad (4.5.8)$$

A finite-difference method may employ either an explicit scheme or an implicit scheme for solution. The main difference between the two is that in the explicit method, the unknown are solved *sequentially* along a time line from one distance point to the next, While in the implicit method the unknown values on a given time line are all determined *simultaneously*. The explicit method is simpler but can be unstable, which means that small values of Δx and Δt are required for convergence of the numerical procedure. The explicit method is convenient because results are given at the grid points, and it can treat slightly varying channel geometry from section to section, but it is less efficient than the implicit method and hence not suitable for routing flood flows over a long time period.

The implicit method is mathematically more complicated, but with the use of computers this is not a serious problem once the method is programmed. The method is

stable for large computation steps with little loss of accuracy and hence works much faster than the explicit method. The implicit method can also handle channel geometry varying significantly from one channel cross section to the next.

4.6.1.1 Explicit Scheme

The finite-difference representation is shown by the mesh of points on the time-distance plane shown in Fig. 4.5.1. Assuming that at time t (time line j) the hydraulic quantities u are known, the problem is to determine the unknown quantity at point $(i, j + 1)$ at time $t + \Delta t$, that is, u_i^{j+1}

The simplest scheme determines the partial derivatives at point $(i, j + 1)$ in terms of the quantities at adjacent points $(i-1, j)$, (i, j) , and $(i+1, j)$ using

$$\frac{\partial u_i^{j+1}}{\partial t} = \frac{u_i^{j+1} - u_i^j}{\Delta t} \quad (4.5.9)$$

and

$$\frac{\partial u_i^j}{\partial x} = \frac{u_{i+1}^j - u_{i-1}^j}{2\Delta x} \quad (4.5.10)$$

A forward-difference scheme is used for the time derivative and a central-difference scheme is used for the spatial derivative. Note that the spatial derivative is written using known terms on time line j . Implicit schemes on the other hand use finite-difference approximations for both the temporal and spatial derivatives in terms of the unknown time line $j+1$.

The discretization of the x - t plane into a grid for the integration of the finite-difference equations introduces numerical errors into the computation. A finite-difference

scheme is stable if such errors are not amplified during successive computation from one time line to the next. The numerical stability of the computation depends on the relative grid size. A necessary but insufficient condition for stability of an explicit scheme is the *Courant condition* (Courant and Friedrichs, 1948). For the kinematic wave equations, the Courant condition is

$$\Delta t \leq \frac{\Delta x_i}{C_k} \quad (4.5.11)$$

Where C_k is the kinematic wave celerity. The Courant condition requires that the time step be less than the time for a wave to travel the distance Δx_i . If Δt is so large that the Courant condition is not satisfied, then there is, in effect, an accumulation or piling up of water. The Courant condition does not apply to the implicit scheme.

For computational purposes in an explicit scheme, Δx is specified and kept fixed throughout the computations, while Δt is determined at each time step. To do this, at Δt_i just meeting the Courant condition is computed at each grid point i on time line j , and the smallest Δt_i is used. Because the explicit method is unstable unless Δt is small, it is sometimes advisable to determine the minimum Δt_i at a time line j then reduce it by some percentage. The Courant condition does not guarantee stability, and therefore is only a guideline.

4.6.1.2 Implicit Scheme

Implicit schemes use finite-difference approximations for both the temporal and spatial derivative in terms of the dependent variable on the unknown time line. As a simple example the space and time derivatives can be written for the unknown point $(i+1, j+1)$ as

$$\frac{\partial u_{i+1}^{j+1}}{\partial x} = \frac{u_{i+1}^{j+1} - u_i^{j+1}}{\Delta x} \quad (4.5.12)$$

and

$$\frac{\partial u_{i+1}^{j+1}}{\partial t} = \frac{u_{i+1}^{j+1} - u_{i+1}^j}{\Delta t} \quad (4.5.13)$$

This scheme is used in Sec. 4.6 for the kinematic wave model, a more complex implicit scheme, referred to as a weighted 4-point implicit scheme is used for the full dynamic wave model.

4.6.2 Numerical Solution Of The Kinematic Wave Equations

As shown, the continuity and momentum equations for the kinematic wave can be combined to produce an equation with Q as the only dependent variable:

$$\frac{\partial Q}{\partial x} + \alpha\beta Q^{\beta-1} \frac{\partial Q}{\partial t} = q \quad (4.6.1)$$

The objective of the numerical solution is to solve (4.6.1) for $Q(x, t)$ at each point on the x - t grid, given the channel parameter α and β , the lateral inflow $q(t)$, and the initial and boundary conditions. In particular, the purpose of the solution is to determine the outflow hydrograph $Q(L, t)$. The numerical solution of the kinematic wave equation is more flexible than the analytical solution described in Sec. 4.4; it can more easily handle variation in the channel properties and in the initial and boundary conditions, and it serves as an introduction to numerical solution of the dynamic wave equations.

To solve Eq. (4.6.1) numerically, the time and space derivatives of Q are approximated on the x - t grid as shown in Fig. 4.6.1. The unknown value is Q_{i+1}^{j+1} . The values of Q on the j^{th} time line have been previously determined, and so has Q_i^{j+1} .

and

$$\frac{\partial u_{i+1}^{j+1}}{\partial t} = \frac{u_{i+1}^{j+1} - u_{i+1}^j}{\Delta t} \quad (4.5.13)$$

This scheme is used in Sec. 4.6 for the kinematic wave model, a more complex implicit scheme, referred to as a weighted 4-point implicit scheme is used for the full dynamic wave model.

4.6.2 Numerical Solution Of The Kinematic Wave Equations

As shown, the continuity and momentum equations for the kinematic wave can be combined to produce an equation with Q as the only dependent variable:

$$\frac{\partial Q}{\partial x} + \alpha\beta Q^{\beta-1} \frac{\partial Q}{\partial t} = q \quad (4.6.1)$$

The objective of the numerical solution is to solve (4.6.1) for Q (x, t) at each point on the x-t grid, given the channel parameter α and β , the lateral' inflow q(t), and the initial and boundary conditions. In particular, the purpose of the solution is to determine the outflow hydrograph Q (L,t). The numerical solution of the kinematic wave equation is more flexible than the analytical solution described in Sec. 4.4; it can more easily handle variation in the channel properties and in the initial and boundary conditions, and it serves as an introduction to numerical solution of the dynamic wave equations.

To solve Eq. (4.6.1) numerically, the time and space derivatives of Q are approximated on the x- t grid as shown in Fig. 4.6.1. The unknown value is Q_{i+1}^{j+1} . The values of Q on the j^{th} time line have been previously determined, and so has Q_i^{j+1} .

4.6.2.1 Linear Scheme

The backward-difference method is used to set up the finite-difference equations. The finite-difference form of the space derivative of Q_{i+1}^{j+1} is found by substituting the values of Q on the $(j+1)^{\text{th}}$ time line into (4.5.12):

$$\frac{\partial Q}{\partial x} \approx \frac{Q_{i+1}^{j+1} - Q_i^{j+1}}{\Delta x} \quad (4.6.2)$$

The finite-difference form of the time derivative is found likewise by substituting

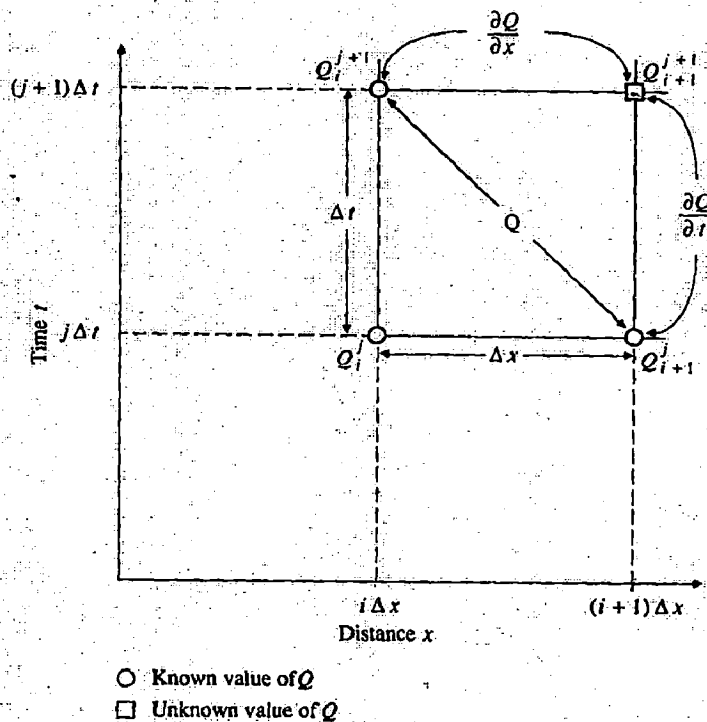


Figure 4.4 Finite difference box for solution of the linear kinematic wave equation showing the finite difference equations.

the values of Q on the $(i+1)^{\text{th}}$ distance line into (4.5.13):

$$\frac{\partial Q}{\partial t} \approx \frac{Q_{i+1}^{j+1} - Q_{i+1}^j}{\Delta t} \quad (4.6.3)$$

if the value of Q_{i+1}^{j+1} were used for Q in the term $\alpha\beta Q^{\beta-1}$ in Eq. (4.6.1), the resulting equation would be nonlinear in Q_{i+1}^{j+1} . To create a linear equation, the value of Q used in $\alpha\beta Q^{\beta-1}$ is found by averaging the values across the diagonal in the box shown in Fig 9.6.1

$$Q \approx \frac{Q_{i+1}^j + Q_i^{j+1}}{2} \quad (4.6.4)$$

The value of lateral inflow q is found by averaging the values on the $(i+1)^{\text{th}}$ distance line (these are assumed to be given in the problem).

$$q \approx \frac{q_{i+1}^{j+1} + q_{i+1}^j}{2} \quad (4.6.5)$$

By substituting Eqs. (4.6.2) to (4.6.5) into (4.6.1), the finite-difference form of the linear kinematic wave is obtained:

$$\frac{Q_{i+1}^{j+1} - Q_i^{j+1}}{\Delta x} + \alpha\beta \left(\frac{Q_{i+1}^j + Q_i^{j+1}}{2} \right)^{\beta-1} \left(\frac{Q_{i+1}^{j+1} - Q_i^j}{\Delta t} \right) = \frac{q_{i+1}^{j+1} + q_{i+1}^j}{2} \quad (4.6.6)$$

This equation, solved for the unknown Q_{i+1}^{j+1} , is

$$Q_{i+1}^{j+1} = \frac{\left[\frac{\Delta t}{\Delta x} Q_i^{j+1} + \alpha\beta Q_{i+1}^j \left(\frac{Q_{i+1}^j + Q_i^{j+1}}{2} \right)^{\beta-1} + \Delta t \left(\frac{q_{i+1}^{j+1} + q_{i+1}^j}{2} \right) \right]}{\left[\frac{\Delta t}{\Delta x} + \alpha\beta \left(\frac{Q_{i+1}^j + Q_i^{j+1}}{2} \right)^{\beta-1} \right]} \quad (4.6.7)$$

Q was chosen as the dependent variable because this results in smaller relative errors than if cross-sectional area A were chosen as the dependent variable - (Henderson, 1966) This is shown by taking the logarithm of (4.3.3):

$$\ln A = \ln \alpha + \beta \ln Q \quad (4.6.8)$$

and differentiating

$$\frac{dQ}{Q} = \frac{1}{\beta} \left(\frac{dA}{A} \right) \quad (4.6.9)$$

to define the relationship between the relative errors dA/A and dQ/Q . Using either Manning's equation or the Darcy-Weishach equation, β is generally less than 1, and it follows that the discharge estimation error would be magnified by the ratio $1/\beta$ if the cross-sectional area were the dependent variable instead of the flow rate.

4.7 DEVELOPMENT OF KINEMATIC WAVE MODEL FOR CHINDWIN RIVER

4.7.1 Variables List

The variables used in the program are described in brief, following are enlisted below:

n	=	Manning roughness coefficient.
t	=	Time interval .
d1	=	Distance between Mawalaik and Kalewa station
d2	=	Distance between Kalewa and Monywa station
s1	=	Slope between Mawalaik and Kalewa station
s2	=	Slope between Kalewa and Monywa station
p1	=	Perimeter of Kalewa station
p2	=	Perimeter of Monywa station
Q	=	Daily discharge
h	=	Daily stage

4.7.2 Data Used

n	=	0.045
t	=	24 x 60 x 60 secs
d1	=	41.89 km
d2	=	129.83 km
s1	=	0.00119504
s2	=	5.1156E-05
p1	=	1178.67 m
p2	=	848.64 m

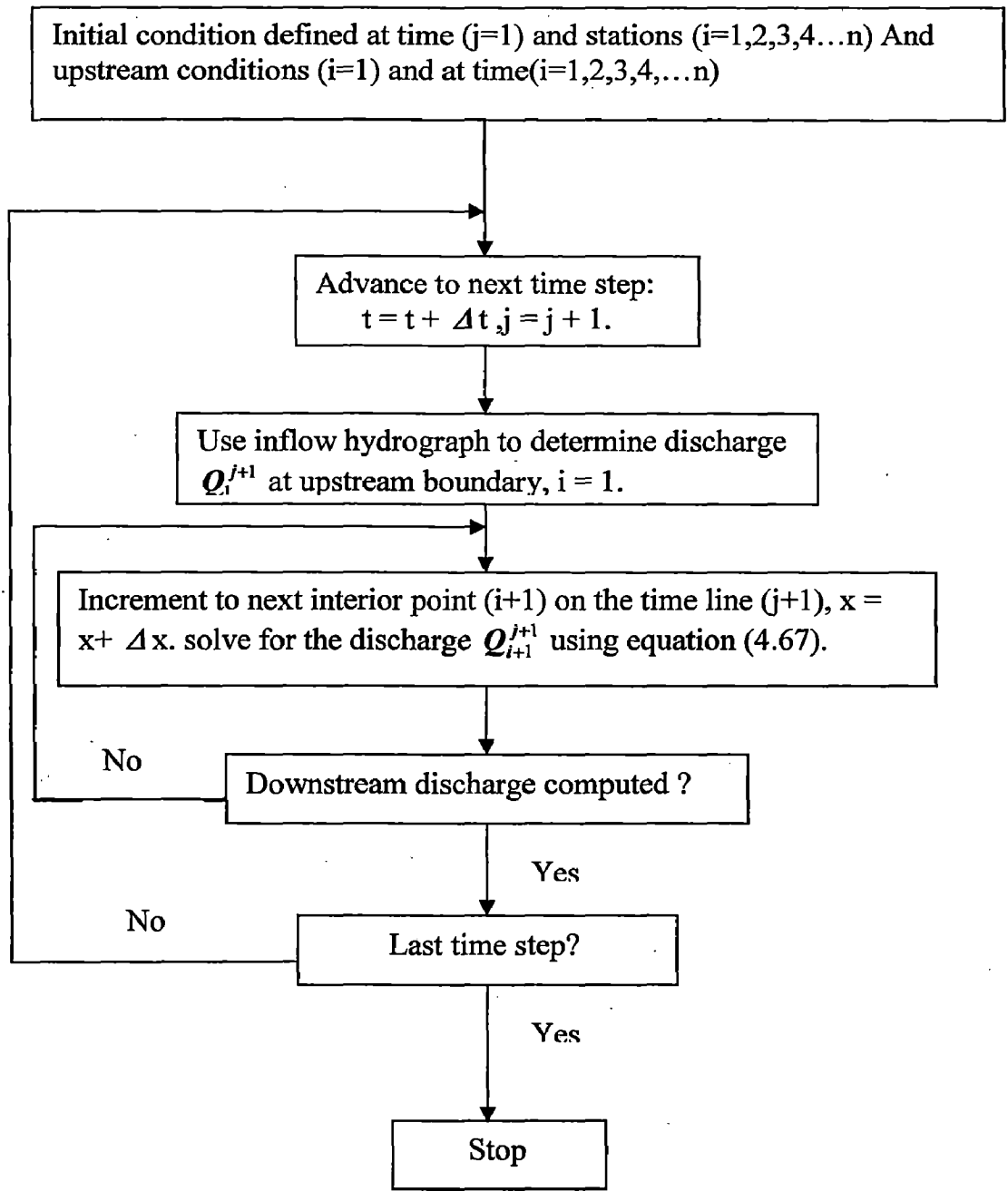


Fig 4.5 Flow chart for linear Kinematic wave computation.

Program for the Kinematic Wave model is developed in Visual C++ and it is given in Appendix

4.8: PERFORMANCE OF KINEMATIC WAVE MODEL AT DIFFERENT STATIONS FOR DIFFERENT SEASONS

(i) Following are the graphs which shows the efficiency of different stations at different seasons for daily discharge prediction

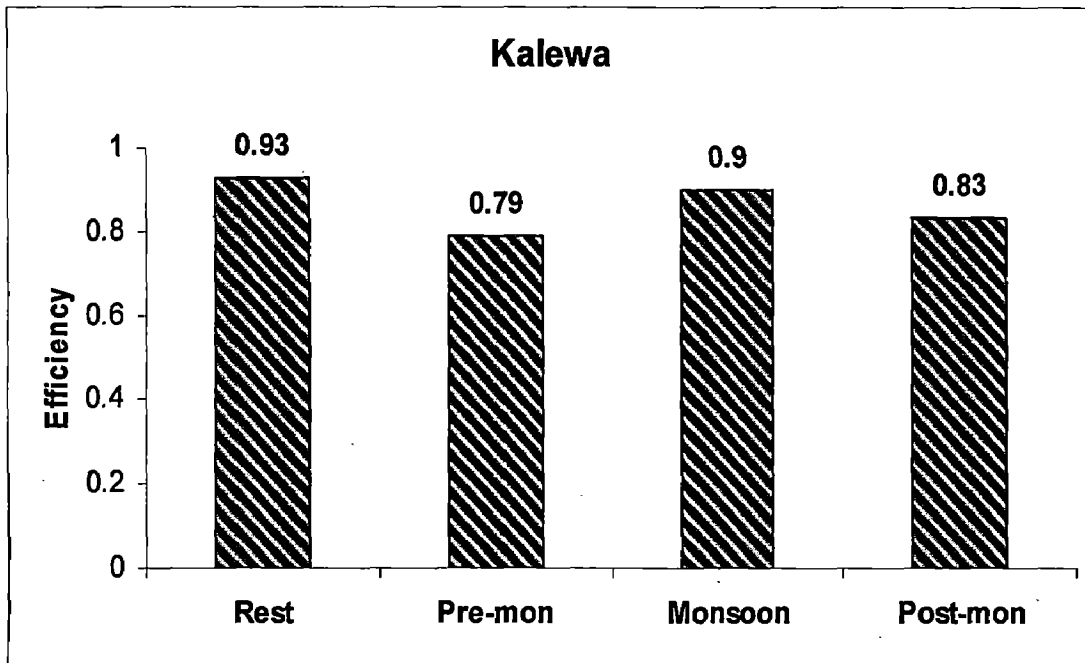


Fig (4.6): Percentage Efficiency of Kalewa station over a year for daily discharge prediction.

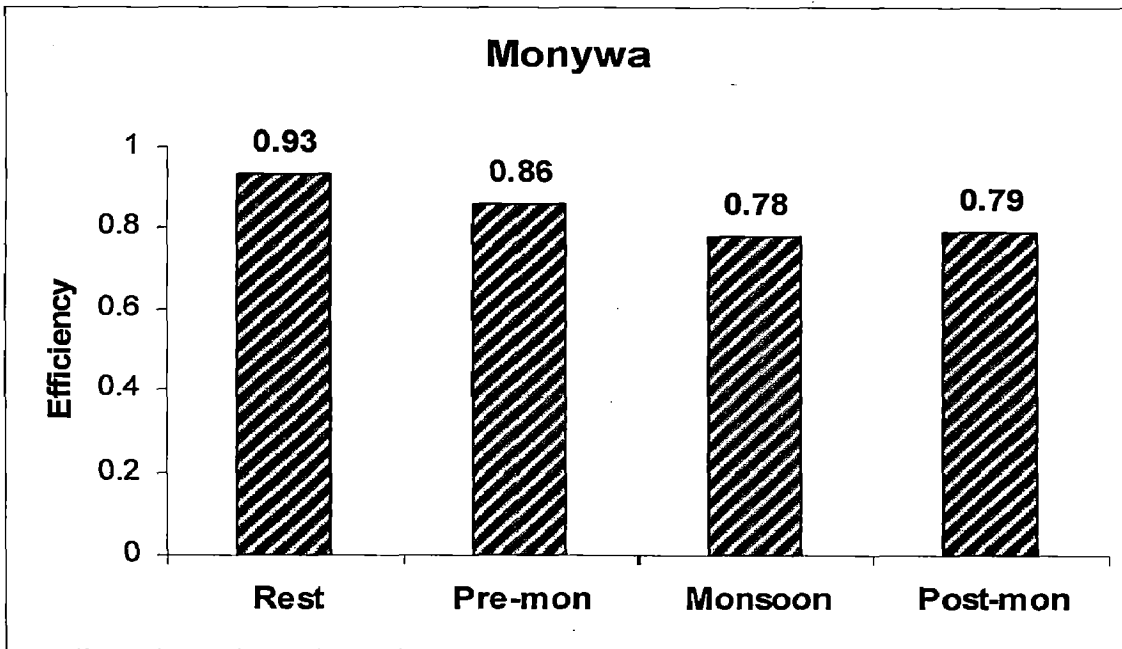
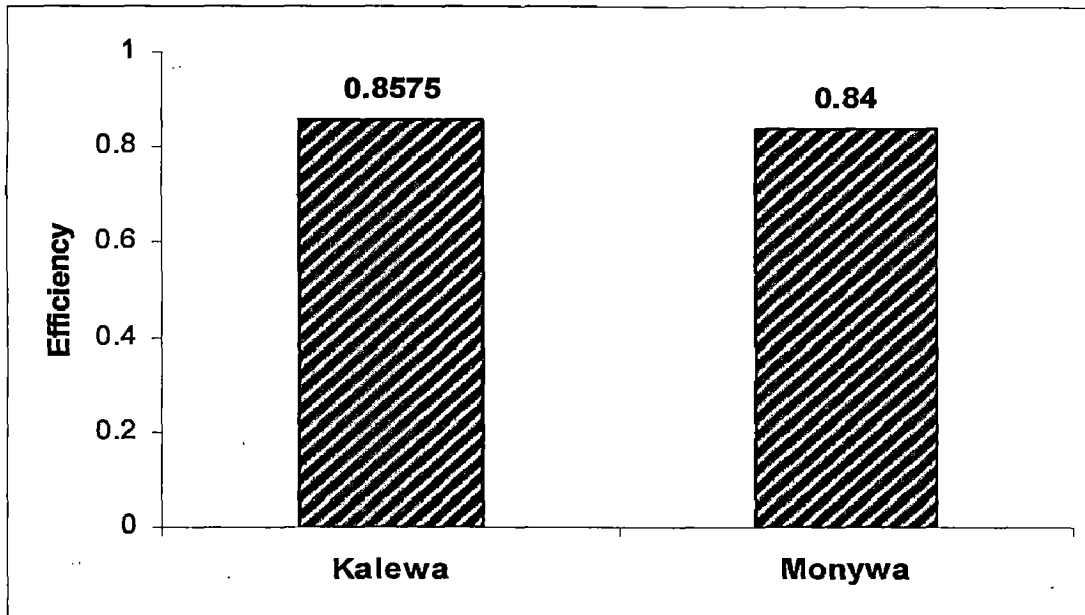
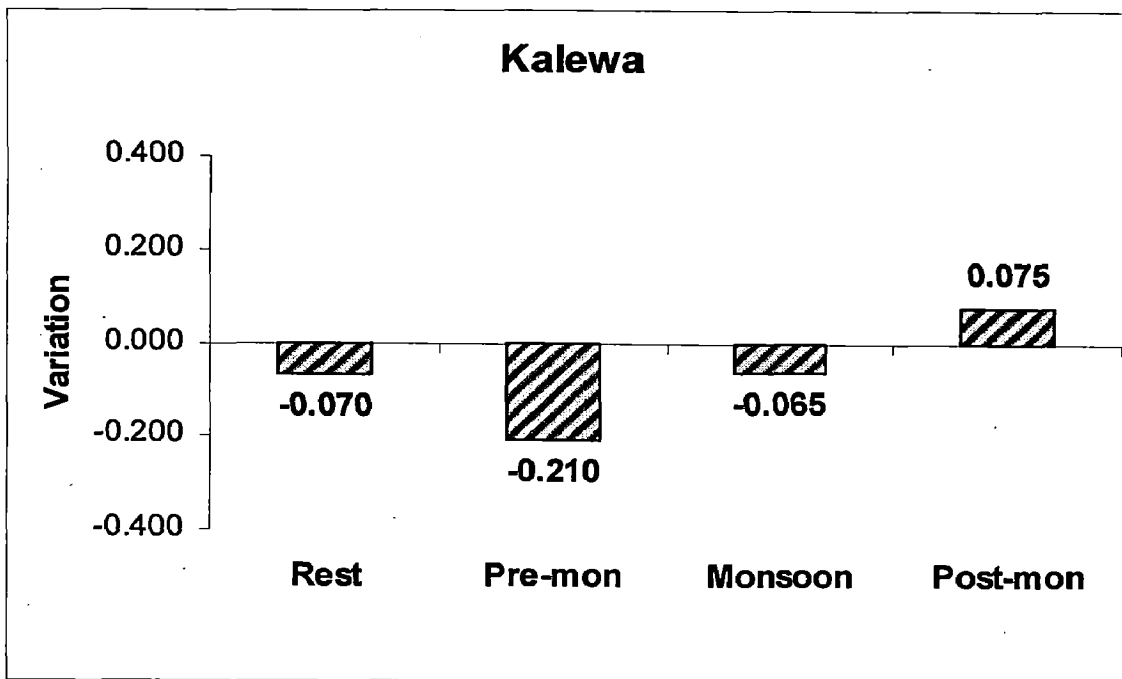


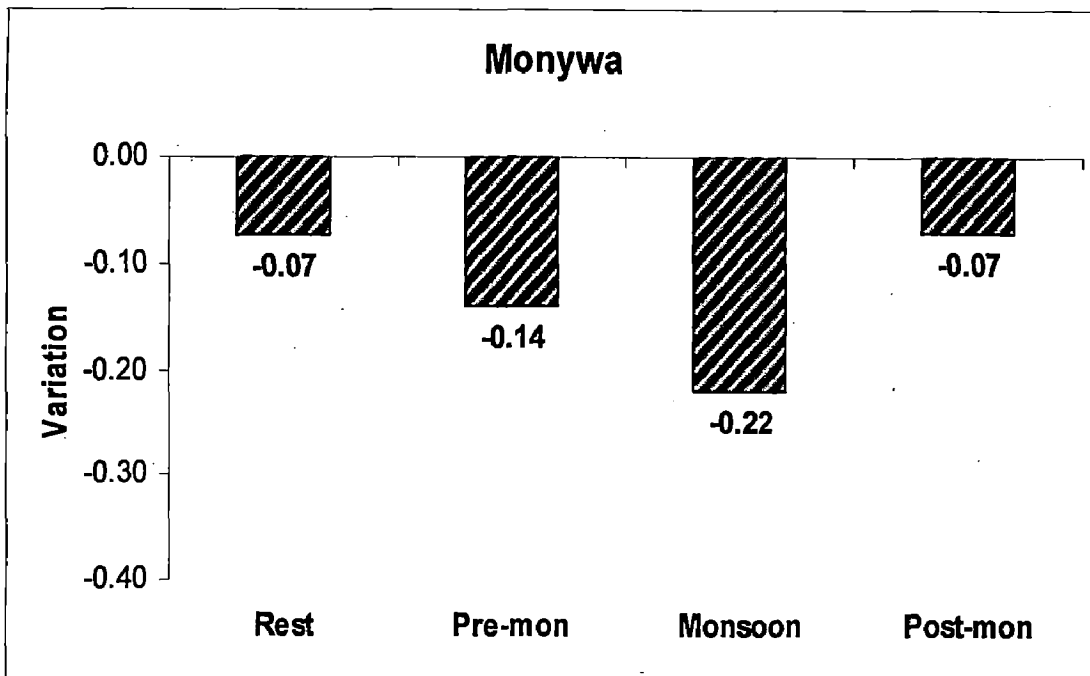
Fig (4.7) Efficiency of Monywa station over a year for daily discharge prediction.



Fig(4.8): Average Efficiency of Monywa and Kalewa for daily discharge prediction.



Fig(4.9): Variation in computed discharge with observed discharges at Kalewa station over a year.



Fig(4.10): Variation in computed discharge at Monywa station over a year.

(ii) Graphs showing the efficiency of stations over a year for daily stage prediction

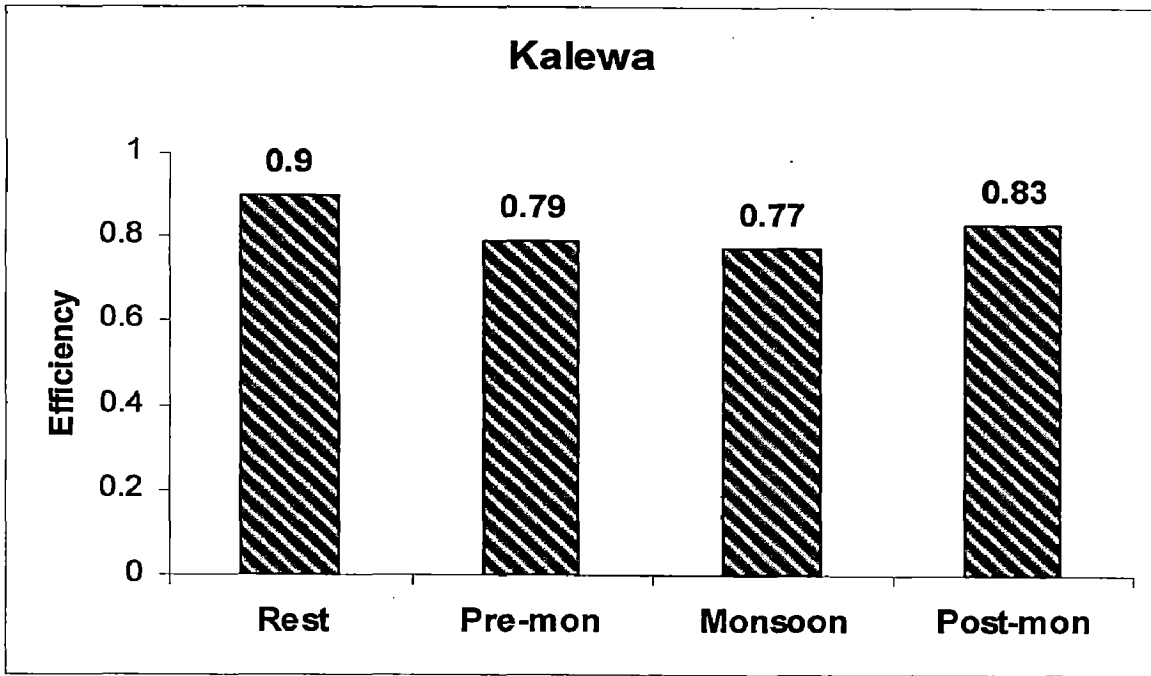


Fig (4.11): Efficiency of Kalewa station over a year for daily stage prediction

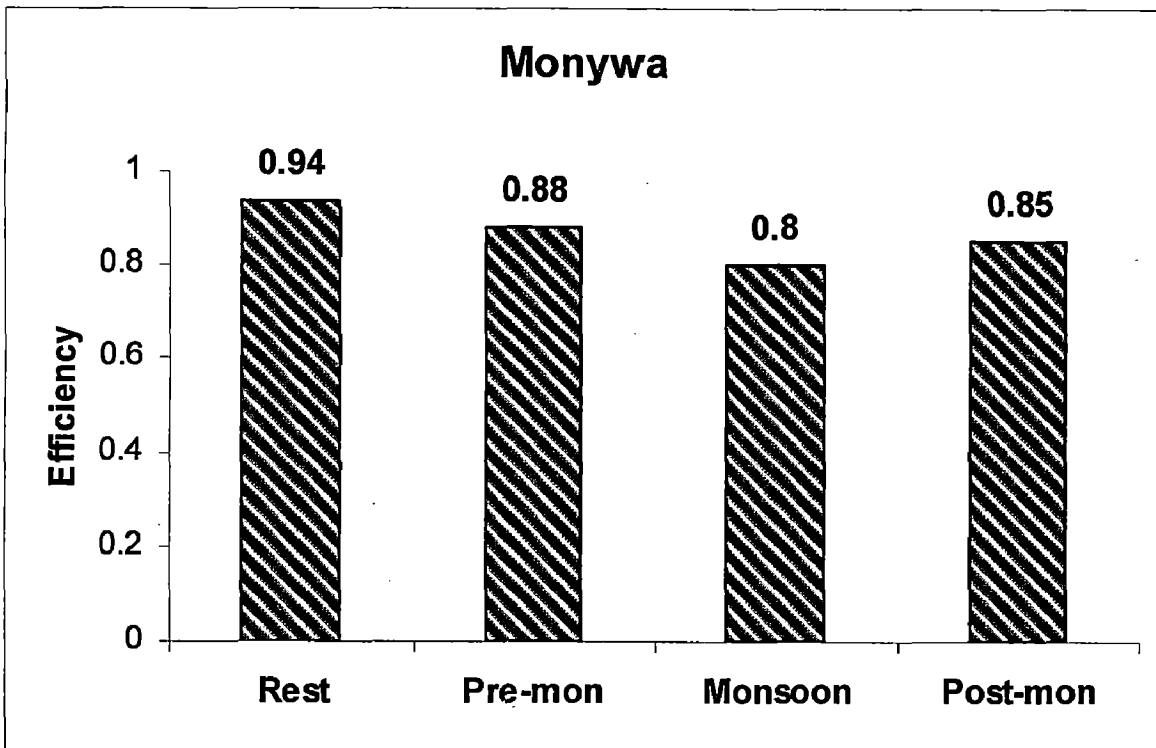
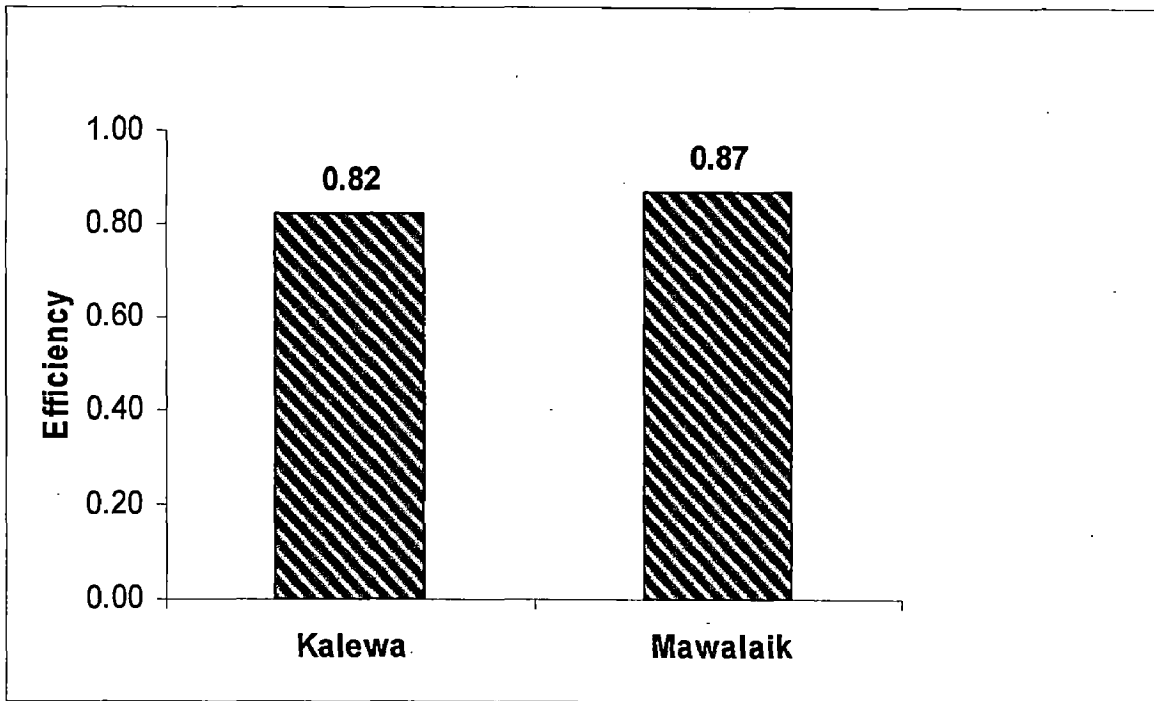
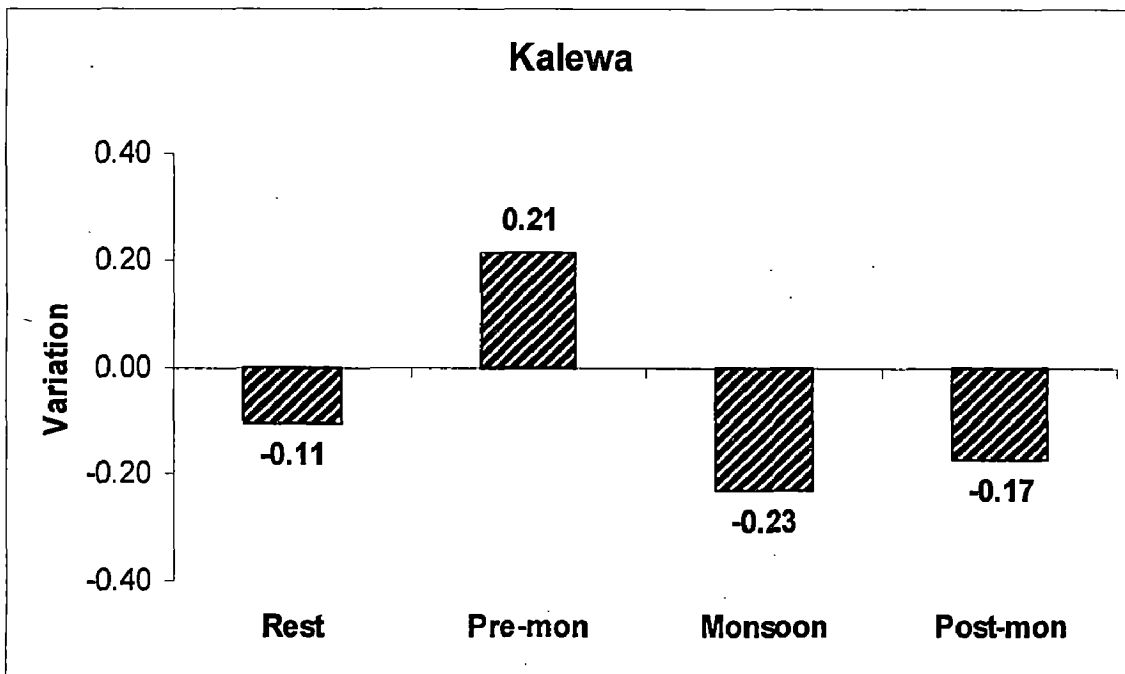


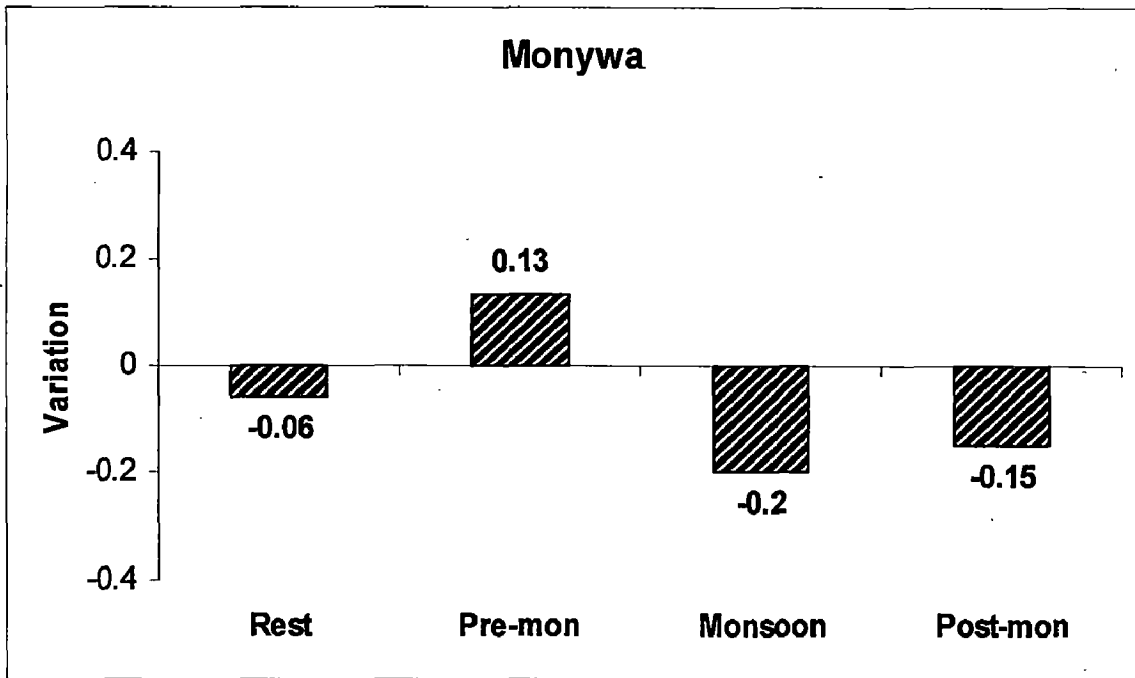
Fig (4.12): Efficiency of Monywa station over a year for daily stage prediction



Fig(4.13): Average Efficiency of Monywa and Kalewa for daily stage prediction.



Fig(4.14): Variation in computed stage with observed stage at Kalewa station over a year.



Fig(4.15): Variation in computed stage at Monywa station over a year.

**4.9: SUMMARY OF KINEMATIC WAVE MODEL AT DIFFERENT STATIONS
FOR DIFFERENT SEASONS**

4.9.1 Summary Of Kinematic Wave Model At Different Stations For Daily

Discharge Prediction:

Table (4.1a) Summary of Kalewa station for rest and pre-monsoon

Rest			Pre-monsoon		
Observed	Computed	Efficiency	Observed	Computed	Efficiency
923	909.811	0.985711	549	536.121	0.976541
919	896.796	0.975839	547	523.344	0.956753
914	883.775	0.966931	551	514.656	0.93404
901	871.16	0.966881	551	507.926	0.921826
883	859.656	0.973563	552	501.482	0.908482
865	848.171	0.980545	552	495.166	0.89704
849	836.706	0.985519	552	488.575	0.8851
848	825.259	0.973183	551	482.255	0.875236
843	813.831	0.965399	549	474.825	0.864891
923	802.501	0.869449	551	466.086	0.845891
839	791.18	0.943004	557	457.523	0.821406
839	780.822	0.930658	558	448.455	0.803683
826	770.388	0.932673	556	439.892	0.791173
813	760.831	0.935831	558	431.917	0.774045
808	751.366	0.929908	559	424.063	0.75861
804	741.984	0.922866	558	416.741	0.746848
799	733.067	0.917481	556	409.79	0.737032
795	723.8	0.91044	554	403.065	0.727554
790	715.295	0.905437	552	396.786	0.718815
786	707.485	0.900108	550	390.92	0.710764
771	699.617	0.907415	547	385.439	0.704642
760	691.927	0.91043	545	379.901	0.697066
749	683.943	0.913142	543	374.721	0.690094
738	675.843	0.915776	540	372.471	0.689761
739	668.09	0.904046	537	374.587	0.697555
739	660.58	0.893884	544	380.224	0.698941
739	653.665	0.884526	582	385.705	0.662723
732	649.879	0.887813	586	388.91	0.663669
732	648.478	0.885899	586	389.635	0.664906
735	648.127	0.881805	549	536.121	0.976541
923	909.811	0.985711	547	523.344	0.956753
Average efficiency		0.92859	Average efficiency		0.789072

Table(4.1b) Summary of Kalewa station for monsoon and post monsoon

Monsoon			Post-monsoon		
Observed	Computed	Efficiency	Observed	Computed	Efficiency
4665	4809.04	0.969123	4787	4841.07	0.988705
5621	5081.88	0.904088	5009	4860.04	0.970262
6286	5388.36	0.8572	5463	5136	0.940143
6465	5623.45	0.86983	8181	5843.33	0.714256
6353	5854.08	0.921467	9673	6625.32	0.684929
6803	6195.71	0.910732	9916	7338.66	0.740083
7583	664.37	0.087613	9804	7868.78	0.802609
7895	7065.26	0.894903	9477	8250.42	0.870573
8539	7525.8	0.881344	8950	8444.06	0.94347
9034	8026.76	0.888506	9179	8566.96	0.933322
9459	8503.4	0.898975	8563	8555.96	0.999178
9986	8968.42	0.898099	8017	8441.12	0.947097
9983	9367.88	0.938383	7865	8326.58	0.941312
10107	9730.27	0.962726	8261	8223.16	0.995419
10353	10033.9	0.969178	7492	7962.29	0.937228
10750	10350.2	0.962809	7050	7743.64	0.901611
10533	10499.7	0.996839	6231	7376.23	0.816204
9907	10514.3	0.9387	6751	7153.18	0.940427
9431	10354.7	0.902057	6387	6883.77	0.922222
9015	10186.6	0.870039	5712	6642.25	0.837141
9286	10196.9	0.901906	5866	6423.51	0.904959
10262	10504.2	0.976398	5444	6187.32	0.863461
11320	11029.2	0.974311	4806	5931.03	0.765911
12670	11733.3	0.926069	4374	5662.02	0.705528
14157	12599.5	0.889984	4077	5394.68	0.676802
15690	13636.5	0.86912	3663	5141.92	0.596254
17967	14954.6	0.832337	3517	4897.39	0.607509
20020	16217.4	0.81006	3295	4666.34	0.583812
21350	17473.6	0.818436	3436	4483.14	0.695244
21713	18479.6	0.851085	3409	4356.4	0.722089
4665	4809.04	0.969123	4787	4841.07	0.988705
Average efficiency		0.8997	Average efficiency		0.8304

Table(4.2a) Summary of Monywa station for rest and pre-monsoon

Rest			Pre-monsoon		
Observed	Computed	Efficiency	Observed	Computed	Efficiency
1321	1313.01	0.993952	739	736.459	0.996562
1305	1294.39	0.99187	728	728.776	0.998935
1289	1276.13	0.990016	720	721.095	0.998481
1273	1258.13	0.988319	725	713.483	0.984114
1257	1240.67	0.987009	771	705.946	0.915624
1244	1223.48	0.983505	816	698.486	0.855988
1233	1206.64	0.978621	832	691.09	0.830637
1220	1190.12	0.975508	830	683.765	0.823813
1220	1173.91	0.962221	828	676.472	0.816995
1212	1157.99	0.955437	812	669.167	0.824097
1201	1142.35	0.951166	792	661.859	0.835681
1193	1127.01	0.944686	768	654.532	0.852255
1183	1111.96	0.939949	749	647.202	0.864088
1177	1097.22	0.932218	736	639.891	0.869417
1164	1082.77	0.930215	723	632.602	0.874968
1156	1068.6	0.924394	720	625.35	0.868542
1156	1054.72	0.912388	712	618.146	0.868183
1148	1041.1	0.906882	704	610.996	0.867892
1140	1027.1	0.900965	696	603.911	0.867688
1132	1014.69	0.896369	696	596.902	0.857618
1121	1001.91	0.893764	704	589.976	0.838034
1108	989.383	0.892945	701	583.976	0.833061
1100	977.1	0.888273	696	576.372	0.828121
1092	965.043	0.883739	688	569.783	0.828173
1082	953.213	0.880973	672	563.488	0.838524
1076	941.608	0.8751	672	557.578	0.829729
1076	930.239	0.864534	704	552.037	0.784143
1076	919.211	0.854285	768	546.783	0.711957
1076	908.593	0.844417	824	541.732	0.657442
1074	898.406	0.836505	739	736.459	0.996562
1321	1313.01	0.993952	728	728.776	0.998935
Average efficiency		0.9245	Average efficiency		0.8588

Table(4.2b) Summary of Monywa station for monsoon and post monsoon

Monsoon			Post-monsoon		
Observed	Computed	Efficiency	Observed	Computed	Efficiency
5584	5765.85	0.967434	5890	6051.31	0.972613
5506	5676.55	0.969025	6196	5954.26	0.960985
6317	6019.45	0.952897	6973	5887.19	0.844284
7244	6986.41	0.964441	7251	5883.52	0.811408
7472	6975.3	0.933525	9184	5947.05	0.647545
7320	6993.99	0.955463	10900	6068.9	0.55678
7648	6051.66	0.791274	11283	6229.28	0.552094
8536	7140	0.836457	11273	6411.89	0.568783
9008	8262.6	0.917251	11167	6597.22	0.590778
9600	8421.23	0.877211	10583	6778.2	0.64048
10350	9611.43	0.928641	10497	6942.2	0.661351
10933	6830.13	0.624726	9793	7080.64	0.723031
11603	7068.95	0.609235	9168	7195.78	0.78488
11543	7322.72	0.634386	9304	7290.75	0.783615
11723	7584.32	0.646961	9573	7352.58	0.768054
12027	7854.37	0.653061	8976	7388.46	0.823135
12170	8114.82	0.666789	8408	7387.34	0.878608
12080	8352.32	0.691417	7816	7366.15	0.942445
11527	8550.82	0.741808	7688	7322.82	0.9525
11020	8713.07	0.79066	7632	7262.14	0.951538
10433	8860.73	0.849298	7196	7187.91	0.998876
10647	9025.7	0.847722	6965	7100.08	0.980606
11640	9229.34	0.792899	6606	6998.44	0.940593
12767	9487.94	0.743161	5884	6883.46	0.830139
14077	9815.36	0.697262	5362	6756.81	0.739871
15443	10226.1	0.662184	5077	6620.99	0.695885
16057	10747.5	0.669334	4811	4477.75	0.930732
17333	11365.5	0.655715	4555	4329.03	0.950391
18370	12072.2	0.657169	4267	4179.15	0.979412
18820	12828.9	0.681663	5890	6051.31	0.972613
5584	5765.85	0.967434	6196	5954.26	0.960985
Average efficiency		0.78032	Average efficiency		0.7936

4.10.2 Summary Of Kinematic Wave Model At Different Stations For Daily Stage

Prediction:

Table (4.3 a) Summary of Kalewa station for rest and pre-monsoon

Rest			Pre-monsoon		
Observed	Computed	Efficiency	Observed	Computed	Efficiency
2.28	2.64	0.8636	1.93	1.47	0.6871
2.27	2.64	0.8598	1.92	1.46	0.6849
2.26	2.63	0.8593	1.9	1.45	0.6897
2.25	2.62	0.8588	1.89	1.47	0.7143
2.24	2.59	0.8649	1.88	1.47	0.7211
2.23	2.55	0.8745	1.88	1.48	0.7297
2.22	2.51	0.8845	1.87	1.48	0.7365
2.21	2.47	0.8947	1.86	1.48	0.7432
2.2	2.47	0.8907	1.86	1.47	0.7347
2.19	2.46	0.8902	1.85	1.46	0.7329
2.18	2.64	0.8258	1.84	1.47	0.7483
2.17	2.45	0.8857	1.83	1.51	0.7881
2.16	2.45	0.8816	1.82	1.51	0.7947
2.15	2.42	0.8884	1.81	1.5	0.7933
2.14	2.39	0.8954	1.8	1.51	0.8079
2.13	2.38	0.895	1.79	1.52	0.8224
2.12	2.37	0.8945	1.78	1.51	0.8212
2.11	2.36	0.8941	1.77	1.5	0.82
2.11	2.35	0.8979	1.76	1.49	0.8188
2.1	2.34	0.8974	1.75	1.48	0.8176
2.09	2.33	0.897	1.74	1.46	0.8082
2.08	2.3	0.9043	1.74	1.45	0.8
2.08	2.27	0.9163	1.73	1.44	0.7986
2.07	2.24	0.9241	1.72	1.43	0.7972
2.06	2.21	0.9321	1.72	1.41	0.7801
2.05	2.21	0.9276	1.72	1.4	0.7714
2.05	2.21	0.9276	1.73	1.43	0.7902
2.04	2.21	0.9231	1.74	1.65	0.9455
2.04	2.19	0.9315	1.74	1.67	0.9581
2.03	2.19	0.9269	1.74	1.67	0.9581
2.03	2.2	0.9227	1.93	1.47	0.6871
Average efficiency		0.8945	Average efficiency		0.7894

Table (4.3 b) Summary of Kalewa station for monsoon and post monsoon

Monsoon			Post-monsoon		
Observed	Computed	Efficiency	Observed	Computed	Efficiency
6.16	7.87	0.7827	7.2	7.97	0.9034
6.2	7.85	0.7898	7.21	7.95	0.9069
6.29	8.67	0.7255	7.22	8.14	0.887
6.6	9.22	0.7158	7.31	8.53	0.857
6.67	9.37	0.7118	7.57	10.68	0.7088
6.55	9.29	0.7051	7.78	11.77	0.661
6.65	9.63	0.6906	7.99	11.94	0.6692
6.8	10.23	0.6647	9.17	11.86	0.7732
6.91	10.47	0.66	9.27	11.63	0.7971
10.04	10.96	0.9161	9.29	11.25	0.8258
10.18	11.31	0.9001	9.327	11.41	0.8174
10.31	11.61	0.888	8.85	10.97	0.8067
10.43	11.99	0.8699	8.86	10.57	0.8382
10.103	11.99	0.8426	8.89	10.45	0.8507
10.61	12.07	0.879	8.232	10.75	0.7658
10.69	12.22	0.8748	8.01	10.16	0.7884
10.76	12.47	0.8629	8	9.82	0.8147
10.8	12.33	0.8759	9	9.19	0.9793
10.8	11.93	0.9053	7.97	9.59	0.8311
10.76	11.59	0.9284	7.86	9.31	0.8443
10.72	11.3	0.9487	7.79	8.76	0.8893
10.73	11.49	0.9339	7.72	8.9	0.8674
10.8	12.16	0.8882	7.65	8.51	0.8989
10.92	12.83	0.8511	7.57	7.97	0.9498
10.08	13.51	0.7461	7.79	7.48	0.9586
10.21	14.15	0.7216	7.7	7.13	0.9201
10.48	14.76	0.71	7.32	6.8	0.9235
10.74	15.58	0.6893	7.23	6.66	0.9144
10.98	16.29	0.674	7.15	6.42	0.8863
10.21	16.77	0.6088	7.08	6.57	0.9224
10.39	16.9	0.6148	7.07	6.54	0.919
Average efficiency		0.7728	Average efficiency		0.8304

Table (4.4 a) Summary of Monywa station for rest and pre-monsoon

Rest			Pre-monsoon		
Observed	Computed	Efficiency	Observed	Computed	Efficiency
2.15	2.29	0.939	1.7	1.43	0.811
2.13	2.28	0.934	1.69	1.42	0.81
2.12	2.26	0.938	1.69	1.41	0.801
2.11	2.24	0.942	1.68	1.4	0.8
2.09	2.22	0.941	1.67	1.41	0.816
2.08	2.2	0.945	1.67	1.46	0.856
2.07	2.18	0.95	1.66	1.53	0.915
2.06	2.17	0.949	1.65	1.55	0.935
2.04	2.15	0.949	1.65	1.55	0.935
2.03	2.15	0.944	1.64	1.55	0.942
2.02	2.14	0.944	1.64	1.52	0.921
2.01	2.13	0.944	1.63	1.49	0.906
2	2.12	0.943	1.62	1.46	0.89
1.98	2.1	0.943	1.62	1.44	0.875
1.97	2.1	0.938	1.61	1.42	0.866
1.96	2.08	0.942	1.6	1.4	0.857
1.95	2.07	0.942	1.6	1.4	0.857
1.94	2.07	0.937	1.59	1.39	0.856
1.93	2.06	0.937	1.58	1.38	0.855
1.92	2.05	0.937	1.58	1.37	0.847
1.91	2.04	0.936	1.57	1.37	0.854
1.9	2.03	0.936	1.57	1.38	0.862
1.89	2.01	0.94	1.56	1.38	0.87
1.88	2	0.94	1.55	1.37	0.869
1.87	1.99	0.94	1.55	1.36	0.86
1.86	1.97	0.944	1.54	1.34	0.851
1.86	1.96	0.949	1.54	1.34	0.851
1.85	1.96	0.944	1.53	1.38	0.891
1.84	1.96	0.939	1.53	1.46	0.952
1.83	1.96	0.934	1.52	1.54	0.987
1.82	1.96	0.929	1.7	1.43	0.811
Average efficiency		0.945	Average efficiency		0.873

Table (4.4 b) Summary of Monywa station for monsoon and post monsoon

Monsoon			Post-monsoon		
Observed	Computed	Efficiency	Observed	Computed	Efficiency
5	6.08	0.822	5.95	6.03	0.987
5.25	5.71	0.919	5.68	5.88	0.966
5.1	5.67	0.899	5.83	6.03	0.967
5.8	6.1	0.951	5.81	6.4	0.908
5.79	6.52	0.888	5.92	6.52	0.908
5.84	6.61	0.884	5.83	7.32	0.796
4.85	6.55	0.74	5.95	7.91	0.752
4.88	6.69	0.729	6.23	8.03	0.776
4.92	7.06	0.697	6.23	8.03	0.776
4.99	7.25	0.688	5.97	7.99	0.747
6.06	7.49	0.809	5.78	7.81	0.74
6.16	7.73	0.797	5.65	7.78	0.726
6.27	7.92	0.792	5.35	7.56	0.708
6.38	8.14	0.784	5.44	7.32	0.743
6.61	8.12	0.814	5.59	7.38	0.757
6.636	8.19	0.81	5.74	7.49	0.766
6.76	8.3	0.814	5.55	7.24	0.767
6.88	8.37	0.822	5.15	7	0.736
6.99	8.33	0.839	5.53	6.76	0.818
6.09	8.12	0.75	5.51	6.7	0.822
6.16	7.94	0.776	5.58	6.68	0.835
6.32	7.76	0.814	5.55	6.5	0.854
6.3	7.83	0.805	5.5	6.39	0.861
6.4	8.16	0.784	5.35	6.23	0.859
6.62	8.55	0.774	5.29	5.88	0.9
6.66	8.91	0.747	5.23	5.59	0.936
6.86	9.29	0.738	5.16	5.42	0.952
7.08	9.46	0.748	5.09	5.26	0.968
7.36	9.78	0.753	5.02	5.1	0.984
7.66	10.05	0.762	4.82	4.92	0.98
7.97	10.19	0.782	4.85	4.95	0.98
Average efficiency		0.798	Average efficiency		0.848

5.1 GENERAL

The developed stage-discharge relationship has been tested for different stations, over a year and its efficiency is found to be satisfactory. It has been found to be 88%, 99.02%, 86% , 89% , and 89% ,for Hkamti,Homalin,Mawalaik,Kalewa and Monywa respectively. Similarly the efficiency of Kinematic Wave model has been tested separately for daily stage prediction and for daily discharge prediction and it is found to be satisfactory. For daily stage prediction efficiency of Kinematic Wave model is 82% and 87% at Kalewa and Monywa station respectively. For daily discharge prediction efficiency of Kinematic Wave model is 85.75%, and 84%, at Kalewa and Monywa station respectively.

5.2 CONCLUSIONS

The following conclusions can be drawn from this study:

- (1) The performance of Stage-Discharge relation for daily stage forecasting at five sites of Chindwin River for different season have been investigated. And it has been found that:
 - Accuracy of prediction of Stage-Discharge relationship is best at Homalin station.
 - At Hkamti station Stage-Discharge relationship gives best accuracy during monsoon season.
 - At Homalin station Stage-Discharge relationship gives good accuracy during all seasons.

- At Mawalaik station Stage-Discharge relationship gives best accuracy in rest of the year.
 - At Kalewa station Stage-Discharge relationship gives best accuracy during monsoon season.
 - At Monywa station Stage-Discharge relationship gives best accuracy in rest of the year.
- (2) The performance of Kinematic wave model for daily discharge and stage forecasting at two sites of lower Chindwin river for different season have been investigated. And it has been found that:
- The performance of kinematic wave model at both stations for forecasting of daily discharge is quite good. Between two stations, performance at Kalewa station is better than Monywa station.
 - The performance of kinematic wave model at both stations for forecasting of daily stage is quite good. Between two stations, performance at Monywa station is better than Kalewa station.
 - The performance of kinematic wave model for forecasting of daily discharge at Kalewa and Monywa stations gives best accuracy during rest of the year.
 - The performance of kinematic wave model for forecasting of daily stages at Kalewa and Monywa stations gives best accuracy during rest of the year.

5.3 SUGGESTIONS FOR FURTHER WORK

The analysis and results reported in this work leave sufficient scope for further investigation, which could not be taken up owing to time constraint, unavailability of data and are briefed as follows:

- (1) Incorporation of all the stations of Chindwin river in Kinematic wave model, which could not be done due to unavailability of data.
- (2) For getting more accurate results Stage-Discharge relationship should be developed separately for different seasons.
- (3) Comparisons should be made between the Kinematic wave model output and that from Neurosolution on the same river.

REFERENCES:

Abramowitz, M. and Stegun, I.A., ed., Handbook of Mathematical Functions With Formulas, Graphs, and Mathematical Tables, 9th ed., Dover Publications, New York, 1972.

Ang, A.H.S. and Tang, W.H., Probability Concepts in Engineering Planning and Design, Vol. I: Basic Principles, John Wiley & Sons, Inc., 1975.

Benjamin, J.R. and Cornell, C.A., Probability, Statistics, and Decisions for Civil Engineers, McGraw-Hill, New York, 1970

Berry, J.K. 1987. 'Fundamental operations in computer-assisted map analysis', *International Journal of Geographic Information Systems*, 2, 119-136.

Bowman, K.O. and Shenton, L.R., "Approximate Percentage Points for Pearson Distributions," *Biometrika*, 66(1):147-151, 1979a.

Bowman, K.O. and Shenton, L.R., "Further Approximate Pearson Percentage Points and Cornish-Fisher," *Communication Statistics-Simulation*, B8 (3):231-244, 1979b

Burrough, P.A. and McDonnell, R.A. 1998. *Principles of Geographical Information Systems*. Oxford University Press. p. 333.

B.B. Ross and V.O. Shanholtz , A one-dimensional finite element for modelling the hydrology of small upland watersheds. In: *Proceedings of the Hydrologic Transport Modelling Symposium*, Amer. Soc. of Agric. Eng. (1979), pp. 42-59.

Chow, V.T, Maidment, D.R. and Mays, L.W. 1988. *Applied Hydrology McGraw-Hill*, p 572.

Davis, C.S. and Stephens, M.A., "Approximate Percentage Points Using Pearson Curves," Royal Statistical Society, 322-327, 1983.

De Roo, A.P.J., L. Hazelhoff and P.A. Burrough 1989. 'Soil erosion modelling using 'ANSWERS' and Geographical Information Systems'. *Earth Surface Processes and Landforms*, 14, 517-532.

De Saint-Venant Barre' , Theory of unsteady water flow, with applications to floods and to propagations of tides in river channels. *French Academy of Science* 73 (1871), pp. 148–154.

De Saint-Venant Barre' , Theory of unsteady water flow, with applications to floods and to propagations of tides in river channels. *French Academy of Science* 73 (1871), pp. 237–240.

D.H. Keuning , Application of finite element method to open channel flow. In: *Journal of Hydraulics Division* 102, ASCE (1976), pp. 459–467 No. HY4

D.L. Fread , Effects of time step size in implicit dynamic routing. In: *Water Resources Bulletin* 9, AWRA (1973), pp. 339–351 No. 2 .

Epstein, B., "Some Application of the Mellin Transform in Statistics." *Annals of Mathematical Statistics*, 19:370-379. 1948.

Fisher, R.A. and Cornish, E.A., "The Percentile Points of Distributions Having Known Cumulants," *Technometrics*, 2(2):209-225, 1960.

Fread, D.L. 1993. '*Flow Routing*'. Chapter 10 In: Maidment, D.R., *Handbook of Hydrology*. McGraw Hill, 10.1-10.36.

F.M. Henderson , *Open Channel Flow*. (1st edition ed.),, McMillan Publishing Co., New York (1966).

Gardner, G.W., et al., "A Comparison of Sensitivity Analysis and Error Analysis Based on a Stream Ecosystem Model," *Ecological Modeling*, 12, 1981.

Giffin, W.C., *Transform Techniques for Probability Modeling*, Academic Press, 1975.

I.L. Nwaogazie , *Finite element modelling of streamflow routing*. In: *Thesis presented to the Oklahoma State University, Stillwater, Oklahoma* (1982) in partial fulfillment of the requirements for the degree of Doctor of Philosophy

J.A. Liggett and D.A. Wollhiser , *Difference solution of shallow-water equation*. In: (1st edition ed.), *Journal of the Engineering Mechanics Division* **95**, ASCE (1967), pp. 39–71 No. EM2 .

J.A. Cunge, *On the subject of a flood propagation method (Muskingum Method)*, *J. Hydraulic Res., Int. Assoc. Hydraulic Res.* **7** (1969) (2), p. 205.

M.A. Median, Jr. and K. Helfrick , *Evaluation of infiltration models in kinematic wave approximation to forested watershed overland flow*. In: *Proceedings of the Hydrologic Transport Modelling Symposium*, Amer. Soc. of Agric. Eng. (1979), pp. 218–233.

- Goel, N.K., Hydrological data collection, processing and analysis (lecture notes, unpublished)
- Kendall, M., Stuart, A., and Ord, J.K., Kendall's Advanced Theory of Statistics, Vol. 1: Distribution Theory, 5th Edition, Oxford University Press, New York, 1987
- King, D., Daroussin, J., Jamagne, M., Le Bas, C. and Montanarella, L. 1997. The 1:1,000,000 soil geographical database of Europe. In: Bruand, A. et al. (eds.) *The use of pedotransfer in soil hydrology research in Europe*. INRA Orléans and EC/JRC Ispra.
- Kirkby, M.J. 1976. 'Hydrological Slope Models: The Influence of Climate'. In: E. Derbyshire (Ed.), *Geomorphology and Climate*, John Wiley.
- Kite, G.W., Ellehoj, E. and Dalton, A. 1996. 'GIS for Large-Scale Watershed Modelling'. In: Singh, V.P. and Fiorentino, M. (eds.) *Geographical Information Systems in Hydrology*. Kluwer. 443 p.
- Lilly, A. 1997. A description of the HYPRES database (Hydraulic Properties of European Soils). In: Bruand, A. et al. (eds.) *The use of pedotransfer in soil hydrology research in Europe*. INRA Orléans and EC/JRC Ispra.
- M. Amein and C.S. Fang, Implicit flood routing in natural channels. In: *Journal of the Hydraulics Division* 96, ASCE (1970), pp. 2481–2500 No. HY12 .
- M.J. Lighthill and G.B. Whitham, On kinematic waves. I — Flood movement in long rivers, *Proc. Roy. Soc. Lond., Ser. A* 229 (1955), p. 281. [MathSciNet](#) | [Abstract](#) + [References in Scopus](#) | [Cited By in Scopus](#)

Natural Environment Research Council, Flood studies report: Volume III flood routing studies, Natural Environment Research Council, Wallingford, England (1975), p. 76

O.C. Zienkiewicz , *The Finite Element Methods in Engineering Science*. (3rd edition ed.), McGraw-Hill Publishing Co., New York (1977).

Park, C.S, "The Mellin Transform in Probabilistic Cash Flow modeling," *The Engineering Economist*, 32(2):115-134. Winter, 1987.

R.K. Price, A river catchment flood model, *Proc. Inst. Civ. Engrs* **65** (1978) (2), p. 655.

[Abstract-Compendex](#) | [Abstract + References in Scopus](#) | [Cited By in Scopus](#)

R.K. Price, Flood routing methods for British rivers, *Proc. Instn Civ. Engrs, London* **55**

(1973), p. 913. [Abstract-Compendex](#) | [Abstract-FLUIDEX](#) | [Abstract + References in](#)

[Scopus](#) | [Cited By in Scopus](#)

R.K. Price, Variable parameter diffusion method for flood routing, *Rep. IN 115*,

Hydraulics Research Station, Japan (1973).

R.L. Cooley and S.A. Moin , Finite element solution of Saint-Venant equations. In:

Journal of the Hydraulics Division **102**, ASCE (1976), pp. 759–776 No. HY6

Singh, V.P. 1996. *Kinematic Wave Modeling in Water Resources*. John Wiley & Sons, 1399 p.

Solomon, H. and Stephen, M.A., "Approximations to Density Functions Using Pearson

Curves," *Journal of American Society of Statisticians*, 73 (361): 153-160, 1978

- S Hayami, On the propagation of flood waves, *Bulletin No. 1*, Disaster Prevention Research Institute, Kyoto University, London (1951).
- Tomlin, C.D. 1990. Geographic information systems and cartographic modelling. Prentice Hall, New York
- Tung, Y.K. and Mays. L.W., "Optimal Risk-Based Design of Hydraulic Structures," Technical Report CRWR-171, Center for Research in Water Resources, University of Texas, Austin, Texas, 1980.
- Tung, Y.K. and Hathorn, W.E., "Probability Distribution for Critical DO Location in Streams," *Ecological Modeling*, 42:45-60, 1988.
- T Hayashi, Propagation and deformation of flood waves in natural channels, *80th Anniversary Bulletin*, Chuo University, Japan (1965), pp. 67–80.
- Than, H, H, Flood Risk Mapping of Lower Part Of Chindwin Basin, M.Tech, Thesis (2005)
- T.J. Chung , Finite Element Analysis in Fluid Dynamics. (1st edition ed.), McGraw-Hill Publishing Co., New York (1978).
- Van Deursen, W.P.A. 1995 'Geographical Information Systems and Dynamic Models: development and application of a prototype spatial modelling language. *Netherlands Geographic Studies*, 190. See also <http://www.frw.ruu.nl/pcraster.html>.
- Yen, B.C., Cheng, S.T., and Melching, C.S., "First-order Reliability Analysis," in *Stochastic and Risk Analysis in Hydraulic Engineering*, Ed. by B.C. Yen, Water Resources Publications, Littleton, CO, 1986.

Wesseling, C.G., Karssenber, D.J., Burrough, P.A. and Van Deursen, W.P.A. 1996. 'Integrated dynamic environmental models in GIS: The development of a Dynamic Modelling language. *Transactions in GIS*,1-1, 40-48.

Wösten, J.H.M. 1998 Personal Communication on HYPRES results.

APPENDIX

```
#include<iostream.h>
#include<math.h>
#include<fstream.h>
void main()
{
    int i,j;
    double Q[35][3],h[35][3],t,d1,d2,a,c,b,s1,s2,p1,p2,n;
    cout<<"input the flow of river at intial time step and at all station :"<<endl;
    cout<<"Input the Time interval 't' and distance between the station"<<endl;
    ifstream din;
    din.open("intial.txt");
    for(j=0,i=0;i<3;i++)
    {
        din>>Q[j][i];
    }
    din>>t;
    din>>d1>>d2;
    din>>s1>>s2;
    din>>p1>>p2;
    din>>n;
    din.close();

    din.open("upstream.txt");
    for(j=1,i=0;j<31;j++)

        din>>Q[j][i];
    din.close();

    for(j=0;j<31;j++)
    {
        b=pow(((n*pow(p1,(2/3)))/(1.49*pow(s1,0.5))),0.6);
        a=t/d1;

        for(i=0;i<2;i++)
        {
```

```

        c=(Q[j][i+1]+Q[j+1][i])/2.0;

        Q[j+1][i+1]=(a*Q[j+1][i]+b*(0.6)*Q[j][i+1]*pow(c,(-
0.4)))/(a+b*pow(c,(-0.4)));

        b=pow(((n*pow(p2,(2/3)))/(1.49*pow(s2,0.5))),0.6);
        a=t/d2;
    }
}
ofstream fout;
fout.open("downstream.txt");
for(j=0;j<31;j++)
{
    for(i=0;i<3;i++)
        fout<<Q[j][i]<<" ";
    fout<<endl;
}
fout.close();
for(j=0;j<31;j++)
{
    h[j][1]=pow((Q[j][1]/354.0),(1/2.08))+0.7;
    h[j][2]=pow((Q[j][2]/993.57),(1/1.307))+0.9;
}
fout.open("stage.txt");
for(j=0;j<31;j++)
{
    fout<<h[j][1]<<" ";
    fout<<h[j][2];
    fout<<endl;
}

fout.close();
}

```